University of California
Los Angeles

Modeling Volatility Using High Frequency Data

A dissertation submitted in partial satisfaction
of the requirements for the degree
Doctor of Philosophy in Economics

by

Miao Sun

2016

Abstract of the Dissertation

Modeling Volatility Using High Frequency Data

by

Miao Sun

Doctor of Philosophy in Economics

University of California, Los Angeles, 2016

Professor Bryan C. Ellickson, Chair

This dissertation explores the volatility of stock prices over the course of a trading day. I reformulate the Heston stochastic volatility model as a model of the high-frequency evolution of the scaled increments of quadratic variation. I use the generalized method of moments to estimate three of the parameters of the model: the speed of mean reversion, the asymptotic mean, and the volatility of volatility. This continuous-path model works very well most of the time, and most of the failures are localized to a few short intervals.

The dissertation of Miao Sun is approved.

Francis Longstaff

Rosa Matzkin

Aaron Tornell

Bryan C. Ellickson, Committee Chair

University of California, Los Angeles

2016

To my parents.

Table of Contents

List of Figures

List of Tables

Acknowledgments

I would like to thank first and foremost my advisor Bryan Ellickson, who has been constantly providing guidance and support for me. I would also like to thank the other members of my committee Aaron Tornell, Rosa Matzkin and Francis Longstaff for all of their help. I would especially like to thank my group members Benjamin Hood, Duke Whang, Hongxiang Xu and Sibo Yan for their comments and inspiration.

Vita

2009 B.S. (Statistics), Peking University.

2010 M.A. (Economics), University of California, Los Angeles.

CHAPTER 1

Stock-Price Volatility: I

This dissertation explores the volatility of stock prices over the course of a trading day. I view the daily pattern of volatility as a realization of a continuous-time mean-reverting stochastic process, a Heston (1993) model of stochastic volatility. Using the generalized method of moments (GMM), I estimate three of the parameters that characterize this model: the asymptotic mean, the speed of mean reversion and the volatility of volatility.[1] Estimating the asymptotic mean and the speed of mean reversion will be the focus of this chapter. Estimating volatility of volatility will be the focus of Chapter 2.

This research follows in a line of doctoral dissertations at UCLA over the past few years that use high-frequency data to explore stock price volatility during the trading day. The common theme is that realized variation computed from stock prices sampled once a second is a useful estimator of the quadratic variation of the stock price process over short intervals of time, intervals as short as 100 seconds.

Consider the following setting (see Protter (2004) and Shreve (2004)). Let the interval $[0, 1]$ denote time for a specific trading day, and let $S = (S_t)_{t\in[0,1]}$ denote a stock price process on $[0, 1]$. Define the log price process X by $X_t = \log(S_t)$ for $t \in [0, 1]$. Consider an Itô process characterized by the stochastic differential equation

$$dX_t = \mu_t\, dt + \sigma_t\, dW_t \qquad (t \in [0, 1]) \tag{1.1}$$

[1] I do not estimate the correlation parameter between the Wiener process driving the price process and the Wiener process driving the volatility process. That "leverage parameter" is incidental to the focus of this dissertation.

where W is a standard Brownian motion. The drift process $\mu = (\mu_t)_{t\in[0,1]}$ and volatility process $\sigma = (\sigma_t)_{t\in[0,1]}$ are stochastic processes defined on the same stochastic basis[2] $(\Omega, \mathcal{F}, \mathbb{F}, \mathbb{P})$ as the Wiener process W and adapted to $\mathbb{F}$. If μ and σ are constant, then the log price process X is called *geometric Brownian motion.* The *quadratic variation* process of the stochastic process X is the stochastic process $[X, X] = ([X, X]_t)_{t\in[0,1]}$ given by

$$[X, X]_t = \int_0^t \sigma_s^2 ds \qquad (t \in [0, 1]) \tag{1.2}$$

To simplify notation in later derivations, I define $\zeta_t = \sigma_t^2$ and write equation 1.2 in the form

$$[X, X]_t = \int_0^t \zeta_s ds \qquad (t \in [0, 1]) \tag{1.3}$$

The instantaneous value ζ_t is, of course, not observable. However, the theory of semimartingales provides a way to estimate the path of the process $[X, X]$, called the realized variation. Realized variation uses the price process X (which is observable) to provide a good estimate of quadratic variation. Let $\Pi^N = \{t_0, t_1, \ldots, t_N\}$ be a partition of $[0, 1]$ where

$$0 = t_0 < t_1 < \ldots < t_N = 1$$

and

$$t_j - t_{j-1} = \delta^N := \frac{1}{N} \qquad (j = 1, \ldots, N)$$

δ^N is called the *mesh* of the partition. In all of the empirical work discussed here, the mesh is 1 second, corresponding to prices sampled once a second. Because there are $N = 23,400$ $(= 6.5 * 60 * 60)$ seconds in a 6.5-hour trading day and a trading day corresponds to one "unit" of time, the mesh $\delta^N = 1/23400$.

The *realized variation* of the stochastic process $X = (X_t)_{t\in[0,1]}$ for the partition

[2]The triple $(\Omega, \mathcal{F}, \mathbb{P})$ is a probability space and $\mathbb{F} = (\mathcal{F}_t)_{t\in[0,1]}$ is a filtration.

Π^N is

$$RV_t^N = \sum_{t_j \leq t} (\Delta X_{t_j})^2 \qquad (t \in [0,1]) \tag{1.4}$$

where $\Delta X_{t_j} = X_{t_j} - X_{t_{j-1}}$ is the log return over the interval $[t_{j-1}, t_j]$. In other words, the value of the realized variation at time t is the cumulative sum of the squared log returns at time t. In particular, for $t = 1$

$$RV_1^N = \sum_{j=1}^{N} (\Delta X_{t_j})^2 \tag{1.5}$$

In much of the financial econometrics literature, RV_1^N (rather than the process RV^N) is called the realized variation.

An important conclusion in semimartingale theory (see Protter (2004)) states that, for any sequence of partitions Π^N for which $\delta^N \to 0$ as $N \to \infty$, the realized variation process converges uniformly in probability on compact sets to the quadratic variation process.[3] It follows that realized variation over an interval is a consistent estimator for the increment to quadratic variation over the same interval. Provided that the processes μ and σ satisfy some regularity conditions, the paths of the price process X defined by the stochastic differential equation 1.1 are continuous with probability one, and the same is true for the paths of the quadratic variation process 1.3.

In her thesis, Zhou (2007) found that, except for occasional jumps, the plot of cumulative squared one-second log returns over a trading day is quite smooth, a curve that can be fit reasonably well on most days by a straight line with a strictly positive intercept, which reflects the elevated level of volatility at the beginning of the day. She examined the behavior of realized variation for every stock in the Dow-Jones Industrials for every trading day from the beginning of 2000 to the end of 2006. These plots exhibit an astonishing regularity across stocks and over

[3]The result in Protter (2004) is, in fact, more general: the times t_j are allowed to be stopping times. I do not require that level of generality.

Figure 1.1: Realized variation process $RV_t^N \times 10^4$, 01/06/2011

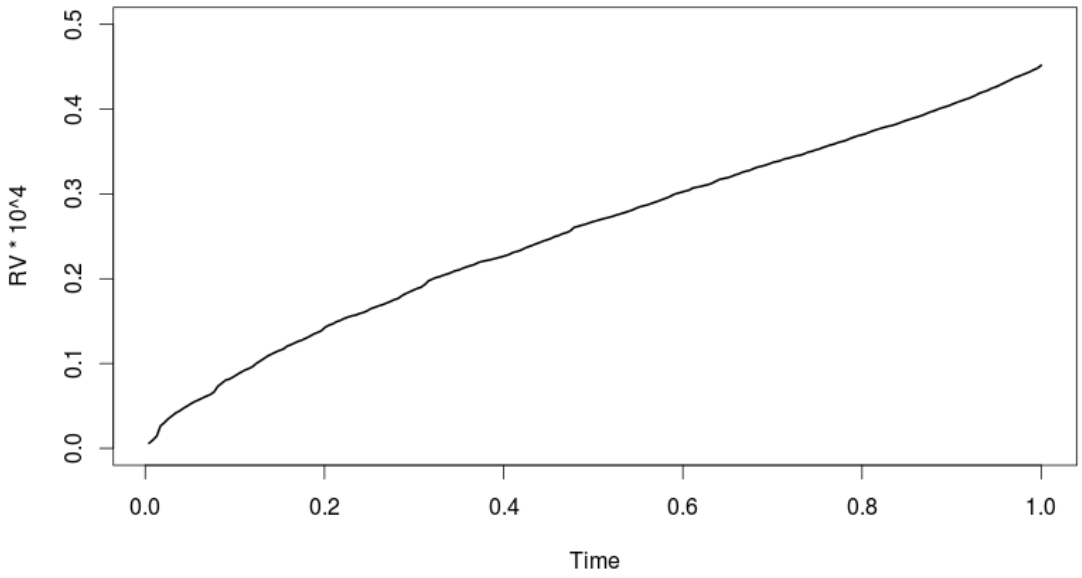

time: apart from a few big jumps, the realized variation (which, of course, starts at 0) has a concave shape for the first half hour or so of the trading day and then flattens out to a straight line for the rest of the day.

Figure 1.1 shows a plot of realized variation for SPY — an exchange traded fund (ETF) that tracks the S&P 500 Index — on a random day, January 6th, 2011 (which lies outside Zhou (2007)'s sample). Because the path of realized variation is a good approximation to the path of quadratic variation, the slope of this graph at time t is a good measure of the local (squared) volatility of the stock at time t. This suggests that, after half an hour or so, stock prices settle down to a constant volatility, the signature of geometric Brownian motion. This pattern fits the initial portion of the "u-shape" found in the literature (see Wood, McInish and Ord (1985)). One interpretation is that, when markets are closed, uncertainty about market-clearing prices builds; when the market opens, "the market" does its job and uncertainty eventually settles down to the constant level

σ of a geometric Brownian motion. But convergence need not be to a geometric Brownian motion — the volatility process itself may be stochastic.

The fact that realized variation is a consistent estimator of quadratic variation for any compact interval of the time line suggests a way to explore the question whether volatility is stochastic: divide the trading day into blocks several seconds in length, and examine the realized variation over each of these *blocks*. Let

$$\Pi^M = \{t_0, t_1, \ldots, t_M\}$$

where $\Pi^M \subset \Pi^N$,

$$0 = t_0 < t_1 < \ldots < t_M = 1$$

and $t_i - t_{i-1} = h = 1/M$ for $i = 1, 2, \ldots, M$. If the 6.5-hour trading day is divided into 100-second blocks, then $M = 23400/100 = 234$ and $h = 100\delta^N = 1/234$. For a block $[t, t+h] \subset [0,1]$ with $t \in \Pi^M$ and $t + h \in \Pi^M$, I define the *quadratic variation over block* $[t, t+h]$ by

$$\zeta_{t,t+h} = \frac{1}{h}\left([X,X]_{t+h} - [X,X]_t\right) = \frac{1}{h}\int_t^{t+h} \zeta_s \, ds \tag{1.6}$$

and the *realized variation over block* $[t, t+h]$ by

$$\varphi_{t,t+h} = \frac{1}{h}\left(RV^N_{t+h} - RV^N_t\right) = \frac{1}{h}\sum_{t_i \in (t,t+h] \cap \Pi^N} (\Delta X_{t_i})^2 \tag{1.7}$$

In both of these definitions, I multiply by $1/h$ so that the increments scale to a rate per unit time (i.e., a rate per trading day). It is important not to confuse these *scaled* variations with the unscaled variations

$$[X,X]_{t+h} - [X,X]_t \; = \int_t^{t+h} \zeta_s \, ds \quad \text{and} \quad RV^N_{t+h} - RV^N_t = \sum_{t_i \in (t,t+h] \cap \Pi^N} (\Delta X_{t_i})^2$$

which, with $h = 1/234$, have the scale of a rate per 100-second block rather

Figure 1.2: Realized variation by block $\varphi_{t,t+h} \times 10^4$, 01/06/2011

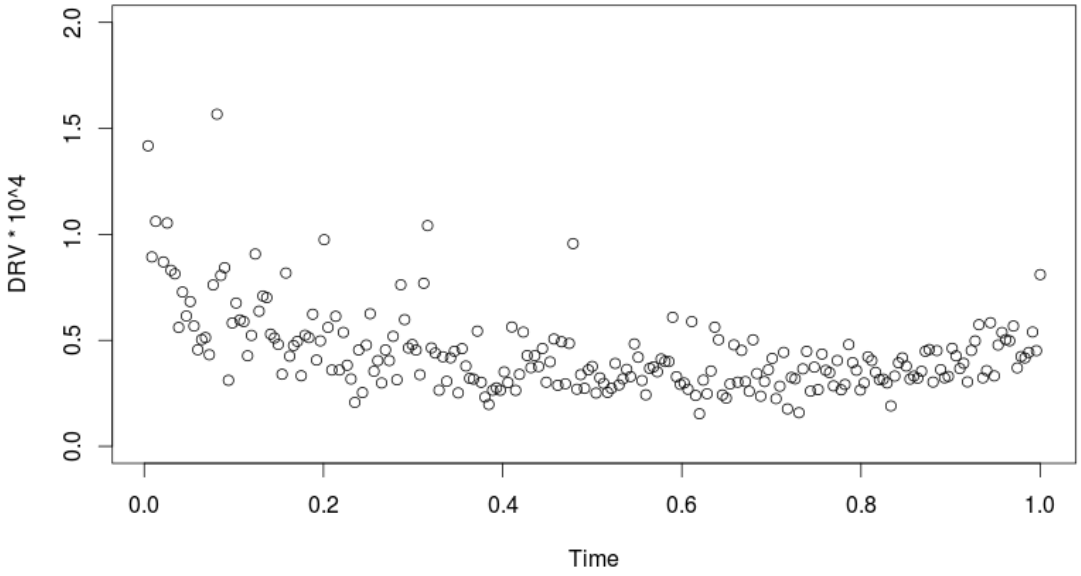

than a rate per trading day. From now on I will refer to $\zeta_{t,h+h}$ and $\varphi_{t,t+h}$ as the quadratic variation and realized variation respectively without adding explicitly the qualification "scaled".

Figure 1.2 exhibits a plot of realized variation block by block for SPY on January 6, 2011, the same day exhibited in Figure 1.1. The higher value of volatility at the beginning of the trading day is apparent, as is the tendency for the process to settle down. Whether the variation in the increments to realized variation is due to sampling variation around a constant value (as for a geometric Brownian motion) or to stochastic volatility is hard to judge without a model.

The Heston (1993) model is probably the most commonly applied model of stochastic volatility. It proposes a specific model for the volatility σ_t of equation 1.1, or rather its square ζ_t. The ζ process is a mean-reverting Markov process

characterized by the stochastic differential equation

$$d\zeta_t = \kappa(\bar{\zeta} - \zeta_t)dt + \gamma\sqrt{\zeta_t}\, dB_t \qquad (t \in [0,1]) \tag{1.8}$$

where B is a Wiener process that is possibly correlated with the Wiener process W that drives the price process in equation 1.1. The parameters $\bar{\zeta}$, κ and γ correspond to the asymptotic mean of the volatility process, the speed of reversion to this asymptotic mean, and the volatility of volatility respectively. These parameters are assumed to be strictly positive and to satisfy the Feller condition (see Feller (1951))

$$\gamma^2 < 2\kappa\bar{\zeta} \tag{1.9}$$

which guarantees that ζ_t is almost surely positive for all t. No restriction is imposed on the drift process μ of the price equation 1.1.

The Heston stochastic differential equation 1.8 does not have a closed-form solution. However, one can solve for the distribution of ζ_t for each t and, in particular, derive expressions for the expectation and variance of ζ_t for each t. The Heston model of the volatility process ζ is mathematically equivalent to the Cox-Ingersoll-Ross (1985) (henceforth CIR (1985)) interest rate model studied on page 151 to 153 of Shreve (2004), although of course there are some differences in notation. In particular, it is shown that (I will provide a detailed derivation of this equation in section 1.1)

$$\zeta_{t_i} - \zeta_{t_{i-1}} = \beta(\bar{\zeta} - \zeta_{t_{i-1}}) + \gamma e^{-\kappa h}\int_{t_{i-1}}^{t_i} e^{\kappa s}\sqrt{\zeta_s}\, dB_s \qquad (i = 1, 2, \ldots, M) \tag{1.10}$$

where $[t_{i-1}, t_i]$ is a block defined by the partition Π^M and $\beta = 1 - e^{-\kappa h}$.

Equation 1.10 can be interpreted as a stochastic difference equation

$$\zeta_{t_i} - \zeta_{t_{i-1}} = \beta(\bar{\zeta} - \zeta_{t_{i-1}}) + \varepsilon_{t_i} \qquad (i = 1, 2, \ldots, M) \tag{1.11}$$

with slope β, no constant term and an innovation sequence $(\varepsilon_{t_i})_{i=1}^{M}$ that is a martingale difference. The slope of the regression model measures the speed of mean reversion: on average the fraction β of the gap between $\zeta_{t_{i-1}}$ and the daily asymptotic mean $\bar{\zeta}$ is eliminated over the block $[t_{i-1}, t_i]$. Ellickson, Hood, Liu, Whang and Zhou (2012)[4] (henceforth EHLWZ (2012)) estimates equation 1.11 using the ordinary least square (OLS) method, by assuming that the instantaneous volatility ζ_t can be approximated by the quadratic variation $\zeta_{t,t+h}$ over the block $[t, t+h]$, and that $\zeta_{t,t+h}$ can be approximated by the realized variation $\varphi_{t,t+h}$ over the same block.

The results are very impressive: the speed of mean reversion appears to be roughly constant over the entire period, and t-statistics are very large. Mean reversion is rapid: on the order of 80% of the gap between volatility and its asymptotic mean is expected to vanish in five minutes. What emerges is a plausible portrait of the equilibrating dynamics of volatility within the trading day. The volatility process is approximated reasonably well by a continuous-path, stationary Markov process, the Heston model, that reverts with high speed to its asymptotic mean. Disequilibrium occurs at the market open, but that effect wears off quickly, and the market settles down to an equilibrium in which shocks to volatility are balanced by reversion to the mean.

The estimation of the Heston model in EHLWZ (2012) is the starting point for this dissertation. Their regression-based method is easy to compute, and the estimation results are successful. However, it suffers from some drawbacks. First, this method does not distinguish between instantaneous volatility at a specific time and quadratic variation over a block. If, as their paper claims, the mean reversion of the volatility process is rapid, replacing ζ_t by $\zeta_{t,t+h}$ could potentially introduce large error. That is to say, this method does not perfectly deal with the key

[4]EHLWZ (2012) draws from the doctoral dissertations of Hood (2011), Liu (2011), Whang (2012) and Zhou (2007).

challenge that the volatility process is unobservable. Second, the standard errors seem too small and the t-statistics too large. This renders statistical inference based on them suspicious. Third, the authors do not use the Heston model to estimate the asymptotic mean $\bar{\zeta}$, choosing instead to estimate that parameter using the median of the realized variations for the blocks, and they do not estimate γ. Fourth, their paper does not address the issue of error in variables introduced by using the observable realized variation $\varphi_{t,t+h}$ in place of the unobservable quadratic variation $\zeta_{t,t+h}$ despite the considerable literature casting doubt on the reliability of the approximation.[5]

In this dissertation I develop an easy-to-compute, GMM-type estimator that addresses these problems with the EHLWZ (2012) methodology. In this chapter, I develop a difference equation that describes the evolution of the conditional expectation of the quadratic variation from one block to the next, a characterization that parallels the structure of the continuous-time stochastic differential equation of Heston in a natural way. This difference equation provides the basis for the moment conditions that I employ, using GMM, to estimate the asymptotic mean and speed of mean reversion of the Heston model. In Chapter 2, I derive a second moment condition that is used to estimate the volatility of volatility. In both chapters I estimate the model using high-frequency data for SPY (the exchange-traded fund that tracks the S&P 500 index) for all trading days from the start of 2007 until the end of 2014.

[5]As high-frequency asset price data became widely available in the late 1990's, financial econometricians began to explore the potential of using realized variation to estimate quadratic variation over the trading day. However, experience using the notion of realized variation was not successful, leading to the widespread suspicion of its value as an estimator of quadratic variation and to the development of methods not based on realized variation. See Anderson, Bollerslev, Diebold and Labys (2002) for an early exploration of this issue, and Aît-Sahalia and Jacod (2014) or Mykland and Zhang (2012) for more recent commentary.

1.1 Estimating the Heston Model

The setting is a single trading day in which a log stock price process and its volatility are described by the Heston model: they satisfy the stochastic differential equations 1.1 and 1.8 respectively, repeated here for convenience:

$$dX_t = \mu_t \, dt + \sigma_t \, dW_t \qquad (t \in [0,1])$$

and

$$d\zeta_t = \kappa(\bar{\zeta} - \zeta_t)dt + \gamma\sqrt{\zeta_t} \, dB_t \qquad (t \in [0,1])$$

I assume that the trading day $[0,1]$ has been partitioned into M blocks, each of length $h = 1/M$.

The goal in this section is to develop estimators for the parameters κ and $\bar{\zeta}$ of the Heston model, given observed realized variation $\varphi_{t,t+h}$ over these blocks. Note that the instantaneous volatility ζ_t and the quadratic variation $\zeta_{t,t+h}$ over blocks are not observable.

To simplify notation in later discussion, I define parameters

$$\alpha = e^{-\kappa h} \tag{1.12}$$

$$\beta = 1 - e^{-\kappa h} \tag{1.13}$$

Thus, the goal is equivalent to developing estimators for the parameters β and $\bar{\zeta}$.

1.1.1 Deriving a moment condition for GMM

In this subsection, I derive a stochastic difference equation describing the evolution of the quadratic variation $\zeta_{t,t+h}$ from one block $[t, t+h]$ to the next.

The starting place is the stochastic difference equation 1.10 describing the evo-

lution of the instantaneous volatility ζ_t. I rewrite it as a lemma, and as promised in the introduction, derive it now.

Lemma 1.1. *In the Heston model,*

$$\zeta_{t+h} = \alpha\zeta_t + \beta\bar{\zeta} + e^{-\kappa(t+h)}\gamma \int_t^{t+h} e^{\kappa s}\sqrt{\zeta_s}\, dB_s \tag{1.14}$$

Proof. This proof follows directly from the analysis of the CIR model in Shreve (2004), page 152.

Define $f(t,z) = e^{\kappa t}z$, The function f has partial derivatives $f_t = \kappa e^{\kappa t}z$, $f_z = \kappa e^{\kappa t}$ and $f_{zz} = 0$. The Itô-Doeblin formula implies that

$$\begin{aligned}
d(e^{\kappa t}\zeta_t) &= df(t,\zeta_t) \\
&= f_t(t,\zeta_t)\, dt + f_z(t,\zeta_t)\, d\zeta_t + \frac{1}{2}f_{zz}(t,\zeta_t)\, d[\zeta,\zeta]_t \\
&= \kappa e^{\kappa t}\zeta_t\, dt + e^{\kappa t}\left[\kappa(\bar{\zeta} - \zeta_t) + \gamma\sqrt{\zeta_t}\, dB_t\right] \\
&= \kappa e^{\kappa t}\bar{\zeta} + \gamma e^{\kappa t}\sqrt{\zeta_t}\, dB_t
\end{aligned}$$

Integrating both sides over the interval $[t, t+h]$ yields

$$e^{\kappa(t+h)}\zeta_{t+h} - e^{\kappa t}\zeta_t = \bar{\zeta}(e^{\kappa(t+h)} - e^{\kappa t}) + \gamma \int_t^{t+h} e^{\kappa s}\sqrt{\zeta_s}\, dB_s$$

Rearranging terms and using the definitions of α and β in equations 1.12 and 1.13, the result follows. □

Equation 1.14 is a difference equation for the instantaneous volatility ζ_t. What I want is a difference equation for the quadratic variation $\zeta_{t,t+h}$ over the blocks of the partition Π^M.

The following lemma expresses the conditional expectation of ζ_{t+h} relative to the information set $\mathcal{F}_t$ as a convex combination of ζ_t and $\bar{\zeta}$.

Lemma 1.2. *In the Heston model,*

$$\mathbb{E}[\zeta_{t+h} \mid \mathcal{F}_t] = \alpha\zeta_t + \beta\bar{\zeta} \tag{1.15}$$

Proof. The result follows from equation 1.14 and the fact that the Itô integral $\int_0^{t+h} e^{\kappa s}\sqrt{\zeta_s}\, dB_s$ is a martingale with zero expectation. □

Lemma 1.2 allows me to interpret β as the weight attached to the asymptotic mean $\bar{\zeta}$ in equation 1.15, which expresses the conditional expectation of ζ_{t+h} as a convex combination of ζ_t and $\bar{\zeta}$. Equation 1.15 can also be written in the form

$$\mathbb{E}[\zeta_{t+h} - \zeta_t \mid \mathcal{F}_t] = \beta\left(\bar{\zeta} - \zeta_t\right) \tag{1.16}$$

Thus, β can be interpreted as the average fraction of the gap between ζ_t and the asymptotic mean $\bar{\zeta}$ eliminated over the block $[t, t+h]$.

The next lemma establishes a link between the conditional mean of the quadratic variation $\zeta_{t,t+h}$ over the block $[t, t+h]$ and the instantaneous volatility ζ_t at the beginning of that block.

Lemma 1.3. *In the Heston model,*

$$\mathbb{E}\left[\zeta_{t,t+h} \mid \mathcal{F}_t\right] = a_1\zeta_t + b_1\bar{\zeta} \tag{1.17}$$

where

$$a_1 = \frac{1 - e^{-\kappa h}}{\kappa h} \qquad b_1 = 1 - a_1$$

Proof. Using the definition of $\zeta_{t,t+h}$ in equation 1.6 and interchanging expectation and integration with respect to time,

$$\mathbb{E}\left[\zeta_{t,t+h} \mid \mathcal{F}_t\right] = \mathbb{E}\left[\frac{1}{h}\int_t^{t+h} \zeta_s ds \mid \mathcal{F}_t\right] = \frac{1}{h}\int_t^{t+h} \mathbb{E}\left[\zeta_s \mid \mathcal{F}_t\right] ds$$

Using equation 1.15 to substitute for the conditional expectation and evaluating the integrals,

$$\begin{aligned}
\mathbb{E}\left[\zeta_{t,t+h} \mid \mathcal{F}_t\right] &= \frac{1}{h}\int_t^{t+h} \left[e^{-\kappa(s-t)}\zeta_t + \left(1 - e^{-\kappa(s-t)}\right)\bar{\zeta}\right] ds \\
&= \left(\frac{1}{h}\int_t^{t+h} e^{-\kappa(s-t)} ds\right)\zeta_t + \left(\frac{1}{h}\int_t^{t+h} \left(1 - e^{-\kappa(s-t)}\right) ds\right)\bar{\zeta} \\
&= \frac{1 - e^{-\kappa h}}{\kappa h}\zeta_t + \left(1 - \frac{1 - e^{-\kappa h}}{\kappa h}\right)\bar{\zeta}
\end{aligned}$$

□

Lemma 1.3 states that the conditional mean of the quadratic variation $\zeta_{t,t+h}$ over the block $[t, t+h]$ is a convex combination of the instantaneous volatility ζ_t at the beginning of the block and the asymptotic mean $\bar{\zeta}$. Although the weights are different from those in equation 1.15, the similarity in form of equation 1.15 and equation 1.17 is no surprise at all: Equation 1.17 is just an integrated version of equation 1.15 — the average of quantities that are convex combinations of two given numbers with different weights is just a convex combination of the two numbers with the average weight. A simple application of calculus shows that

$$\beta = 1 - e^{-\kappa h} > 1 - \frac{1 - e^{-\kappa h}}{\kappa h} = b_1$$

Thus, the weight of the asymptotic mean in equation 1.15 is always larger than that in equation 1.17. This makes sense, as the instantaneous volatility ζ_{t+h} is more forward-looking and less sticky than quadratic variation over the block $[t, t+h]$ and consequently exhibits faster mean reversion.

Now I am ready to establish the relationship between the conditional mean of the quadratic variation $\zeta_{t+h,t+2h}$ given the information set $\mathcal{F}_t$ and the conditional mean of the quadratic variation $\zeta_{t,t+h}$ over the preceding block.

Proposition 1.1. *In the Heston model,*

$$\mathbb{E}\left[\zeta_{t+h,t+2h} \mid \mathcal{F}_t\right] = \alpha\, \mathbb{E}\left[\zeta_{t,t+h} \mid \mathcal{F}_t\right] + \beta\, \bar{\zeta} \tag{1.18}$$

or equivalently,

$$\mathbb{E}\left[\zeta_{t+h,t+2h} - \alpha\, \zeta_{t,t+h} - \beta\, \bar{\zeta} \mid \mathcal{F}_t\right] = 0 \tag{1.19}$$

Proof. By the law of iterated expectations,

$$\mathbb{E}\left[\zeta_{t+h,t+2h} \mid \mathcal{F}_t\right] = \mathbb{E}\left[\mathbb{E}\left[\zeta_{t+h,t+2h} | \mathcal{F}_{t+h}\right] | \mathcal{F}_t\right]$$

Using equation 1.17 to substitute for the inner conditional expectation on the right-hand side gives

$$\mathbb{E}\left[\zeta_{t+h,t+2h} \mid \mathcal{F}_t\right] = \mathbb{E}\left[a_1\zeta_{t+h} + b_1\bar{\zeta} \mid \mathcal{F}_t\right] = a_1\, \mathbb{E}\left[\zeta_{t+h} \mid \mathcal{F}_t\right] + b_1\, \bar{\zeta}$$

Using equation 1.15 to substitute for $\mathbb{E}\left[\zeta_{t+h} \mid \mathcal{F}_t\right]$ yields

$$\mathbb{E}\left[\zeta_{t+h,t+2h} \mid \mathcal{F}_t\right] = a_1\left(\alpha\zeta_t + \beta\bar{\zeta}\right) + b_1\bar{\zeta} = a_1\alpha\zeta_t + (a_1\beta + b_1)\bar{\zeta}$$

Using equation 1.17 to replace ζ_t

$$\begin{aligned}
\mathbb{E}\left[\zeta_{t+h,t+2h} \mid \mathcal{F}_t\right] &= a_1\alpha\frac{\mathbb{E}\left[\zeta_{t,t+h} \mid \mathcal{F}_t\right] - b_1\bar{\zeta}}{a_1} + (a_1\beta + b_1)\bar{\zeta} \\
&= \alpha\mathbb{E}\left[\zeta_{t,t+h} \mid \mathcal{F}_t\right] + (-\alpha b_1 + a_1\beta + b_1)\bar{\zeta} \\
&= \alpha\mathbb{E}\left[\zeta_{t,t+h} \mid \mathcal{F}_t\right] + (a_1\beta + (1-\alpha)b_1)\bar{\zeta}
\end{aligned}$$

Because

$$a_1\beta + (1-\alpha)b_1 = \left(\frac{\beta}{kh}\right)\beta + \beta\left(1 - \frac{\beta}{kh}\right) = \beta$$

the result follows. □

Proposition 1.1 establishes that the conditional expectation of $\zeta_{t+h,t+2h}$ with respect to the information set $\mathcal{F}_t$ is a convex combination of the conditional expectation of $\zeta_{t,t+h}$ with respect to the same information set $\mathcal{F}_t$ and the asymptotic mean $\bar{\zeta}$ of the process ζ. Note that the coefficients in equation 1.18 are the same as those in equation 1.15. This seems surprising at first, but it is actually quite natural: equation 1.18 is just a time-averaged version of equation 1.15 plus the law of iterated expectations.

Proposition 1.1 provides interpretations of β that are parallel to those provided by Lemma 1.2. On the one hand, β is the weight attached to the asymptotic mean $\bar{\zeta}$ in the expression for conditional expectation of $\zeta_{t+h,t+2h}$ as a convex combination of conditional expectation of $\zeta_{t,t+h}$ and $\bar{\zeta}$. On the other hand, equation 1.18 can be rewritten in the form

$$\mathbb{E}\left[\zeta_{t+h,t+2h} - \zeta_{t,t+h} \mid \mathcal{F}_t\right] = \beta \left(\bar{\zeta} - \mathbb{E}\left[\zeta_{t,t+h} \mid \mathcal{F}_t\right]\right) \tag{1.20}$$

Thus, β can be interpreted as the average fraction of the gap between conditional expectation of $\zeta_{t,t+h}$ and the asymptotic mean $\bar{\zeta}$ eliminated over the block $[t + h, t + 2h]$.

Rewrite equation 1.19 as

$$\mathbb{E}\left[\eta_{t,t+2h} \mid \mathcal{F}_t\right] = 0 \tag{1.21}$$

where

$$\eta_{t,t+2h} := \zeta_{t+h,t+2h} - \alpha\, \zeta_{t,t+h} - \beta\, \bar{\zeta} \tag{1.22}$$

or

$$\zeta_{t+h,t+2h} = \alpha\, \zeta_{t,t+h} + \beta\, \bar{\zeta} + \eta_{t,t+2h} \tag{1.23}$$

Equation 1.23 is a stochastic difference equation that describes the evolution of the quadratic variation $\zeta_{t,t+h}$ from one block $[t, t + h]$ to the next, and it has

the important property that the error term has a conditional mean of zero, as in equation 1.21.

Equation 1.19 gives a candidate for a moment condition suitable for the GMM procedure, provided that the quadratic variation $\zeta_{t,t+h}$ over a block $[t, t+h]$ can be approximated by the realized variation $\varphi_{t,t+h}$ over the same block.

1.1.2 Errors in variables

I now address the error in variables introduced by using the observable realized variation $\varphi_{t,t+h}$ in place of the unobservable quadratic variation $\zeta_{t,t+h}$. The error-in-variables problem, also called the measurement error problem, refers to the phenomenon that an otherwise exogenous regressor necessarily becomes endogenous when measured with error.

Standard assumptions about measurement errors are that they are zero mean and uncorrelated with contemporaneous observables. This idea applies naturally in my context. The observable realized variation is an error-ridden measure of the unobservable quadratic variation:

$$\varphi_{t,t+h} = \zeta_{t,t+h} + \nu_{t,t+h} \tag{1.24}$$

and

$$\varphi_{t+h,t+2h} = \zeta_{t+h,t+2h} + \nu_{t+h,t+2h} \tag{1.25}$$

Substituting equations 1.24 and 1.25 into equation 1.23, the relationship in equation 1.23 can be expressed in terms of the observable realized variation:

$$\varphi_{t+h,t+2h} = \alpha\, \varphi_{t,t+h} + \beta\, \bar{\zeta} + (\nu_{t+h,t+2h} - \alpha\, \nu_{t,t+h} + \eta_{t,t+2h}) \tag{1.26}$$

I claim that, in order to satisfy the conditional moment condition

$$\mathbb{E}\left[\varphi_{t+h,t+2h} - \alpha\, \varphi_{t,t+h} - \beta\, \bar{\zeta} \mid \mathcal{F}_t\right] = 0 \tag{1.27}$$

or equivalently,

$$\mathbb{E}\left[\nu_{t+h,t+2h} - \alpha\, \nu_{t,t+h} + \eta_{t,t+2h} \mid \mathcal{F}_t\right] = 0 \tag{1.28}$$

I only need the following assumption:

Assumption 1.1.

$$\mathbb{E}\left[\nu_{t,t+h} \mid \mathcal{F}_s\right] = 0 \qquad \forall s \leq t \tag{1.29}$$

To see this, note that the first two terms in equation 1.28 are zero under Assumption 1.1, and that the last term is zero according to equation 1.21.

Assumption 1.1 is hardly an "assumption", and it appears quite reasonable — the difference between realized variation and quadratic variation over a block is zero mean and uncorrelated with what happens before the beginning of the block.

1.1.3 GMM estimation

Up to now I have adopted a notation more suitable to the setting of continuous-time finance. In order to apply discrete-time econometrics techniques, I translate the analysis into a discrete-time notation that is consistent with Hayashi (2000). I will describe the econometric problem by focusing on realized variation over blocks defined by the partition $\Pi^M = \{0, h, 2h \ldots, Mh\}$.

The equation to be estimated is the linear regression equation 1.26, a stochastic difference equation describing the evolution of realized variation over blocks:

$$y_i = \boldsymbol{z_i}'\boldsymbol{\delta} + \varepsilon_i \qquad (i = 1, 2, \ldots, n)$$

where

$$y_i = \varphi_{(i+1)h,(i+2)h}$$

is the scalar observable dependent variable,

$$\boldsymbol{z_i} = \begin{bmatrix} 1 \\ \\ \varphi_{ih,(i+1)h} \end{bmatrix}$$

is the 2-dimensional observable vector of regressors,

$$\boldsymbol{\delta} = \begin{bmatrix} \beta\bar{\zeta} \\ 1-\beta \end{bmatrix}$$

is the 2-dimensional coefficient vector,

$$\varepsilon_i = \nu_{(i+1)h,(i+2)h} - \alpha\, \nu_{ih,(i+1)h} + \eta_{ih,(i+2)h}$$

is the scalar unobservable error term, and $n = M - 2$ is the sample size.

The regressor $\varphi_{ih,(i+1)h}$ (the second row of $\boldsymbol{z_i}$) is necessarily endogenous in this setting. To see this, notice that $\varphi_{ih,(i+1)h}$, which depends on the realization of the Heston model over the block $[ih, (i+1)h]$, is necessarily correlated with $\eta_{ih,(i+2)h}$, which depends on the realization of the Heston model over the block $[ih, (i+2)h]$, and hence, is correlated with the error term ε_i. As a consequence, the OLS estimator is not consistent.

To deal with the endogeneity problem, I introduce instrument variables (IVs). IVs should be both valid and relevant: orthogonal to the error term and at the same time correlated with the endogenous regressors. The lagged realized variation and its powers appear to satisfy both conditions: they are orthogonal to the error term under Assumption 1.1 and equation 1.21, and realized variation is typically serially autocorrelated. The number of IVs should be no less than the

number of parameters, 2. In the empirical analysis below, I choose the following 4-dimensional observable vector of instruments:

$$\boldsymbol{x_i} = \begin{bmatrix} 1 \\ \varphi_{(i-1)h,ih} \\ \varphi^{1/2}_{(i-1)h,ih} \\ \varphi^{1/4}_{(i-1)h,ih} \end{bmatrix}$$

The orthogonality conditions associated with these IVs are

$$\begin{aligned} \mathbb{E}\left[\varphi_{t+h,t+2h} - (1-\beta)\varphi_{t,t+h} - \beta\bar{\zeta}\right] &= 0 \\ \mathbb{E}\left[\left(\varphi_{t+h,t+2h} - (1-\beta)\varphi_{t,t+h} - \beta\bar{\zeta}\right)\varphi_{t-h,t}\right] &= 0 \\ \mathbb{E}\left[\left(\varphi_{t+h,t+2h} - (1-\beta)\varphi_{t,t+h} - \beta\bar{\zeta}\right)\varphi^{1/2}_{t-h,t}\right] &= 0 \\ \mathbb{E}\left[\left(\varphi_{t+h,t+2h} - (1-\beta)\varphi_{t,t+h} - \beta\bar{\zeta}\right)\varphi^{1/4}_{t-h,t}\right] &= 0. \end{aligned}$$

However, I am well aware that lagged variables might fail to be proper instruments, either because assumptions of zero correlations might fail due to a more complex pattern of serial correlation than the model assumes, or because these lagged variables are not quite correlated with the variables they are instrumenting. I will examine this issue in Chapter 3.

I have so far stated the complete setting necessary for the generalized method of moments (GMM). One obtains the GMM estimator for the underlying model parameters by minimizing the weighted distance between population moments and their sample versions (see Hansen (1982)).

The GMM estimator is consistent under standard regularity conditions, according to Hayashi (2000), Proposition 3.1. These conditions are Assumptions 3.1 to 3.4 in the book. Assumption 3.1 states that the equation to be esti-

mated is linear, which is automatically satisfied here. Assumption 3.2 requires that $\left(\varphi_{t+h,t+2h}, \varphi_{t,t+h}, \varphi_{t-h,t}, \varphi_{t-h,t}^{1/2}, \varphi_{t-h,t}^{1/4}\right)$ is jointly stationary and ergodic; this is likely satisfied because (1) the ζ process in the Heston model is stationary and ergodic, (2) a measurable function of a stationary and ergodic process is stationary and ergodic, and (3) $\varphi_{t,t+h}$ is a very good approximation of $\zeta_{t,t+h}$ so it should approximately inherit the stationarity and ergodicity properties of the ζ process. Assumption 3.3, the orthogonality condition, and Assumption 3.4, the identification condition, are trivially satisfied. Therefore, the GMM estimator in my setting is consistent.

Because the error terms are autocorrelated, I use a heteroscedasticity and autocorrelation consistent (HAC) covariance matrix estimator with a Bartlett-kernel (see Newey and West (1987)). For numerical considerations, I also re-scale the second, third and fourth moments to make all the four of the same order of magnitude.

Under the GMM setting, the minimized value of the objective function multiplied by the sample size is asymptotically chi-square distributed, which allows for a specification test of the overidentifying restrictions. Moreover, inference concerning the individual parameters is readily available from the standard formula for the asymptotic covariance matrix.

1.2 Empirical Results

This section examines the empirical performance of the Heston stochastic volatility model in describing the intraday dynamics of stock price volatility. I use the GMM method to estimate the asymptotic mean parameter $\bar{\zeta}$ and the mean reversion parameter β of the model. This analysis is based on the high-frequency data set of prices of the exchange-traded fund SPY in a eight-year sample period from 2007 to 2014. I perform daily, weekly and monthly joint estimation of the parameters

$\bar{\zeta}$ and β. I find that weekly estimation achieves a good balance of good statistical performance with large enough sample size and high temporal resolution.

1.2.1 Data

The data come from the trades component of the NYSE Trades and Quotes (TAQ) database, available at the Wharton WRDS website. These data report price, number of shares, and time of each transaction (to the nearest second). Following the usual practice, the TAQ "condition codes" were used to remove trades from the file that were canceled or otherwise flagged as illegitimate, and the data within each day were sorted by time stamp.[6]

The sample period is 2007 to 2014. These years have witnessed a rapid development of high-frequency trading. On the one hand, high-frequency trading generates an abundance of data. On the other hand, it probably influences how the financial market works. I will address some of these points in Chapter 3. Because this sample period includes the financial crisis in 2008 and 2009, I am able to examine how my model works in an extremely volatile environment. I use data for SPY, an exchange traded fund that tracks the S&P 500 Index.

I sample the data once per second. Following Whang (2012), for a time stamp with more than one trade I use the median-share price, i.e. the median of the distribution of price per share for that second with each share traded in that second treated as a separate observation. One advantage of using the median-share price rather than the volume-weighted price is that there is almost always a transaction with the median-share price. This set of median-share prices sampled every second is the data set used to compute realized variation over blocks.

[6]See Aît-Sahalia and Jacod (2014) for details about the TAQ dataset.

1.2.2 Daily estimation

This subsection examines the estimates of $\bar{\zeta}$ (the asymptotic mean) and β (the speed of mean reversion parameter) for every day in the sample period. The sample period consists of the 1969 trading days from the beginning of 2007 to the end of 2014.

Figure 1.3 plots the time series of the daily estimates for $\bar{\zeta}$, the asymptotic mean. The estimates are multiplied by 10^4. For example, a label of 4 on the vertical axis corresponds to a 2% volatility, or equivalently, a 2% standard deviation of daily return (recall $\sigma_t = \sqrt{\zeta_t}$). The maximum daily estimate of $\bar{\zeta}$ in the entire sample exceeds 10×10^{-4}, but I truncate the vertical axis at that threshold to better reflect the overall picture. The year labels on the horizontal axis mark the start of each year.

The central message of Figure 1.3 is that daily estimation appears to work quite well in the sense that it produces plausible estimates of $\bar{\zeta}$. In general, the time series of $\bar{\zeta}$ looks persistent, consistent with the well-documented stylized fact of volatility clustering. However, volatility can move abruptly; for example, the "Great Recession" from the second half of 2008 to the beginning of 2009 witnessed exceptionally high levels of market volatility, which is clear in the plot.

Figure 1.4 displays a histogram of the daily estimates of $\bar{\zeta}$ (the estimates are multiplied by 10^4). The central message here is the same — the estimates look reasonable. On about half of the days the estimates fall in the range of $[0, 1] \times 10^{-4}$, corresponding to a daily variance of less than 1%, which again seems plausible. The distribution of $\bar{\zeta}$ is asymmetric with a fat right tail: volatility is occasionally quite high, as represented by the bar I label "infinity" at the very right of the histogram.

Daily estimation of β does not perform as well. Figure 1.5 plots the time series of daily estimates of β, the mean reversion parameter. The plot is very

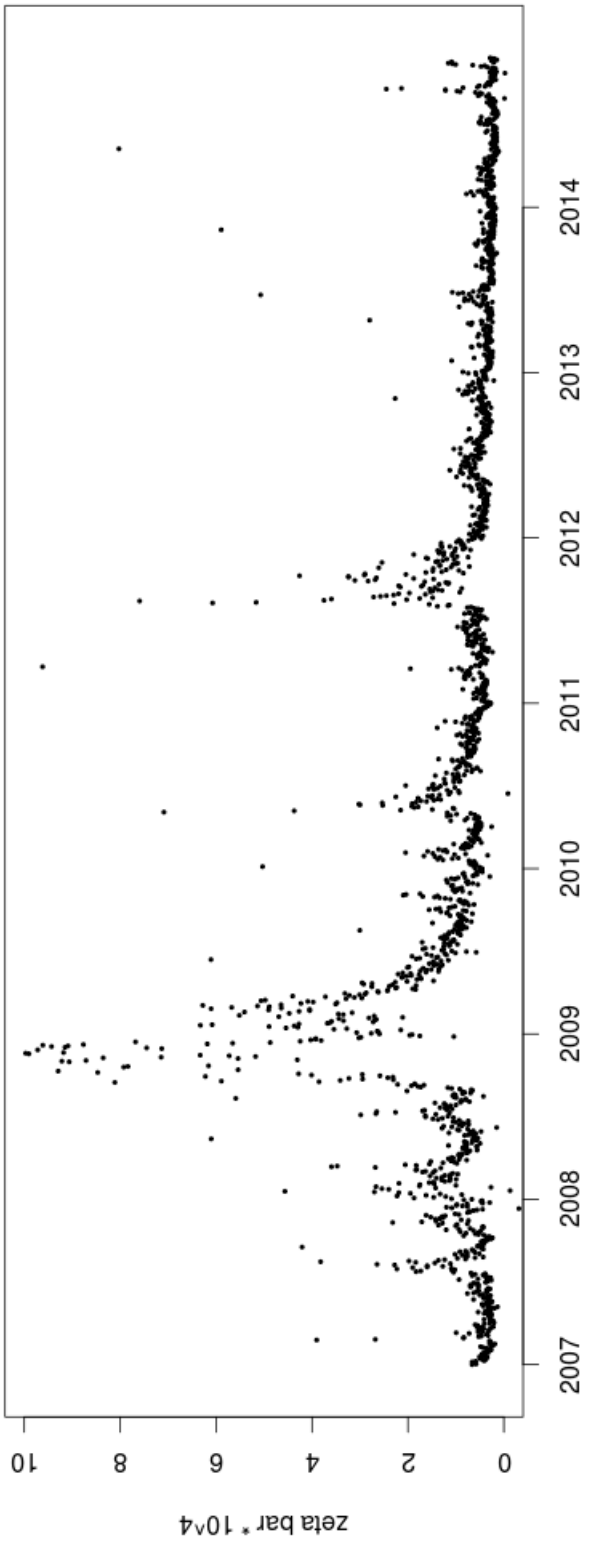

Figure 1.3: Daily estimates of $\bar{\zeta} \times 10^4$

Figure 1.4: Histogram of daily estimates of $\bar{\zeta} \times 10^4$

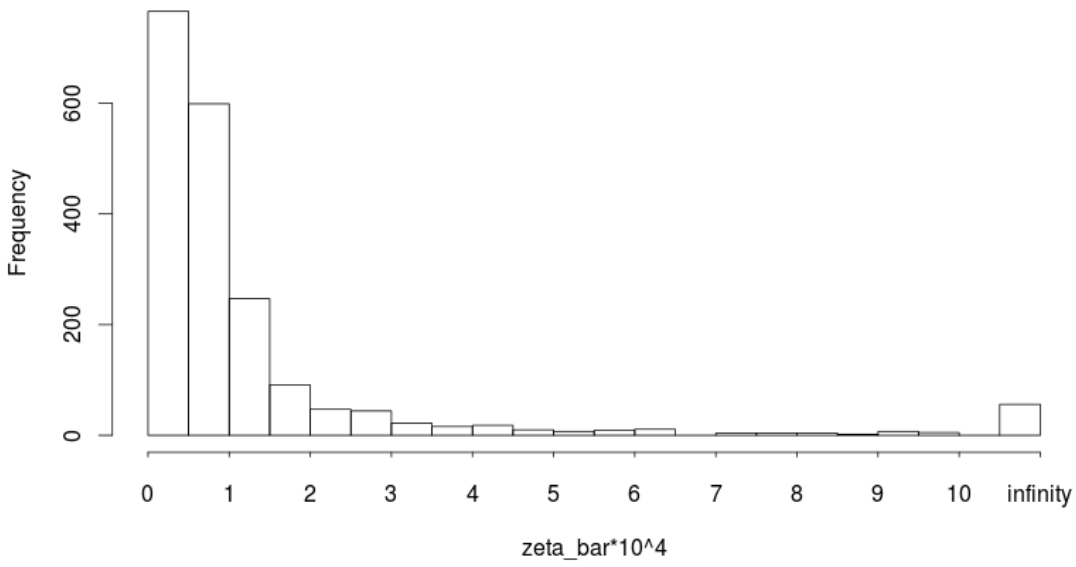

noisy, with no clear pattern. One possible reason for this is that the sample size is not large enough. To give some perspective, the sample size of 232 is the same order of magnitude as the number of daily returns in a year. Figure 1.6 displays a histogram of the daily estimates of β. The very left bar and the very right bar represent daily estimates smaller than zero and larger than unity respectively. Clearly daily estimation works poorly on those days.

1.2.3 Pooled joint estimation

The daily estimates suggest that pooling the data might be a good idea. Specifically, I pool trading days into groups of 5 or 20 successive trading days, which I will refer to as "weeks" or "months". I assume that the parameters $\bar{\zeta}$ and β are constant within each week or month. This seems reasonable because $\bar{\zeta}$ looks highly persistent according to Figure 1.3 and β does not have a clear pattern

Figure 1.5: Daily estimates of β

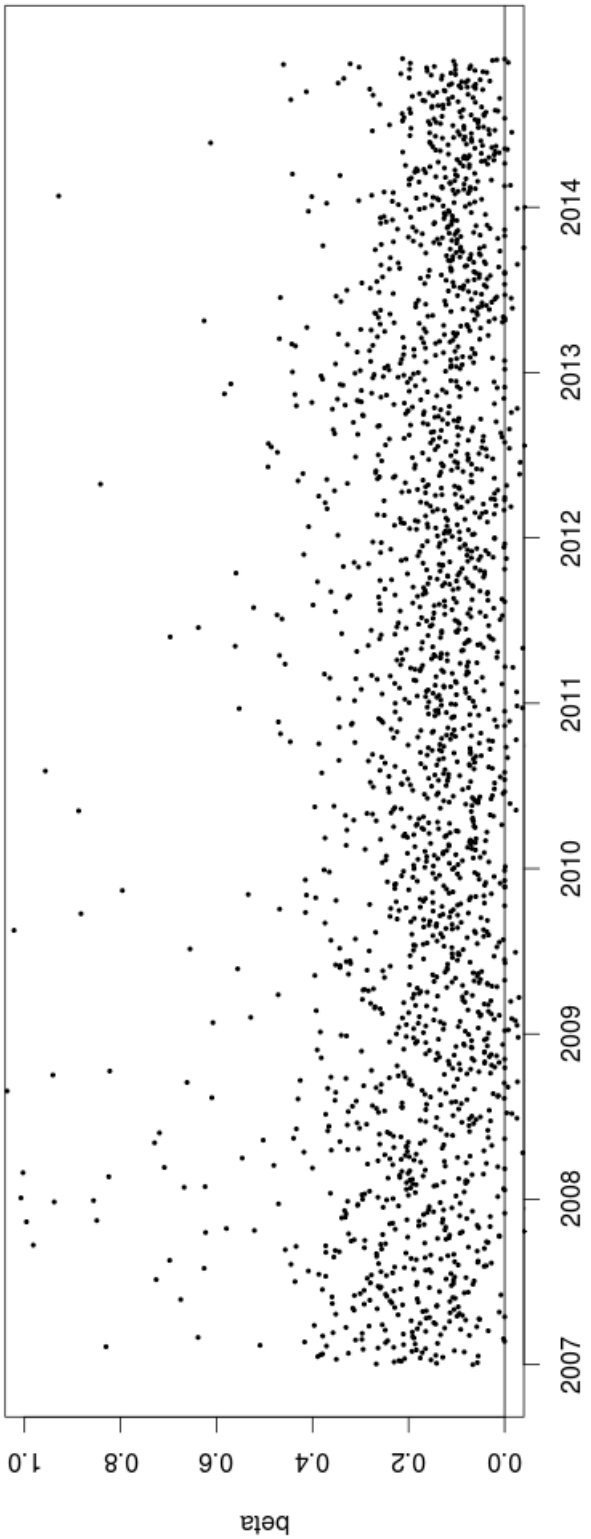

Figure 1.6: Histogram of daily estimates of β

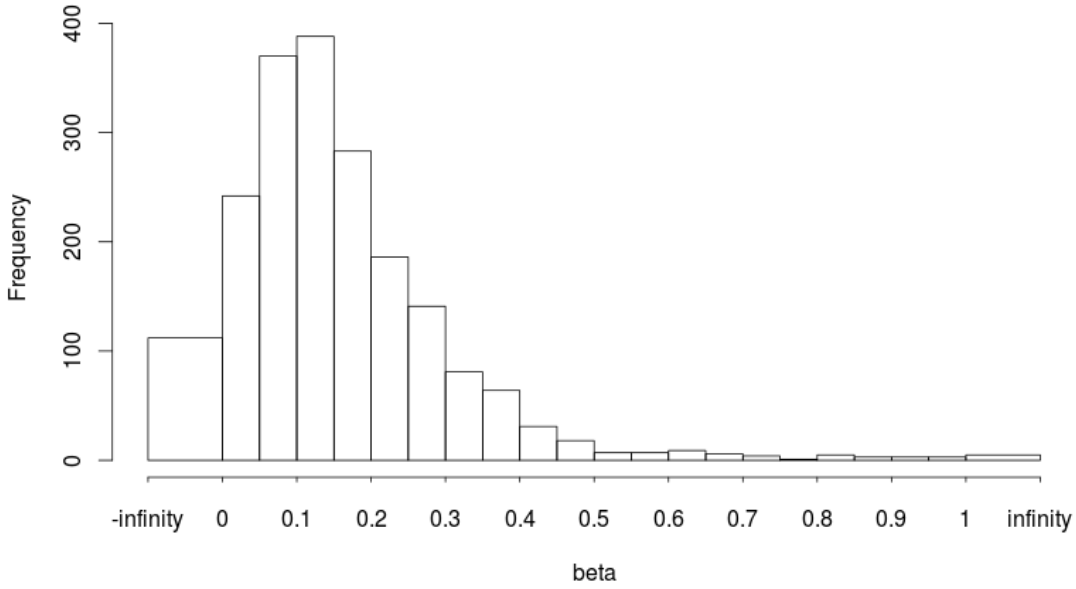

according to Figure 1.5.

Table 1.1 displays measures of statistical performance of daily, weekly and monthly joint estimation of $\bar{\zeta}$ and β. The top panel reports significance of estimates of the two parameters. A parameter is called "good" if the null hypothesis that it is zero is rejected at 5% significance level in favor of an alternative that it is positive, where the test statistic is the "z-score", which is asymptotically standard normal under standard regularity conditions. The first row of the panel reports the percentage of days, weeks and months (together with the counts in parentheses) where the joint estimation yields good estimates for both parameters. On 53% of all days in the sample, or 1041 days out of 1969, estimates for both parameters are significant and positive. This ratio rises to 88%, or 344 weeks out of 393, for weekly estimation. This is what I hoped when I introduced the idea of pooling: a sample size five times as large as that of the daily estimation should help produce a more accurate estimate and a smaller standard error. This

Table 1.1: Performance of joint estimation of $\bar{\zeta}$ and β, daily, weekly and monthly

	Daily (1969)	Weekly (393)	Monthly (98)
Good β, Good $\bar{\zeta}$	53% (1041/1969)	88% (344/393)	92% (90/98)
Good β, Bad $\bar{\zeta}$	0% (7/1969)	1% (2/393)	1% (1/98)
Bad β, Good $\bar{\zeta}$	37% (737/1969)	9% (36/393)	2% (2/98)
Bad β, Bad $\bar{\zeta}$	9% (184/1969)	3% (11/393)	5% (5/98)
Good J-stat	88% (1732/1969)	87% (340/393)	48% (47/98)
Bad J-stat	12% (237/1969)	13% (53/393)	52% (51/98)
Good (β, $\bar{\zeta}$ and J-stat)	45% (894/1969)	75% (296/393)	43% (42/98)

ratio increases slightly to 92%, or 90 months out of 98, for monthly estimation. An even longer sample does not seem to provide much help along this dimension.

The next three rows correspond to situations in which the joint estimation does not yield good estimates for both parameters. The "good β bad $\bar{\zeta}$" cases account for less than 1% of days, weeks or months in the sample. On a few occasions, the joint estimation breaks down when it cannot yield a good estimate of $\bar{\zeta}$ and consequently cannot produce a good estimate of β. The "bad β good $\bar{\zeta}$" cases account for 37% of days, 9% of weeks and 2% of months. This demonstrates the power of pooling: a larger sample size by pooling tends to produce a better estimate of β, as long as the joint estimation can yield a good estimate of $\bar{\zeta}$. The "bad $\bar{\zeta}$ bad β" cases account for 9% of days, 3% of weeks and 5% of months. The ratios are not very different from one another, and a good portion of these cases are associated with outliers in the sample of realized variation, either representing true volatility jumps or data errors. I will examine these situations in more detail in Chapter 3.

The middle panel of Table 1.1 takes into consideration the GMM specification test. A "good J-stat" means that the model is not rejected at a 10% significance level by the J-test: i.e., the J-statistic is smaller than the corresponding percentile of the relevant chi-square distribution. The model passes the specification test on

88% of all days in the sample, or 1732 days out of 1969. This ratio drops slightly to 87%, or 340 out of 393, for weekly estimation and dramatically to 48%, or 47 out of 98, for monthly estimation. This is most likely because the assumption that the parameters are constant for each day or week hold reasonably well but the corresponding assumption for each month is badly violated — volatility could well vary by a large amount over a month, as suggested by Figure 1.3.

The bottom row of Table 1.1 reports the percentages of days, weeks and months in which the joint estimation yields good estimates of both parameters $\bar{\zeta}$ and β as well as a good J-stat. I will call them "good days", "good weeks" and "good months", respectively. Good weeks account for 75% of weeks, much higher than the percentages of good days and good months.

The central message of Table 1.1 is that weekly estimation enjoys the best statistical performance: it provides a large enough sample size and the parameters are approximately constant over that period of time.

1.2.4 Good days versus good weeks

I have focused on statistical performance when comparing daily and weekly joint estimation. This subsection complements that comparison by taking into consideration another criterion, temporal resolution. A natural tradeoff between good statistical performance and temporal resolution arises in my context: weekly pooled estimation enjoys better statistical performance than daily estimation, but it may fail to capture rapid movement of $\bar{\zeta}$ over time.

To address this, Figure 1.7 and Figure 1.8 plot the time series of $\bar{\zeta}$ for good days and good weeks respectively, and Figure 1.9 and Figure 1.10 plot the time series of β for good days and good weeks respectively. The two plots for $\bar{\zeta}$ look similar. One does not lose much resolution in moving from daily to weekly estimation. However, weekly estimates of β improve upon daily estimates: there is little evidence that

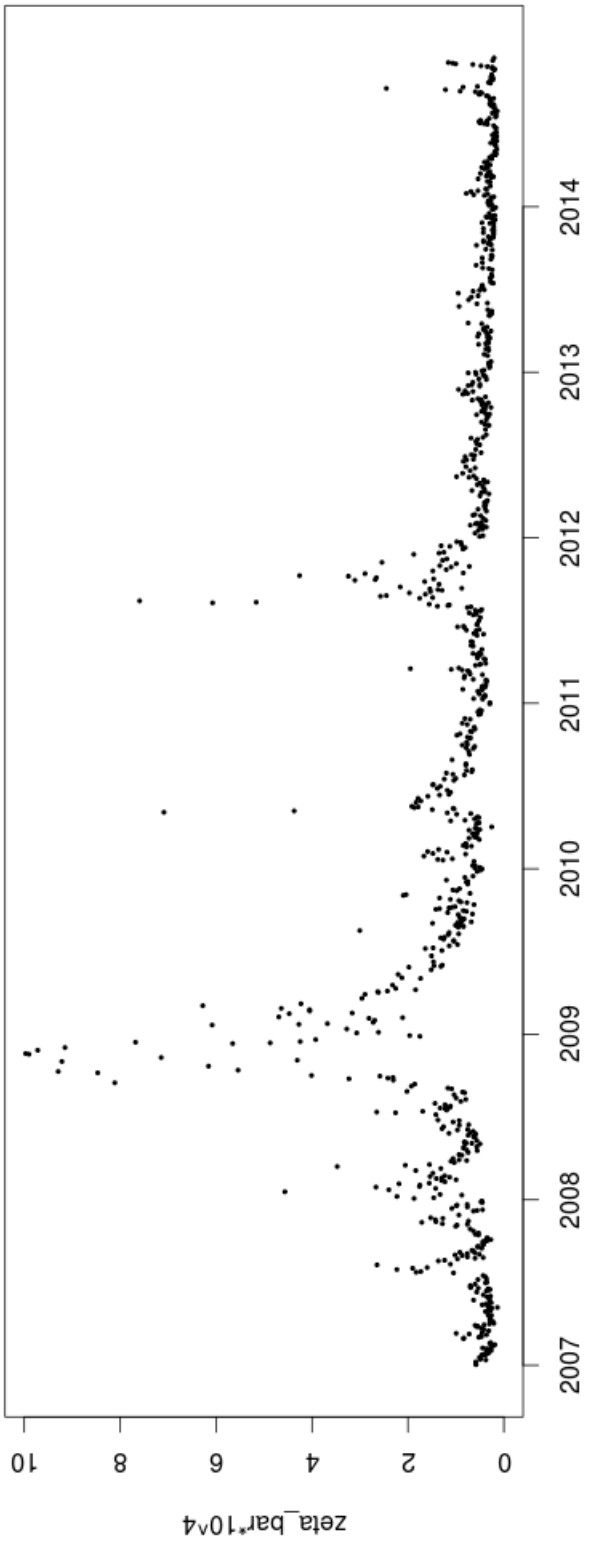

Figure 1.7: Estimates of $\bar{\zeta} \times 10^4$, good days

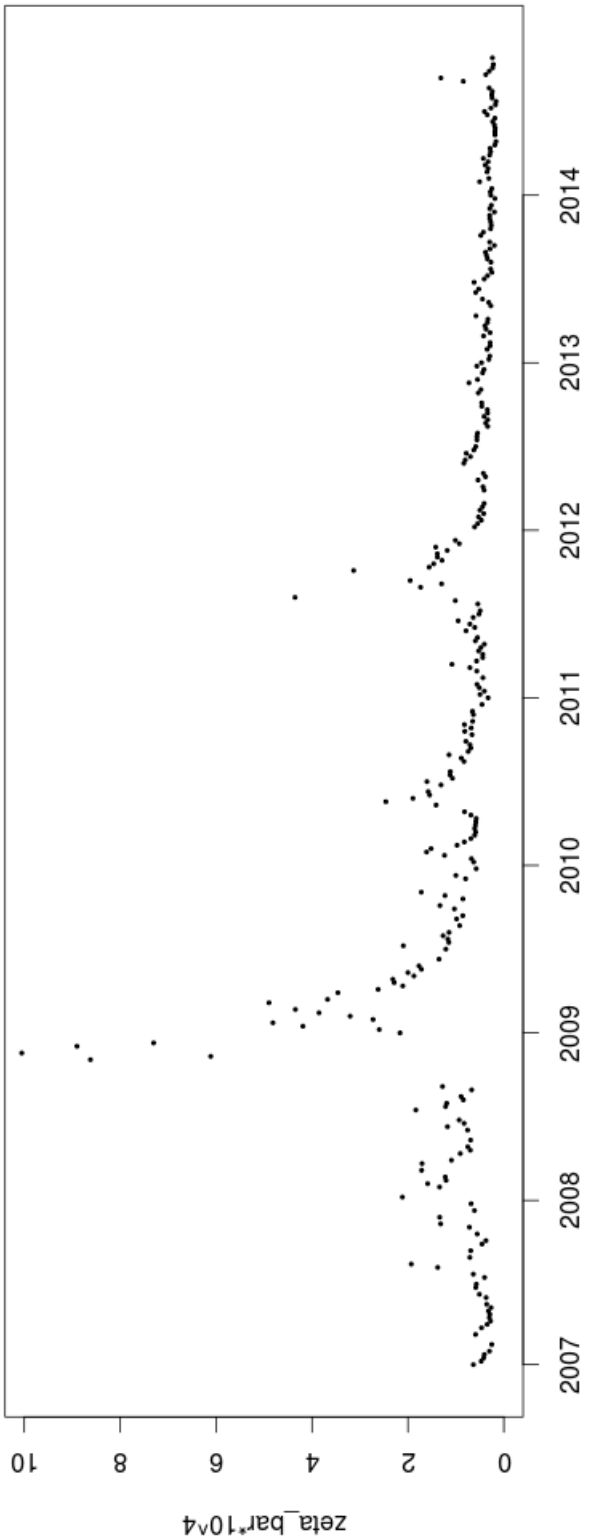

Figure 1.8: Estimates of $\bar{\zeta} \times 10^4$, good weeks

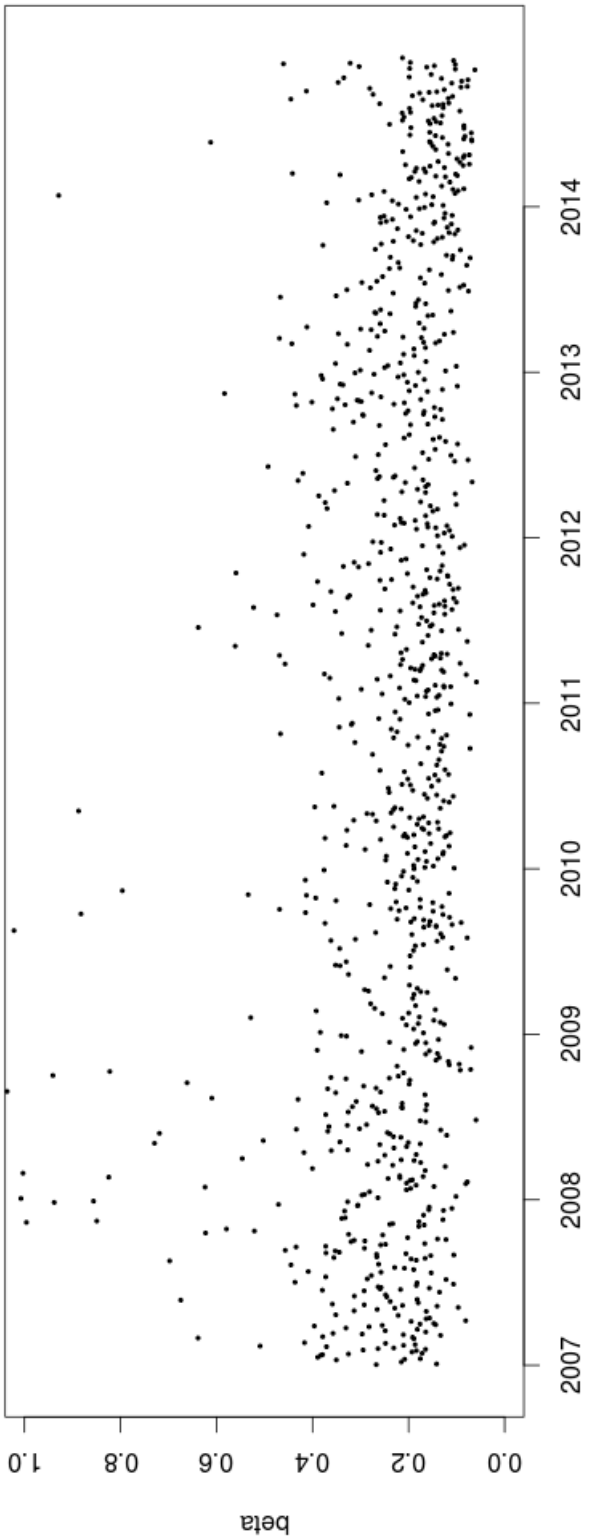

Figure 1.9: Estimates of β, good days

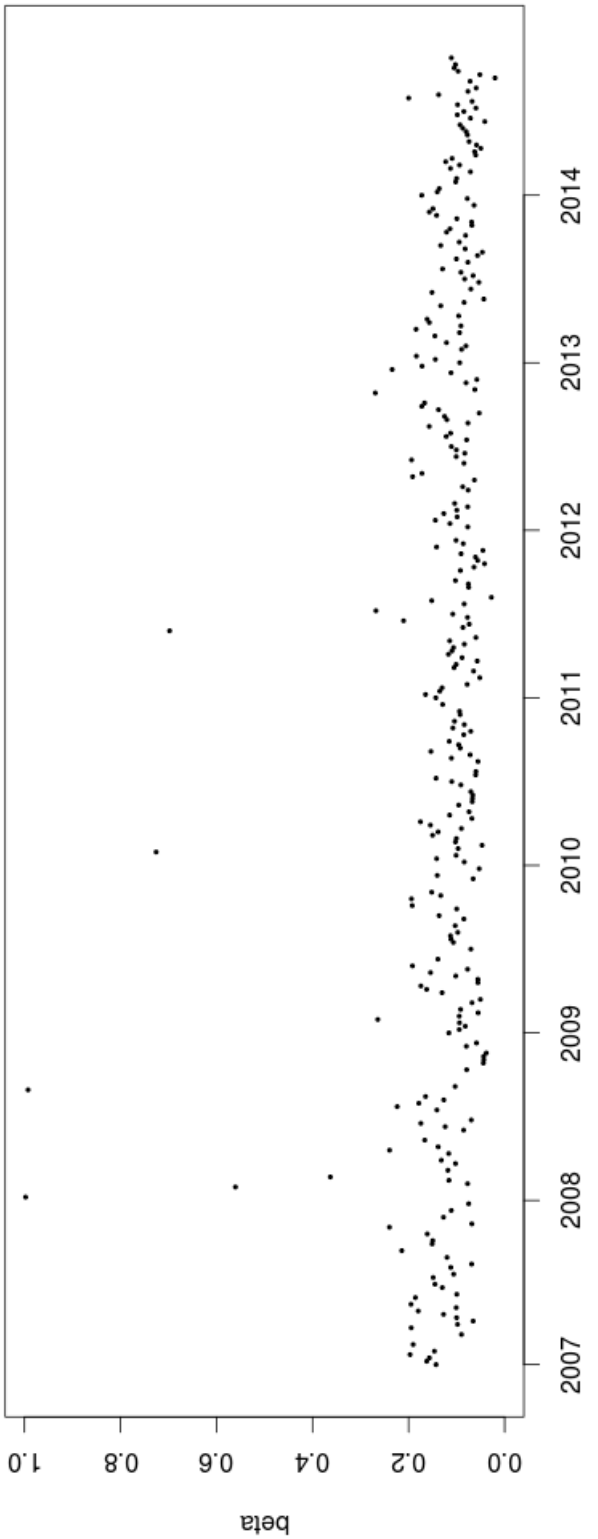

Figure 1.10: Estimates of β, good weeks

Table 1.2: Estimates of $\bar{\zeta} \times 10^4$ and β, good weeks

	$\bar{\zeta} \times 10^4$	β
median	0.59	0.10
lower quantile	0.37	0.08
upper quantile	1.15	0.14
mean	1.06	0.13
median standard error	0.04	0.03
median z-score	14	3.2

β varies significantly over time.

To summarize, weekly estimation achieves a good balance of sample size and high temporal resolution. For this reason, weekly estimates for good weeks will be the focus of the empirical analysis that follows.

1.2.5 Estimation results for good weeks

I now examine the weekly estimation in more detail for good weeks. Table 1.2 reports the summary statistics of weekly estimates of $\bar{\zeta}$ and β in good weeks only. The median estimate of $\bar{\zeta}$ is 0.59×10^{-4}, corresponding to a 0.77% standard deviation of daily return, or a 12% standard deviation of yearly return, which seems plausible given the historic volatility of U.S stock indexes. The lower and upper quantiles of 0.37×10^{-4} and 1.15×10^{-4} correspond to 10% and 17% yearly standard deviation respectively.[7] The mean is 1.06×10^{-4}, only slightly smaller than the upper quantile. This suggests that there are a few large positive estimates. The median z-score of the estimates is 14, which is reasonably high. As a comparison, this z-score is smaller than the corresponding t-statistics as high as a few hundred reported in EHLWZ (2012). This is probably because my estimation

[7]The annual standard deviation of postwar U.S. stock market return is about 16%, according to Cochrane (2005).

Figure 1.11: Histogram of estimates of $\bar{\zeta} \times 10^4$, good weeks

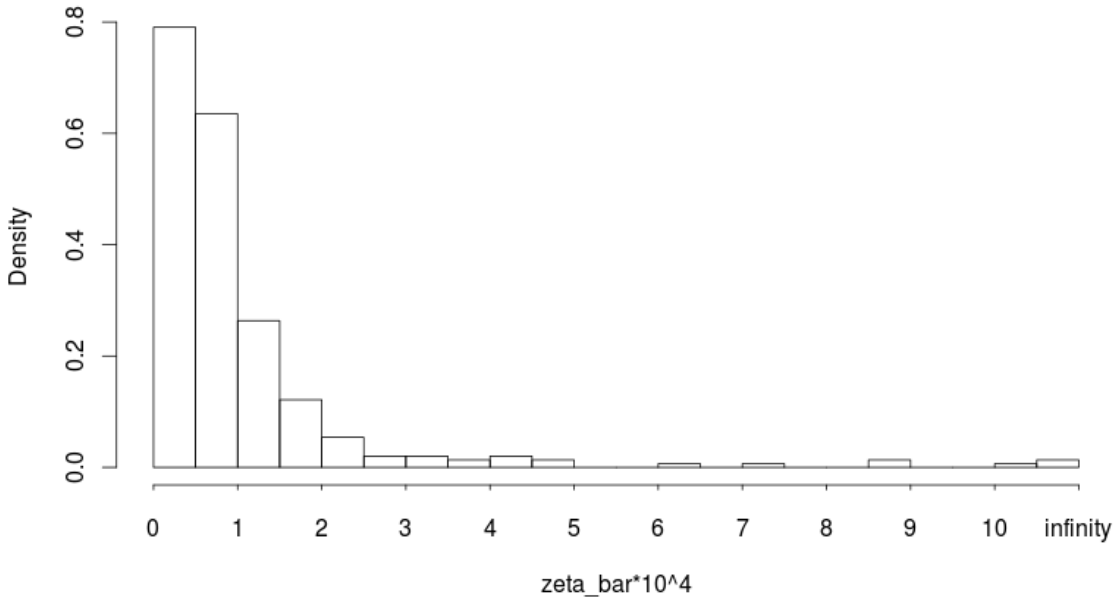

using GMM yields a more accurate estimate of the standard error than OLS.

Figure 1.11 displays the histogram of $\bar{\zeta}$ in good weeks only. The two highest bars lie in the range of $[0, 1] \times 10^{-4}$, which contains the median and lower quantile $\bar{\zeta}$ reported in Table 1.2. The distribution is highly skewed to the right, with a few outliers that are larger than 5×10^{-4}. However, these outliers are not suspicious but rather represent a good feature of the estimation: volatility can sometimes be exceptionally high, for example, during the financial crisis of 2008 - 2009.

The second column of Table 1.2 reports the summary statistics of weekly estimates of β in good weeks only. The median, lower and upper quantiles are 0.10, 0.08 and 0.14, respectively. I will delay the interpretation of these magnitudes until the next subsection.

Figure 1.12 displays the histogram of β in good weeks only. Compared to the daily estimates in Figure 1.6, weekly estimates are much more concentrated

Figure 1.12: Histogram of estimates of β, good weeks

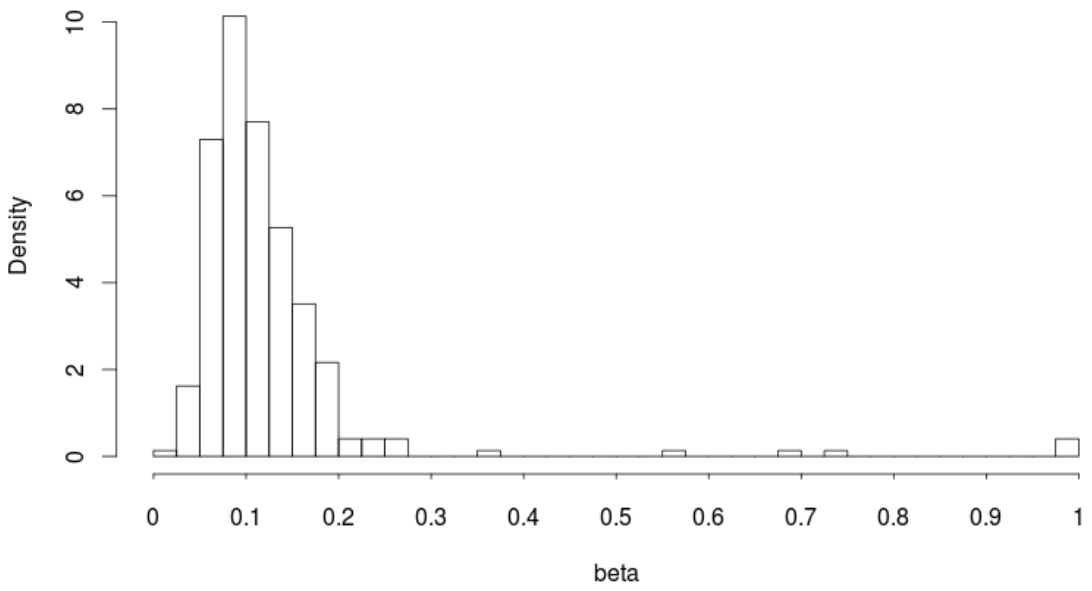

in a smaller range that is clearly above zero. The three highest bars lie in the range of $[0.050, 0.125]$, which contains the median and lower quantile β reported in Table 1.2. However, there are still a few outliers that are larger than 0.3. They are suspicious, as there is hardly any economic reason to have the speed of mean reversion significantly different from one week to another. Indeed, β in good weeks might even be seen as roughly constant.

1.2.6 Speed of mean reversion

In this subsection, I examine more closely my estimates of β as well as two alternative measures of the speed of mean reversion: the parameter κ and the "half-life".

Table 1.3: Measures of the speed of mean reversion, good weeks

	median	lower quantile	upper quantile
β for 100 seconds	10%	8%	14%
β for 5 minutes	27%	21%	36%
β for 10 minutes	47%	38%	60%
β for 30 minutes	85%	76%	93%
κ (rate per day)	25	19	34
half-life	11 minutes	14 minutes	8 minutes

1.2.6.1 Magnitudes of β

Recall from equation 1.16 that β can be interpreted as the average fraction of the gap between instantaneous volatility ζ_t and the asymptotic mean $\bar{\zeta}$ eliminated over the interval $[t, t+h]$. Thus, the median estimate of 0.10 in Table 1.2 suggests that on average about 10% of the gap between the level of the volatility process and its asymptotic mean is eliminated within a 100-second interval.

The magnitude of β depends on the particular length of the interval h. To better illustrate, I translate my estimates of β for 100-second intervals to rates for intervals with different lengths. Rewriting equation 1.13 as

$$\beta_h = 1 - e^{-\kappa h} \tag{1.30}$$

I obtain

$$\beta_{h'} = 1 - (1 - \beta_h)^{\frac{h'}{h}} \tag{1.31}$$

for any h, h'. In particular, setting $h = 1/234$ and h' at a different value will convert the β rate for 100-second intervals to rates for intervals with different lengths.

The top panel of Table 1.3 displays the magnitudes of β for intervals with

length h', computed by the method described above. The central message here is that mean reversion is fast. The median estimates in the first column suggest that the fraction of the gap between volatility and its asymptotic mean expected to evaporate rises from 10% in 100 seconds to 27% in 5 minutes, to 47% in 10 minutes, and 85% in 30 minutes. The lower quantile and upper quantile estimates are shown in the second and third column respectively. Even the lower quantile estimates suggest a very high speed of mean reversion.

These results generally agree with EHLWZ (2012) in the sense that both document a very high speed of mean reversion in a matter of minutes. However, my estimates are smaller than theirs. As shown in the second row of the top panel of Table 1.3, my median estimate of β for a five-minute interval is 27%, while the estimate in EHLWZ (2012) is about 60%. This can be explained by differences in estimation methodology: one key difference is that EHLWZ (2012) excludes an interval pair if the second interval has a large jump in volatility, so their β estimates are naturally biased upwards compared to my estimates, which exclude no intervals.

1.2.6.2 Magnitudes of κ

κ is a natural alternative measure of the speed of mean reversion. Recall that κ is a parameter in the continuous-time stochastic differential equation 1.8 while β is a parameter that I introduced to derive parallel discrete-time stochastic difference equations. κ is related to β in the following two ways. First, one can solve for κ in the equation 1.30:

$$\kappa = -\frac{\log(1-\beta_h)}{h} \tag{1.32}$$

for any h, and consequently, can compute an estimate of κ given an estimate of β. Second, κ, with the dimension of a rate per day (recall that a unit time is a day), measures the instantaneous rate of mean reversion: it is the infinitesimal fraction

of the gap between volatility and its asymptotic mean expected to evaporate in an infinitesimally short interval. Precisely, a simple application of calculus combined with equation 1.30 yields

$$\kappa = \lim_{h \to 0} \frac{1 - e^{-\kappa h}}{h} = \lim_{h \to 0} \frac{\beta_h}{h} \tag{1.33}$$

which clearly gives the interpretation above. Note that the magnitude of κ does not depend on the particular length of the interval h (while β does).

The middle panel of Table 1.3 displays the magnitudes of κ, computed by equation 1.32. The median estimate is 25. This suggests that, for example, within a short time interval as short as one thousandth of a trading day, or 23.4 seconds, the average fraction of gap between volatility and its asymptotic mean eliminated is $25 \times 1/1000 = 2.5\%$ — a very rapid mean reversion. The lower quantile and upper quantile estimates are shown in the second and third column respectively. Even the lower quantile estimate suggests a very high speed of mean reversion.

1.2.6.3 Half-life

The half-life is yet another measure of the speed of mean reversion. It is the amount of time required for the gap between volatility and its asymptotic mean to fall to half its initial value. According to equation 1.30 and the interpretation of β, the half-life H, measured in units of a trading day, satisfies

$$\frac{1}{2} = 1 - e^{-\kappa H} \tag{1.34}$$

from which I can solve

$$H = \frac{\log 2}{\kappa} \tag{1.35}$$

where κ has already been calculated by equation 1.32.

The bottom panel of Table 1.3 displays the magnitudes of the half-life H, com-

puted by equation 1.35. The median estimate is 11 minutes. This suggests that it takes 11 minutes on average for the gap between volatility and its asymptotic mean to fall to half its initial value, which is consistent with β for 10 minutes being 47%, as shown in the third row and first column of Table 1.3. The lower quantile and upper quantile estimates are shown in the second and third column respectively. Even the lower quantile estimate suggests a very high speed of mean reversion.

1.2.7 The asymptotic mean

My GMM estimation approach provides a direct estimate of the asymptotic mean parameter $\bar{\zeta}$, and it is jointly estimated together with β. In this section, I compare my estimates of $\bar{\zeta}$ with alternative local measures of volatility.

1.2.7.1 Comparison to the median and mean realized variation

EHLWZ (2012) used the daily median of the realized variation over blocks as an estimate of the daily asymptotic mean $\bar{\zeta}$. They argued that the median is preferred to the mean, because the median is a robust measure of central tendency given the asymmetry of distribution of realized variation over blocks.

Figure 1.13 compares for good weeks only my weekly estimate of $\bar{\zeta}$ with the median and the mean of the realized variation for all blocks in the same week, together with the 45 degree lines. My GMM estimates are very close to both the median and the mean for a great majority of weeks. My estimates are occasionally significantly larger than the median and are rarely smaller, according to the top plot, while my estimates are sometimes significantly smaller than the mean and are rarely larger, according to the bottom plot.

Figure 1.13: Estimates of $\bar{\zeta}$ versus the median and mean of $\varphi_{t,t+h}$, good weeks

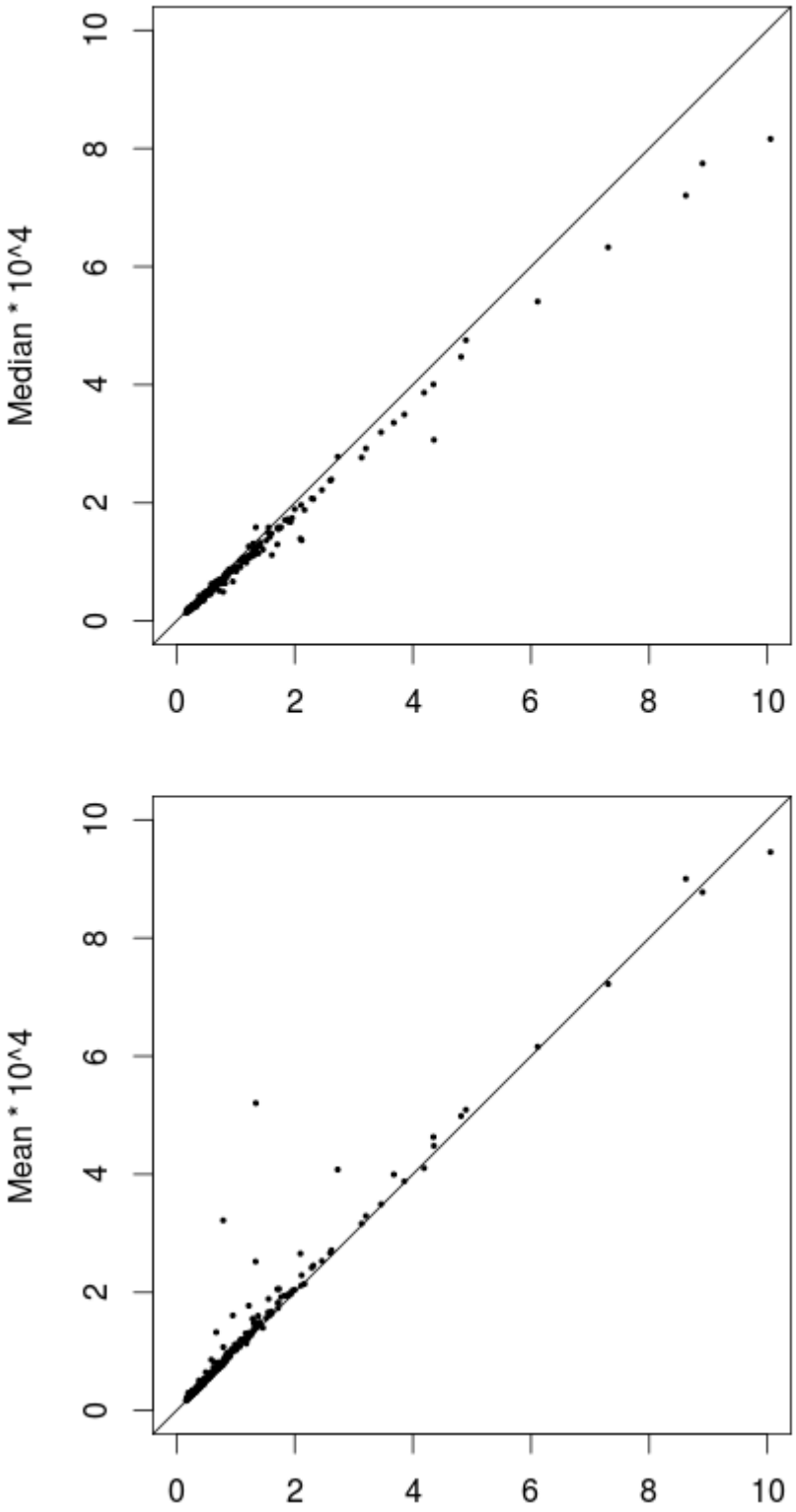

1.2.7.2 Comparison to the VIX

I also compare my asymptotic mean parameter $\bar{\zeta}$ with another local measure of volatility, the VIX. The VIX is the Chicago Board Options Exchange (CBOE) Volatility Index. It was created by Whaley (1993) and is the implied volatility of the S&P 500 index options. (See Whaley (2009)) To construct a weekly time series for the VIX, I use the average value of each daily close. Because the VIX is an annualized standard deviation while $\bar{\zeta}$ has the dimension of variance per day, I re-scale my estimates appropriately. Specifically, assuming 250 trading days in a year, I calculate adjusted $\bar{\zeta}$ as

$$100\sqrt{250\bar{\zeta}}.$$

Note that, because the VIX is expressed as a percent, I need to multiply by 100.

Figure 1.14 compares my weekly estimates of $\bar{\zeta}$ for SPY and the weekly averaged VIX for good weeks. The values are reasonably close to each other, despite the fact that the VIX is a forward-looking indicator measuring volatility that the investors expect to see in the near future while $\bar{\zeta}$ is backward looking. The resemblance of the two plots is not surprising: $\bar{\zeta}$ is not very far backward looking: it measures the settled value of volatility for a week once the week has ended, which we associate with the asymptotic mean of the volatility process. Both are meaningful local measures of volatility.

Figure 1.14: Adjusted $\bar{\zeta}$ versus weekly average VIX, good weeks

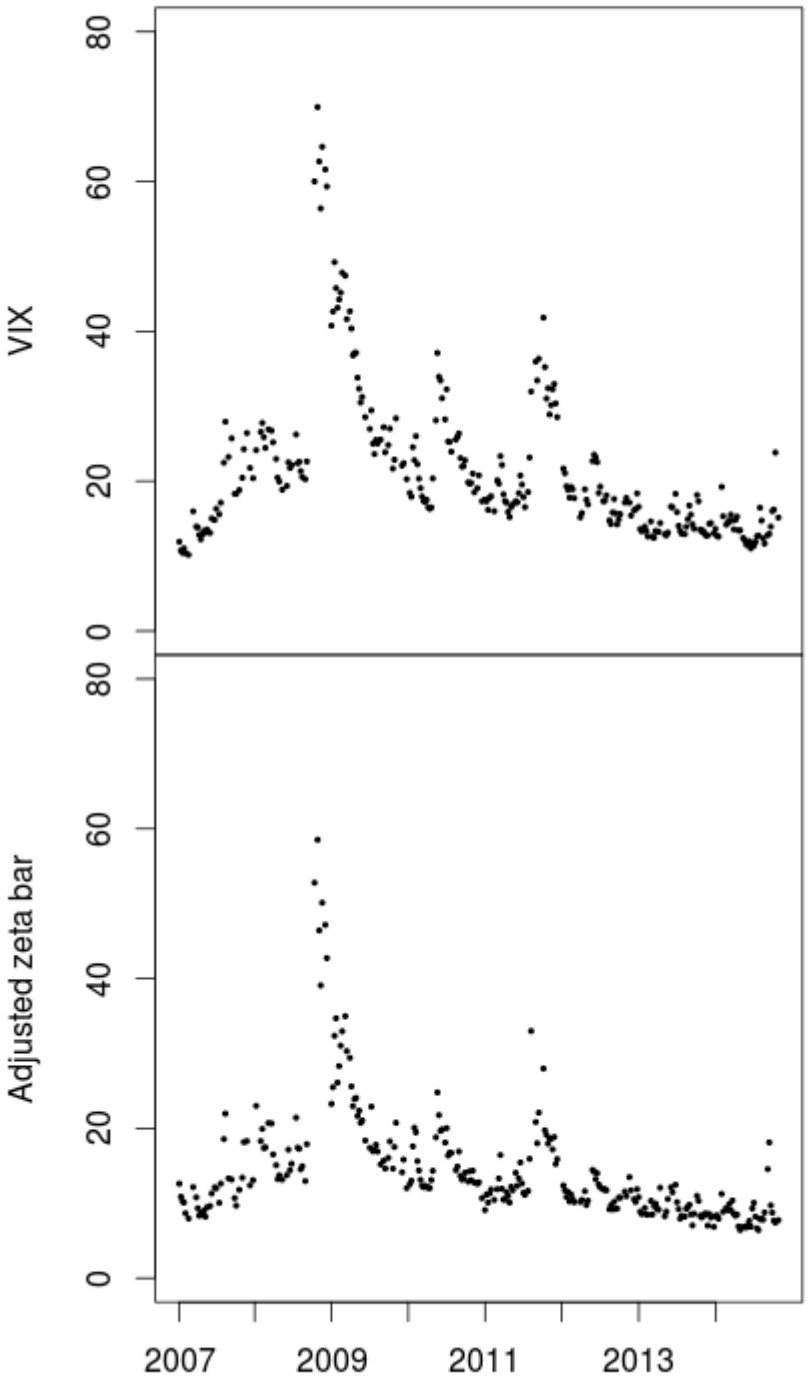

CHAPTER 2

Stock-Price Volatility: II

In Chapter 1 I reformulated the Heston model of stochastic volatility for stock-price processes to develop a model of the evolution of the scaled increments $\zeta_{t,t+h}$ of quadratic variation. I used this model to estimate two of the parameters of the Heston model, the speed of mean reversion κ (or equivalently, β) and the asymptotic mean $\bar{\zeta}$, using the generalized method of moments (GMM). In this chapter I focus on the parameter γ, called the *volatility of volatility*.

In the Heston model, the process $\zeta = (\zeta_t)_{t\geq 0}$ is a stationary ergodic Markov process. Although the stochastic differential equation that characterizes the volatility process ζ has no closed form solution, it is possible to solve for the distribution of ζ_t for each t and, in particular, to derive its expectation and variance. As Shreve (2004) shows, [1]

$$\mathbb{E}\left[\zeta_t\right] = \bar{\zeta} + e^{-\kappa t}(\zeta_0 - \bar{\zeta}) \tag{2.1}$$

and

$$\mathrm{Var}(\zeta_t) = \frac{\gamma^2}{\kappa}(e^{-\kappa t} - e^{-2\kappa t})\ \zeta_0 + \frac{\gamma^2}{2\kappa}(1 - 2e^{-\kappa t} + e^{-2\kappa t})\ \bar{\zeta} \tag{2.2}$$

As $t \to \infty$, the mean and the variance approach limits that are independent of the initial value ζ_0 of the process:

$$\lim_{t\to\infty} \mathbb{E}\left[\zeta_t\right] = \bar{\zeta} \tag{2.3}$$

[1] Shreve (2004) derives these equations for the Cox, Ingersoll, Ross (CIR) model of interest rates. As noted in Chapter 1, the CIR model and the Heston model are identical in form. Because the context is different, the notation here is different from that of Shreve. Equations 2.1 and 2.2 correspond to equations (4.4.36) and (4.4.48) respectively in Shreve (2004).

and

$$\lim_{t\to\infty} \mathrm{Var}(\zeta_t) = \frac{\gamma^2 \bar{\zeta}}{2\kappa} \tag{2.4}$$

In Chapter 1 I exploited the implications of equation 2.3, demonstrating that the volatility process for SPY reverts very quickly to its asymptotic mean $\bar{\zeta}$.

In this chapter I turn my attention to the second moment of $\zeta_{t,t+h}$. In Section 2.1 I derive an equation for the conditional variance $\mathrm{Var}(\zeta_{t,t+h} \mid \mathcal{F}_t)$ that is a linear combination of ζ_t and $\bar{\zeta}$ with weights that are independent of t. I use this conditional variance to derive an expression for $\lim_{t\to\infty} \mathrm{Var}(\zeta_{t,t+h})$, the asymptotic variance of the process as $t \to \infty$. Because I find mean reversion is very fast, in my empirical work I assume that this limiting approximation is a good approximation for most of the trading day. I also derive asymptotic limits for the autocovariance

$$\mathbb{E}[(\zeta_{t,t+h} - \bar{\zeta})(\zeta_{t+jh,t+(j+1)h} - \bar{\zeta})]$$

and the autocorrelation for all lags $j \geq 1$.

In Section 2.2 I derive an explicit expression for the error term

$$\eta_{t,t+2h} := \zeta_{t+h,t+2h} - \alpha\, \zeta_{t,t+h} - \beta\, \bar{\zeta}$$

for the GMM moment condition that featured prominently in Chapter 1 as the sum of an Itô integral over the block $[t, t+h]$ and an Itô integral over the block $[t+h, t+2h]$. I then proceed to derive an equation for the conditional variance $\mathrm{Var}(\eta_{t,t+2h} \mid \mathcal{F}_t)$ that is a linear combination of ζ_t and $\bar{\zeta}$ with weights independent of t. I use the conditional variance to derive a formula for the asymptotic variance $\lim_{t\to\infty} \mathrm{Var}(\eta_{t,t+2h})$ and for the asymptotic autocovariances and autocorrelations of $\eta_{t,t+2h}$ for all lags $j \geq 1$.

Section 2.3 explicitly addresses the errors in variables introduced by using the observable realized variation $\varphi_{t,t+h}$ in place of the unobservable quadratic variation

$\zeta_{t,t+h}$. I show that among the results in Sections 2.1 and 2.2 only those on the autocovariances of $\zeta_{t,t+h}$ for lags $j \geq 1$ and on the autocovariances of $\eta_{t,t+2h}$ for lags $j \geq 2$ are robust to measurement error.

Section 2.4 proposes a GMM estimator of the volatility-of-volatility parameter γ based on the autocovariances of $\zeta_{t,t+h}$ for lags $j \geq 1$.

Section 2.5 explores the empirical properties of the variance, autocovariances and autocorrelations of the $\zeta_{t,t+h}$ process. I find that the results in Section 2.1 are able to explain the relative sizes of the sample autocovariances and autocorrelations of $\zeta_{t,t+h}$ for all lags $j \geq 1$, but fail to account for the relatively large sizes of the sample variance. These pattern are consistent with the analysis of the measurement error problem in Section 2.3.

Section 2.6 explores the empirical properties of the variance, autocovariances and autocorrelations of the error process $\eta_{t,t+2h}$. I find that the results in Section 2.2 are able to explain the relative sizes of the sample autocovariances and autocorrelations of $\eta_{t,t+2h}$ for all lags $j \geq 2$, but they fail to account for the relatively large sizes of the sample variance, and greatly over-predict the autocorrelation (or autocovariance) of $\eta_{t,t+2h}$ for lag 1. These patterns are also consistent with the analysis of the measurement error problem in Section 2.3.

Section 2.7 reports the estimation results of γ for the collection of "good weeks" as characterized in Chapter 1. For 91% of the good weeks, the estimates of γ^2 are significant and satisfy the Feller condition, and the model passes the GMM specification test. I interpret these results as strong evidence of stochastic volatility at high frequency. I conclude that the Heston model is a good model of high-frequency stock-price volatility most of the time.

2.1 The Second Moments of Quadratic Variation $\zeta_{t,t+h}$

This section examines the structural implications of the Heston model on the second moments of $\zeta_{t,t+h}$, the (scaled) quadratic variation over a block.

2.1.1 Conditional variance of $\zeta_{t,t+h}$

I start with the following lemma, which decomposes $\zeta_{t,t+h}$, the quadratic variation over the block $[t, t+h]$, into the sum of its expectation conditional on the information at the beginning of that block and an innovation, an Itô integral over that block.

Lemma 2.1. *In the Heston model,*

$$\zeta_{t,t+h} = \mathbb{E}\left[\zeta_{t,t+h}|\mathcal{F}_t\right] + \int_t^{t+h} \left(\frac{1 - e^{-\kappa(t+h-s)}}{\kappa h}\right) \gamma\sqrt{\zeta_s} dB_s \tag{2.5}$$

Proof. Lemma 1.3 asserts that

$$\mathbb{E}\left[\zeta_{t,t+h} \mid \mathcal{F}_t\right] = a_1\zeta_t + b_1\bar{\zeta}$$

with

$$a_1 = \frac{1 - e^{-\kappa h}}{\kappa h} \qquad b_1 = \frac{kh - e^{-\kappa h}}{\kappa h}$$

Letting $t + h = T$ and $h = T - t$, I have

$$\mathbb{E}\left[\zeta_{t,T} \mid \mathcal{F}_t\right] = a_1\zeta_t + b_1\bar{\zeta}$$

with

$$a_1 = \frac{1 - e^{-\kappa(T-t)}}{\kappa(T-t)} \qquad b_1 = \frac{k(T-t) - e^{-\kappa(T-t)}}{\kappa(T-t)}$$

or equivalently,

$$\kappa\,(T-t)\,\mathbb{E}\left[\zeta_{t,T}|\mathcal{F}_t\right] = \left(1-e^{-\kappa(T-t)}\right)\zeta_t + \left(\kappa(T-t) - \left(1-e^{-\kappa(T-t)}\right)\right)\bar{\zeta}$$

Fix T and let t vary. Define

$$f(t,z) = \left(1-e^{-\kappa(T-t)}\right)z - \left(\kappa(T-t) - \left(1-e^{-\kappa(T-t)}\right)\right)\bar{\zeta}$$

The partial derivatives of f are

$$f_t = -\kappa e^{-\kappa(T-t)}z + \kappa(1-e^{-\kappa(T-t)})\bar{\zeta} \qquad f_z = 1-e^{-\kappa(T-t)} \qquad f_{zz} = 0$$

Applying the Itô-Doeblin formula,

$$\begin{aligned} d\left(\kappa\,(T-t)\,\mathbb{E}\left[\zeta_{t,T}|\mathcal{F}_t\right]\right) &= df(t,\zeta_t) \\ &= \left[-\kappa e^{-\kappa(T-t)}\zeta_t - \kappa(1-e^{-\kappa(T-t)})\bar{\zeta}\right]dt \\ &\quad + (1-e^{\kappa(T-t)})[\kappa(\bar{\zeta}-\zeta_t)\,dt + \gamma\sqrt{\zeta_t}\,dB_t] \end{aligned}$$

Simplifying gives the stochastic differential equation

$$d\left(\kappa(T-t)\mathbb{E}\left[\zeta_{t,T}\mid\mathcal{F}_t\right]\right) = -\kappa\zeta_t dt + \left(1-e^{-\kappa(T-t)}\right)\gamma\sqrt{\zeta_t}\,dB_t$$

Integrating from t to T yields

$$0 - \kappa\,(T-t)\,\mathbb{E}\left[\zeta_{t,T}|\mathcal{F}_t\right] = -\kappa\int_t^T \zeta_s ds + \int_t^T \left(1-e^{-\kappa(T-s)}\right)\gamma\sqrt{\zeta_s}\,dB_s$$

Dividing both sides by $\kappa(T-t)$, writing T once again as $t+h$ and using the definition of $\zeta_{t,t+h}$, we reach the desired conclusion:

$$\zeta_{t,t+h} = \mathbb{E}\left[\zeta_{t,t+h}|\mathcal{F}_t\right] + \int_t^{t+h}\left(\frac{1-e^{-\kappa(t+h-s)}}{\kappa h}\right)\gamma\sqrt{\zeta_s}\,dB_s$$

□

The next lemma expresses the conditional variance of $\zeta_{t,t+h}$ as a linear function of the instantaneous volatility at the beginning of the block and the asymptotic mean of the instantaneous volatility.

Lemma 2.2. *In the Heston model,*

$$Var\left(\zeta_{t,t+h} \mid \mathcal{F}_t\right) = \left(\frac{\gamma}{\kappa h}\right)^2 \left(c_1\ \zeta_t + d_1\ \bar{\zeta}\right) \tag{2.6}$$

where

$$c_1 = \frac{1}{\kappa} - 2he^{-\kappa h} - \frac{1}{\kappa}e^{-2\kappa h}$$
$$d_1 = h - \frac{5}{2\kappa} + \left(\frac{2}{\kappa} + 2h\right)e^{-\kappa h} + \frac{1}{2\kappa}e^{-2\kappa h}$$

Proof. Rewrite equation 2.5 in Lemma 2.1 as

$$\zeta_{t,t+h} - \mathbb{E}\left[\zeta_{t,t+h}|\mathcal{F}_t\right] = \int_t^{t+h} \left(\frac{1 - e^{-\kappa(t+h-s)}}{\kappa h}\right) \gamma\sqrt{\zeta_s} dB_s \tag{2.7}$$

Squaring both sides of equation 2.7, taking the conditional expectation of each

side with respect to $\mathcal{F}_t$ and appealing to Itô's isometry,

$$\begin{aligned}
\text{Var}\left(\zeta_{t,t+h} \mid \mathcal{F}_t\right) &:= \mathbb{E}\left[\left(\zeta_{t,t+h} - \mathbb{E}[\zeta_{t,t+h} \mid \mathcal{F}_t]\right)^2 \mid \mathcal{F}_t\right] \\
&= \mathbb{E}\left[\left(\int_t^{t+h} \left(\frac{1-e^{-\kappa(t+h-s)}}{kh}\right) \gamma\sqrt{\zeta_s}\, dB_s\right)^2 \mid \mathcal{F}_t\right] \\
&= \mathbb{E}\left[\int_t^{t+h} \left[\left(\frac{1-e^{-\kappa(t+h-s)}}{kh}\right) \gamma\sqrt{\zeta_s}\right]^2 ds \mid \mathcal{F}_t\right] \\
&= \left(\frac{\gamma}{\kappa h}\right)^2 \mathbb{E}\left[\int_t^{t+h} \left(1-e^{-\kappa(t+h-s)}\right)^2 \zeta_s\, ds \mid \mathcal{F}_t\right] \\
&= \left(\frac{\gamma}{\kappa h}\right)^2 \int_t^{t+h} \left(1-e^{-\kappa(t+h-s)}\right)^2 \mathbb{E}[\zeta_s \mid \mathcal{F}_t]\, ds \qquad (2.8)
\end{aligned}$$

Recall that Lemma 1.2 establishes that for $s \geq t$,

$$\mathbb{E}[\zeta_s \mid \mathcal{F}_t] = e^{-\kappa(s-t)}\zeta_t + (1-e^{-\kappa(s-t)})\bar{\zeta} \qquad (2.9)$$

Using equation 2.9 to substitute for the conditional expectation in equation 2.8,

$$\begin{aligned}
\text{Var}\left(\zeta_{t,t+h} \mid \mathcal{F}_t\right) &= \left(\frac{\gamma}{\kappa h}\right)^2 \int_t^{t+h} \left(1-e^{-\kappa(t+h-s)}\right)^2 \left(e^{-\kappa(s-t)}\zeta_t + (1-e^{-\kappa(s-t)})\bar{\zeta}\right) ds \\
&= \left(\frac{\gamma}{\kappa h}\right)^2 \left(c_1\, \zeta_t + d_1\, \bar{\zeta}\right)
\end{aligned}$$

where

$$\begin{aligned}
c_1 &= \int_t^{t+h} (1-e^{-\kappa(t+h-s)})^2 e^{-\kappa(s-t)}\, ds \\
&= \int_t^{t+h} (1-2e^{-\kappa(t+h-s)} + e^{-2\kappa(t+h-s)}) e^{-\kappa(s-t)}\, ds \\
&= \int_t^{t+h} (e^{-\kappa(s-t)} - 2e^{-\kappa h} + e^{-\kappa(t+2h-s)})\, ds \\
&= \frac{1}{\kappa} - 2he^{-\kappa h} - \frac{1}{\kappa}e^{-2\kappa h}
\end{aligned}$$

$$c_1 + d_1 = \int_t^{t+h} (1 - e^{-\kappa(t+h-s)})^2 \, ds = \int_t^{t+h} (1 - 2e^{-\kappa(t+h-s)} + e^{-2\kappa(t+h-s)}) \, ds$$
$$= h - \frac{3}{2\kappa} + \frac{2}{k} e^{-\kappa h} - \frac{1}{2\kappa} e^{-2\kappa h}$$

and

$$d_1 = (c_1 + d_1) - c_1 = h - \frac{3}{2\kappa} + \frac{2}{k} e^{-\kappa h} - \frac{1}{2\kappa} e^{-2\kappa h} - \left[\frac{1}{\kappa} - 2he^{-\kappa h} - \frac{1}{\kappa} e^{-2\kappa h} \right]$$
$$= h - \frac{5}{2h} + \left(\frac{2}{\kappa} + 2h \right) e^{-\kappa h} + \frac{1}{2\kappa} e^{-2\kappa h}$$

□

Note that the coefficients c_1 and d_1 do not depend on t or $t + h$, but just on h and the parameters κ and γ of the Heston model.

2.1.2 Asymptotic variance of $\zeta_{t,t+h}$

I now use this conditional variance to derive an expression for $\lim_{t\to\infty} \mathrm{Var}(\zeta_{t,t+h})$, the asymptotic variance of quadratic variation over a block as $t \to \infty$.

Proposition 2.1. *In the Heston model,*

$$\lim_{t\to\infty} Var(\zeta_{t,t+h}) = \left(\frac{\gamma}{\kappa h} \right)^2 \left(h - \frac{1}{\kappa} + \frac{1}{\kappa} e^{-\kappa h} \right) \bar{\zeta} \tag{2.10}$$

Proof. It is important to realize that the expectation of the conditional variance is usually not the unconditional variance of $\zeta_{t,t+h}$. By the law of total variance

$$\mathrm{Var}(\zeta_{t,t+h}) = \mathrm{Var}(\mathbb{E}(\zeta_{t,t+h} \mid \mathcal{F}_t]) + \mathbb{E}[\mathrm{Var}(\zeta_{t,t+h} \mid \mathcal{F}_t)]$$

According to Lemma 1.3,

$$\mathbb{E}[\zeta_{t,t+h} \mid \mathcal{F}_t] = a_1 \zeta_t + (1 - a_1)\bar{\zeta}$$

Consequently,

$$\mathrm{Var}(\mathbb{E}[\zeta_{t,t+h} \mid \mathcal{F}_t]) = \mathrm{Var}(a_1\zeta_t + (1-a_1)\bar{\zeta}) = a_1^2\,\mathrm{Var}(\zeta_t)$$

Taking limits of both sides and using equation 2.4.gives

$$\begin{aligned}\lim_{t\to\infty}\mathrm{Var}(\mathbb{E}[\zeta_{t,t+h} \mid \mathcal{F}_t]) &= a_1^2 \lim_{t\to\infty}\mathrm{Var}(\zeta_t)\\ &= a_1^2\left(\frac{\gamma^2\bar{\zeta}}{2\kappa}\right)\\ &= \left(\frac{\gamma}{\kappa h}\right)^2\frac{(1-e^{-\kappa h})^2}{2\kappa}\bar{\zeta}\end{aligned} \tag{2.11}$$

From Lemma 2.2,

$$\mathrm{Var}(\zeta_{t,t+h} \mid \mathcal{F}_t) = \left(\frac{\gamma}{\kappa h}\right)^2(c_1\,\zeta_t + d_1\,\bar{\zeta})$$

and so

$$\mathbb{E}[\mathrm{Var}(\zeta_{t,t+h} \mid \mathcal{F}_t)] = \left(\frac{\gamma}{\kappa h}\right)^2(c_1\,\mathbb{E}\zeta_t + d_1\,\bar{\zeta})$$

Therefore,

$$\begin{aligned}\lim_{t\to\infty}\mathbb{E}[\mathrm{Var}(\zeta_{t,t+h} \mid \mathcal{F}_t)] &= \left(\frac{\gamma}{\kappa h}\right)^2(c_1\ \lim_{t\to\infty}\mathbb{E}\zeta_t + d_1\bar{\zeta})\\ &= \left(\frac{\gamma}{\kappa h}\right)^2(c_1+d_1)\bar{\zeta}\end{aligned} \tag{2.12}$$

Combining equation 2.11 and equation 2.12, the asymptotic variance is

$$\begin{aligned}\lim_{t\to\infty}\mathrm{Var}(\zeta_{t,t+h}) &= \left(\frac{\gamma}{\kappa h}\right)^2\frac{(1-e^{-\kappa h})^2}{2\kappa}\bar{\zeta} + \left(\frac{\gamma}{\kappa h}\right)^2(c_1+d_1)\bar{\zeta}\\ &= \left(\frac{\gamma}{\kappa h}\right)^2\left(\left(\frac{1}{2\kappa}-\frac{1}{\kappa}e^{-\kappa h}+\frac{1}{2\kappa}e^{-2\kappa h}\right)\right.\\ &\qquad\left.+\left(h-\frac{3}{2\kappa}+\frac{2}{\kappa}e^{-\kappa h}-\frac{1}{2\kappa}e^{-2\kappa h}\right)\right)\bar{\zeta}\\ &= \left(\frac{\gamma}{\kappa h}\right)^2\left(h-\frac{1}{\kappa}+\frac{1}{\kappa}e^{-\kappa h}\right)\bar{\zeta}\end{aligned}$$

□

The limiting procedures in equations 2.11 and 2.12 have a natural interpretation: if t is "large enough", the mean and variance approach their limits because the effects of the initial condition ζ_0 have essentially worn off.

It is instructive to compare the size of the asymptotic variance of $\zeta_{t,t+h}$ to that of the asymptotic variance of ζ_t. To do so, I rewrite equation 2.10 in Proposition 2.1 to express the former as a fraction of the latter:

$$\begin{aligned}\lim_{t\to\infty} \mathrm{Var}(\zeta_{t,t+h}) &= \frac{2}{\kappa h^2}\left(h - \frac{1}{\kappa} + \frac{1}{\kappa}e^{-\kappa h}\right)\frac{\gamma^2\bar{\zeta}}{2\kappa} \\ &= \left(\frac{2}{\kappa h} - \frac{2}{(\kappa h)^2} + \frac{2}{(\kappa h)^2}e^{-\kappa h}\right)\lim_{t\to\infty}\mathrm{Var}(\zeta_t) \qquad (2.13)\end{aligned}$$

To give some practical perspective, recall that $h = 1/234$ throughout my empirical analysis and κ has a median value of 25 according to Table 1.3. With these values,

$$\lim_{t\to\infty} \mathrm{Var}(\zeta_{t,t+h}) \approx 0.96 \lim_{t\to\infty} \mathrm{Var}(\zeta_t)$$

This is not surprising, since a simple application of calculus gives that the fraction approaches unity as the product κh goes to zero:

$$\lim_{\kappa h\to 0}\left(\frac{2}{\kappa h} - \frac{2}{(\kappa h)^2} + \frac{2}{(\kappa h)^2}e^{-\kappa h}\right) = 1$$

This analysis shows that the asymptotic variance of $\zeta_{t,t+h}$ accounts for a large proportion of the variance of ζ_t in the model.

2.1.3 Asymptotic autocovariances and autocorrelations of $\zeta_{t,t+h}$

Since the process $(\zeta_t)_{t\geq 0}$ of the instantaneous volatility in the Heston model is stationary, so is the process $(\zeta_{t,t+h})_{t\geq 0}$ of the quadratic variation over a block. Consequently, it makes sense to talk about asymptotic autocovariances and au-

tocorrelations of $\zeta_{t,t+h}$. Let V_j denote the asymptotic autocovariance of $\zeta_{t,t+h}$ for lag $j \geq 0$:

$$V_j := \lim_{t\to\infty} \mathbb{E}\left[\left(\zeta_{t,t+h} - \bar{\zeta}\right)\left(\zeta_{t+jh,t+(j+1)h} - \bar{\zeta}\right)\right] \tag{2.14}$$

In particular, V_0 is the asymptotic variance, which I have already computed in Proposition 2.1. I now derive expressions for the asymptotic autocovariances for all lags $j \geq 1$.

Proposition 2.2. *In the Heston model,*

$$V_0 = \left(\frac{\gamma}{\kappa h}\right)^2 \left(h - \frac{\beta}{\kappa}\right) \bar{\zeta} \tag{2.15}$$

$$V_1 = \left(\frac{\gamma}{\kappa h}\right)^2 \frac{\beta^2}{2\kappa}\, \bar{\zeta} \tag{2.16}$$

$$V_j = \alpha\, V_{j-1}, \qquad j \geq 2 \tag{2.17}$$

Proof. I have already established equation 2.15 in Proposition 2.1.

To derive an expression for V_1, consider

$$\begin{aligned}
&\lim_{t\to\infty} \mathbb{E}\left[\left(\zeta_{t+h,t+2h} - \alpha\zeta_{t,t+h} - \beta\bar{\zeta}\right)^2\right] \\
&= \lim_{t\to\infty} \mathbb{E}\left[\left(\left(\zeta_{t+h,t+2h} - \bar{\zeta}\right) - \alpha\left(\zeta_{t,t+h} - \bar{\zeta}\right)\right)^2\right] \\
&= \left(1 + \alpha^2\right) V_0 - 2\alpha V_1
\end{aligned}$$

and so

$$V_1 = \frac{1}{2\alpha}\left(\left(1 + \alpha^2\right) V_0 - \lim_{t\to\infty} \mathbb{E}\left[\left(\zeta_{t+h,t+2h} - \alpha\zeta_{t,t+h} - \beta\bar{\zeta}\right)^2\right]\right) \tag{2.18}$$

As I will prove in Proposition 2.4 (whose proof does not rely upon this proposition),

$$\lim_{t\to\infty} \mathbb{E}\left[\left(\zeta_{t+h,t+2h} - \alpha\zeta_{t,t+h} - \beta\bar{\zeta}\right)^2\right] = \left(\frac{\gamma}{\kappa h}\right)^2 (c_2 + d_2)\, \bar{\zeta} \tag{2.19}$$

where

$$c_2 + d_2 = h - \frac{1}{\kappa} + \left(h + \frac{1}{\kappa}\right) e^{-2\kappa h} \tag{2.20}$$

Plugging equation 2.15 and equation 2.19 into equation 2.18 yields

$$\begin{aligned}
V_1 &= \frac{1}{2\alpha}\left(\left(1+\alpha^2\right)\left(\frac{\gamma}{\kappa h}\right)^2\left(h - \frac{1}{\kappa} + \frac{1}{\kappa}e^{-\kappa h}\right)\bar{\zeta} - \left(\frac{\gamma}{\kappa h}\right)^2 (c_2 + d_2)\,\bar{\zeta}\right) \\
&= \frac{1}{2e^{-\kappa h}}\left(\left(1+e^{-2\kappa h}\right)\left(\frac{\gamma}{\kappa h}\right)^2\left(h - \frac{1}{\kappa} + \frac{1}{\kappa}e^{-\kappa h}\right)\bar{\zeta}\right. \\
&\qquad \left. - \left(\frac{\gamma}{\kappa h}\right)^2\left(h - \frac{1}{\kappa} + \left(h + \frac{1}{\kappa}\right)e^{-2\kappa h}\right)\bar{\zeta}\right) \\
&= \left(\frac{\gamma}{\kappa h}\right)^2\left(\frac{1}{2\kappa} - \frac{1}{\kappa}e^{-\kappa h} + \frac{1}{2\kappa}e^{-2\kappa h}\right)\bar{\zeta} \\
&= \left(\frac{\gamma}{\kappa h}\right)^2 \frac{\beta^2}{2\kappa}\,\bar{\zeta}
\end{aligned} \tag{2.21}$$

To compute the autocovariances for lags $j \geq 2$, recall that Proposition 1.1 establishes that

$$\mathbb{E}\left[\zeta_{t+h,t+2h} - \alpha\zeta_{t,t+h} - \beta\bar{\zeta} \mid \mathcal{F}_t\right] = 0$$

Since $\zeta_{t-(j-1)h,t-(j-2)h} - \bar{\zeta}$ is measurable with respect to $\mathcal{F}_t$ when $j \geq 2$, it follows that

$$\mathbb{E}\left[\left(\zeta_{t+h,t+2h} - \alpha\zeta_{t,t+h} - \beta\bar{\zeta}\right)\left(\zeta_{t-(j-1)h,t-(j-2)h} - \bar{\zeta}\right)\right] = 0$$

or

$$\mathbb{E}\left[\left(\left(\zeta_{t+h,t+2h} - \bar{\zeta}\right) - \alpha\left(\zeta_{t,t+h} - \bar{\zeta}\right)\right)\left(\zeta_{t-(j-1)h,t-(j-2)h} - \bar{\zeta}\right)\right] = 0$$

or

$$V_j - \alpha V_{j-1} = 0, \qquad j \geq 2$$

as claimed. □

Note that the autocovariances of $\zeta_{t,t+h}$ for all lags depend on γ^2. Consequently, their expressions in equations 2.15 to 2.17 will potentially play an important role in estimation of γ.

I now consider the autocorrelations of $\zeta_{t,t+h}$. Let R_j denote the asymptotic autocorrelation of $\zeta_{t,t+h}$ for lag j:

$$R_j := \frac{V_j}{V_0} \tag{2.22}$$

It is easy to derive expressions for the autocorrelations of $\zeta_{t,t+h}$ based on the results in Proposition 2.2.

Corollary 2.1. *In the Heston model,*

$$R_0 = 1 \tag{2.23}$$

$$R_1 = \frac{\beta^2}{2\left(-\log\left(1-\beta\right)-\beta\right)} \tag{2.24}$$

$$R_j = \alpha\, R_{j-1}, \qquad j \geq 2 \tag{2.25}$$

Proof. Equation 2.23 is trivial.

Equation 2.25 directly follows from the definition of R_j in equation 2.22 and equation 2.17 in Proposition 2.2.

To establish equation 2.24, use the definition in equation 2.22 and equations 2.15 and 2.16 in Proposition 2.2:

$$\begin{aligned} R_1 := \frac{V_1}{V_0} &= \frac{\frac{\beta^2}{2\kappa}}{h-\frac{\beta}{\kappa}} \\ &= \frac{\beta^2}{2\left(-\log\left(1-\beta\right)-\beta\right)} \end{aligned}$$

where in the last step I use the relationship $\beta = 1 - e^{-\kappa h}$. □

Note that the asymptotic autocorrelations of $\zeta_{t,t+h}$ for all lags depend only on the mean-reversion parameter β. In particular, equation 2.24 expresses R_1, the autocorrelation of $\zeta_{t,t+h}$ for lag 1 as a function of β. Figure 2.1 displays the graph of this function. It suggests that R_1 is approximately affine in β for a wide range

Figure 2.1: R_1 as a function of β in equation 2.24

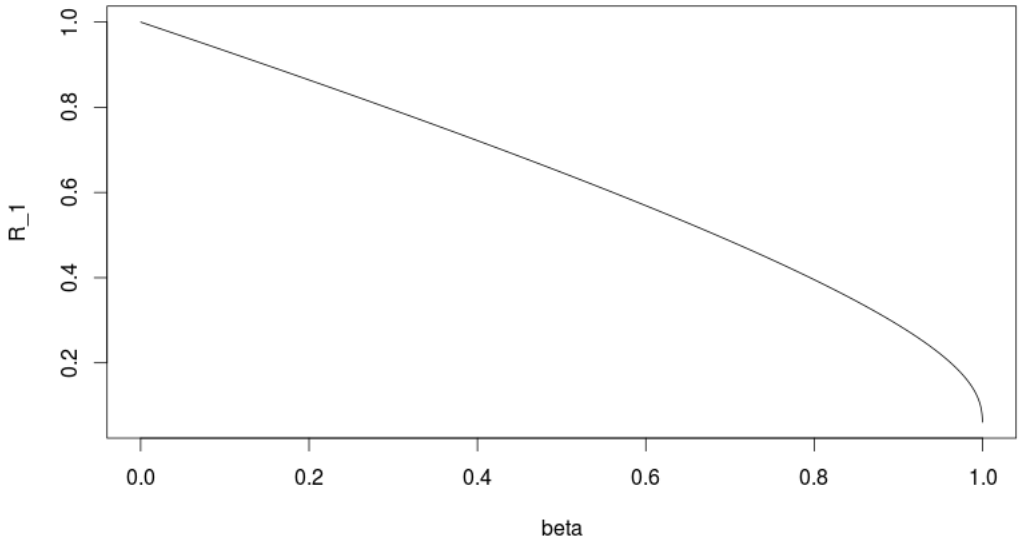

of values of β. This is not surprising, since a Taylor expansion around 0 gives that

$$\frac{\beta^2}{2\left(-\log\left(1-\beta\right)-\beta\right)} = 1 - \frac{2}{3}\,\beta + O(\beta^2)$$

For example, the median value of $\beta = 0.10$ yields $R_1 = 0.93$.

2.2 The Second Moments of the GMM Error $\eta_{t,t+2h}$

I now derive properties of the second moments of the GMM error term $\eta_{t,t+2h}$.

2.2.1 The GMM error $\eta_{t,t+2h}$

I begin by deriving an explicit expression for the GMM error $\eta_{t,t+2h}$ as an Itô integral.

Proposition 2.3. *In the Heston model,*

$$\eta_{t,t+2h} := \zeta_{t+h,t+2h} - \alpha\, \zeta_{t,t+h} - \beta\, \bar{\zeta} \tag{2.26}$$

$$= \int_{t+h}^{t+2h} \left(\frac{1 - e^{-\kappa(t+2h-s)}}{\kappa h} \right) \gamma \sqrt{\zeta_s} dB_s + \int_{t}^{t+h} \left(\frac{e^{-\kappa(t+h-s)} - e^{-\kappa h}}{\kappa h} \right) \gamma \sqrt{\zeta_s} dB_s \tag{2.27}$$

Proof. According to equation 2.6, the GMM error term can be decomposed as

$$\begin{aligned}
\eta_{t,t+2h} &:= \zeta_{t+h,t+2h} - \alpha\, \zeta_{t,t+h} - \beta\, \bar{\zeta} \\
&= \mathbb{E}[\zeta_{t+h,t+2h} \mid \mathcal{F}_{t+h}] + \int_{t+h}^{t+2h} \left(\frac{1 - e^{-\kappa(t+2h-s)}}{\kappa h} \right) \gamma \sqrt{\zeta_s} dB_s \\
&\quad - \alpha \left(\mathbb{E}\left[\zeta_{t,t+h} \mid \mathcal{F}_t\right] + \int_{t}^{t+h} \left(\frac{1 - e^{-\kappa(t+h-s)}}{\kappa h} \right) \gamma \sqrt{\zeta_s} dB_s \right) - \beta\, \bar{\zeta}
\end{aligned}$$

and so

$$\begin{aligned}
\eta_{t,t+2h} = \mathbb{E}[\zeta_{t+h,t+2h} \mid \mathcal{F}_{t+h}] &- \alpha \mathbb{E}\left[\zeta_{t,t+h} \mid \mathcal{F}_t\right] - \beta\, \bar{\zeta} \\
&+ \int_{t+h}^{t+2h} \left(\frac{1 - e^{-\kappa(t+2h-s)}}{\kappa h} \right) \gamma \sqrt{\zeta_s} dB_s \\
&- \int_{t}^{t+h} \left(\frac{e^{-\kappa h} - e^{-\kappa(t+2h-s)}}{\kappa h} \right) \gamma \sqrt{\zeta_s} dB_s
\end{aligned} \tag{2.28}$$

Using equations 1.17 and 1.14,

$$\begin{aligned}
&\mathbb{E}[\zeta_{t+h,t+2h} \mid \mathcal{F}_{t+h}] - \alpha\, \mathbb{E}\left[\zeta_{t,t+h} \mid \mathcal{F}_t\right] - \beta\, \bar{\zeta} \\
&= \left(a_1 \zeta_{t+h} + b_1 \bar{\zeta}\right) - \alpha \left(a_1 \zeta_t + b_1 \bar{\zeta}\right) - \beta\, \bar{\zeta} \\
&= a_1 \left(\zeta_{t+h} - \alpha\, \zeta_t\right) + \left(b_1 - \alpha\, b_1 - \beta\right) \bar{\zeta} \\
&= a_1 \left(\zeta_{t+h} - \alpha\, \zeta_t - \beta\, \bar{\zeta}\right) \\
&= \left(\frac{1 - e^{-\kappa h}}{\kappa h} \right) e^{-\kappa(t+h)} \gamma \int_t^{t+h} e^{\kappa s} \sqrt{\zeta_s}\, dB_s
\end{aligned}$$

and so

$$\begin{aligned}
&\mathbb{E}[\zeta_{t+h,t+2h} \mid \mathcal{F}_{t+h}] - \alpha\, \mathbb{E}\left[\zeta_{t,t+h} \mid \mathcal{F}_t\right] - \beta\, \bar{\zeta} \\
&\quad = \int_t^{t+h} \left(\frac{e^{-\kappa(t+h-s)} - e^{-\kappa(t+2h-s)}}{\kappa h} \right) \gamma \sqrt{\zeta_s}\, dB_s
\end{aligned} \tag{2.29}$$

Substituting equation 2.29 into equation 2.28 yields

$$\eta_{t,t+2h} = \int_{t+h}^{t+2h} \left(\frac{1 - e^{-\kappa(t+2h-s)}}{\kappa h} \right) \gamma \sqrt{\zeta_s} dB_s + \int_t^{t+h} \left(\frac{e^{-\kappa(t+h-s)} - e^{-\kappa h}}{\kappa h} \right) \gamma \sqrt{\zeta_s} dB_s$$

□

Because $\mathbb{E}[\eta_{t,t+2h} \mid \mathcal{F}_t] = 0$, this proposition implies Proposition 1.1. However, because $\mathbb{E}[\eta_{t,t+2h} \mid \mathcal{F}_{t+h}] \neq 0$, the sequence of the GMM errors $\eta_{t,t+2h}$ is not a martingale difference.

2.2.2 Conditional variance of $\eta_{t,t+2h}$

The next lemma expresses the conditional variance of $\eta_{t,t+2h}$ as a linear function of the instantaneous volatility at the beginning of the block and the asymptotic mean of the instantaneous volatility.

Lemma 2.3. *In the Heston model,*

$$Var\left(\eta_{t,t+2h} \mid \mathcal{F}_t\right) = \left(\frac{\gamma}{\kappa h}\right)^2 \left(c_2\, \zeta_t + d_2\, \bar{\zeta}\right) \tag{2.30}$$

where

$$\begin{aligned}
c_2 &= \frac{2}{k} e^{-\kappa h} - 4h e^{-2\kappa h} - \frac{2}{\kappa} e^{-3\kappa h} \\
d_2 &= h - \frac{1}{\kappa} + \left(5h + \frac{1}{\kappa}\right) e^{-2\kappa h} + \frac{2}{\kappa} e^{-3\kappa h}
\end{aligned}$$

Proof. The starting point is Proposition 2.2, which establishes that

$$\eta_{t,t+2h} = \int_t^{t+2h} \psi_s \frac{\gamma}{\kappa h} \sqrt{\zeta_s}\, dB_s \tag{2.31}$$

where[2]

$$\psi_s = \begin{cases} e^{-\kappa(t+h-s)} - e^{-\kappa h} & \text{if } s \in [t, t+h) \\ 1 - e^{-\kappa(t+2h-s)} & \text{if } s \in [t+h, t+2h] \end{cases} \tag{2.32}$$

Squaring both sides of equation 2.31, taking the conditional expectation of each side with respect to $\mathcal{F}_t$ and appealing to Itô's isometry,

$$\begin{aligned} \mathrm{Var}(\eta_{t,t+2h} \mid \mathcal{F}_t) &= \mathbb{E}\left[\eta_{t,t+2h}^2 \mid \mathcal{F}_t\right] \\ &= \mathbb{E}\left[\left(\int_t^{t+2h} \psi_s \frac{\gamma}{\kappa h} \sqrt{\zeta_s}\, dB_s\right)^2 \mid \mathcal{F}_t\right] \\ &= \mathbb{E}\left[\int_t^{t+2h} \left(\psi_s \frac{\gamma}{\kappa h} \sqrt{\zeta_s}\right)^2 ds \mid \mathcal{F}_t\right] \\ &= \left(\frac{\gamma}{\kappa h}\right)^2 \mathbb{E}\left[\int_t^{t+2h} \psi_s^2\, \zeta_s\, ds \mid \mathcal{F}_t\right] \\ &= \left(\frac{\gamma}{\kappa h}\right)^2 \int_t^{t+2h} \psi_s^2\, \mathbb{E}[\zeta_s \mid \mathcal{F}_t]\, ds \end{aligned} \tag{2.33}$$

Recall that Lemma 1.2 establishes that for $s \geq t$,

$$\mathbb{E}[\zeta_s \mid \mathcal{F}_t] = e^{-\kappa(s-t)}\zeta_t + (1 - e^{-\kappa(s-t)})\bar{\zeta} \tag{2.34}$$

Using equation 2.34 to substitute for the conditional expectation in equation 2.33,

$$\begin{aligned} \mathrm{Var}\left(\eta_{t,t+2h} \mid \mathcal{F}_t\right) &= \left(\frac{\gamma}{\kappa h}\right)^2 \left[\int_t^{t+2h} \psi_s^2 e^{-\kappa(s-t)}\, ds\right] \zeta_t \\ &\quad + \left(\frac{\gamma}{\kappa h}\right)^2 \left[\int_t^{t+2h} \psi_s^2 (1 - e^{-\kappa(s-t)})\, ds\right] \bar{\zeta} \\ &= \left(\frac{\gamma}{\kappa h}\right)^2 \left(c_2\, \zeta_t + d_2\, \bar{\zeta}\right) \end{aligned}$$

[2]Note that if $s = t + h$, then $e^{-\kappa(t+h-s)} - e^{-\kappa h} = 1 - e^{-\kappa h}$ and $1 - e^{-\kappa(t+2h-s)} = 1 - e^{-\kappa h}$.

where

$$
\begin{aligned}
c_2 &= \int_t^{t+2h} \psi_s^2 e^{-\kappa(s-t)}\, ds \\
&= \int_t^{t+h} (e^{-\kappa(t+h-s)} - e^{-\kappa h})^2 e^{-\kappa(s-t)}\, ds + \int_{t+h}^{t+2h} (1 - e^{-\kappa(t+2h-s)})^2 e^{-\kappa(s-t)}\, ds \\
&= \int_t^{t+h} (e^{-\kappa(t+2h-s)} - 2e^{-2\kappa h} + e^{\kappa(t-2h-s)})\, ds \\
&\quad + \int_{t+h}^{t+2h} (e^{\kappa(t-s)} - 2e^{-2\kappa h} + e^{-\kappa(t+4h-s)})\, ds \\
&= \frac{2}{k} e^{-\kappa h} - 4h e^{-2\kappa h} - \frac{2}{\kappa} e^{-3\kappa h}
\end{aligned}
$$

$$
\begin{aligned}
c_2 + d_2 &= \int_t^{t+2h} \psi_s^2\, ds \\
&= \int_t^{t+h} (e^{-\kappa(t+h-s)} - e^{-\kappa h})^2\, ds + \int_{t+h}^{t+2h} (1 - e^{-\kappa(t+h-s)})^2\, ds \\
&= \int_t^{t+h} (e^{-2\kappa(t+h-s)} - 2e^{-\kappa(t+2h-s)} + e^{-2\kappa h})\, ds \\
&\quad + \int_{t+h}^{t+2h} (1 - 2e^{-\kappa(t+2h-s)} + e^{-2\kappa(t+2h-s)})\, ds \\
&= h - \frac{1}{\kappa} + (h + \frac{1}{\kappa}) e^{-2\kappa h}
\end{aligned}
$$

and

$$
d_2 = (c_2 + d_2) - c_2 = h - \frac{1}{\kappa} + \left(5h + \frac{1}{\kappa}\right) e^{-2\kappa h} + \frac{2}{\kappa} e^{-3\kappa h}
$$

□

Note that the coefficients c_2 and d_2 do not depend on t or $t+h$, but just on h and the parameters κ and γ of the Heston model.

2.2.3 Asymptotic variance of $\eta_{t,t+2h}$

Now I use this conditional variance to derive an expression for $\lim_{t\to\infty} \mathrm{Var}(\eta_{t,t+2h})$, the asymptotic variance of the GMM error as $t \to \infty$.

Proposition 2.4. *In the Heston model,*

$$\lim_{t\to\infty} Var\left(\eta_{t,t+2h}\right) = \left(\frac{\gamma}{\kappa h}\right)^2 (c_2 + d_2)\,\bar{\zeta} \tag{2.35}$$

where

$$c_2 + d_2 = h - \frac{1}{\kappa} + \left(h + \frac{1}{\kappa}\right) e^{-2\kappa h} \tag{2.36}$$

Proof. Taking the expectation of each side of equation 2.30 in Lemma 2.3, and taking the limit as $t \to \infty$,

$$\begin{aligned}\lim_{t\to\infty} \mathbb{E}[\mathrm{Var}(\eta_{t,t+2h} \mid \mathcal{F}_t)] &= \left(\frac{\gamma}{\kappa h}\right)^2 \left[c_2 \lim_{t\to\infty} \mathbb{E}\zeta_t + d_2\,\bar{\zeta}\right] \\ &= \left(\frac{\gamma}{\kappa h}\right)^2 (c_2 + d_2)\bar{\zeta}\end{aligned} \tag{2.37}$$

where

$$c_2 + d_2 = h - \frac{1}{\kappa} + (h + \frac{1}{\kappa})e^{-2\kappa h}$$

By the law of total variance,

$$\mathrm{Var}(\eta_{t,t+2h}) = \mathbb{E}[\mathrm{Var}(\eta_{t,t+2h} \mid \mathcal{F}_t)] + \mathrm{Var}(\mathbb{E}[\eta_{t,t+2h} \mid \mathcal{F}_t]) \tag{2.38}$$

Since

$$\mathbb{E}[\eta_{t,t+2h} \mid \mathcal{F}_t] = 0$$

equation 2.38 simplifies to

$$\mathrm{Var}(\eta_{t,t+2h}) = \mathbb{E}[\mathrm{Var}(\eta_{t,t+2h} \mid \mathcal{F}_t)] \tag{2.39}$$

Taking the limit of each side of equation 2.39 as $t \to \infty$ and using equation 2.37, the result follows. $\square$

The limiting procedure in equation 2.37 has a natural interpretation: if t is "large enough", the difference $\mathbb{E}(\zeta_t - \bar{\zeta})$ can be ignored because the effects of the initial condition ζ_0 have essentially worn off.

It is instructive to compare the size of the asymptotic variance of $\eta_{t,t+2h}$ to that of the asymptotic variance of ζ_t. To do so, I rewrite equation 2.35 in Proposition 2.4 to express the former as a fraction of the latter:

$$\begin{aligned}\lim_{t\to\infty} \operatorname{Var}(\eta_{t,t+2h}) &= 2\left(\frac{c_2 + d_2}{\kappa h^2}\right)\frac{\gamma^2\bar{\zeta}}{2\kappa} \\ &= \left(\frac{2}{\kappa h} - \frac{2}{(\kappa h)^2} + \left(\frac{2}{\kappa h} + \frac{2}{(\kappa h)^2}\right)e^{-2\kappa h}\right)\lim_{t\to\infty} \operatorname{Var}(\zeta_t) \qquad (2.40)\end{aligned}$$

To give some practical perspective, recall that $h = 1/234$ throughout my empirical analysis and κ has a median value of 25 according to Table 1.3. With these values,

$$\lim_{t\to\infty} \operatorname{Var}(\eta_{t,t+2h}) \approx 0.14 \lim_{t\to\infty} \operatorname{Var}(\zeta_t)$$

The asymptotic variance of the error term is about 14% of the asymptotic variance of ζ_t.

2.2.4 Asymptotic autocovariances and autocorrelations of $\eta_{t,t+2h}$

Since the process $(\zeta_t)_{t\geq 0}$ of the instantaneous volatility in the Heston model is a stationary ergodic process, so is the process $(\eta_{t,t+2h})_{t\geq 0}$ of the GMM error. Consequently, it makes sense to talk about asymptotic autocovariances and autocorrelations of $\eta_{t,t+2h}$. Let U_j denote the asymptotic autocovariance of $\eta_{t,t+2h}$ for lag j:

$$U_j := \lim_{t\to\infty} \mathbb{E}\left[\eta_{t,t+2h}\, \eta_{t+jh,t+(j+2)h}\right] \qquad (2.41)$$

In particular, U_0 is the asymptotic variance, which I have already computed in Proposition 2.4. I now derive expressions for the asymptotic autocovariances for all lags $j \geq 1$.

Proposition 2.5. *In the Heston model,*

$$U_0 = \left(\frac{\gamma}{\kappa h}\right)^2 \left(h - \frac{1}{\kappa} + \left(h + \frac{1}{\kappa}\right) e^{-2\kappa h}\right) \bar{\zeta} \tag{2.42}$$

$$U_1 = \left(\frac{\gamma}{\kappa h}\right)^2 \left(\frac{1}{2\kappa} - h e^{-\kappa h} - \frac{1}{2\kappa} e^{-2\kappa h}\right) \bar{\zeta} \tag{2.43}$$

$$U_j = 0, \qquad j \geq 2 \tag{2.44}$$

Proof. I have already established equation 2.42 in Proposition 2.4.

According to the definition of U_1 in equation 2.41,

$$\begin{aligned}
U_1 &= \lim_{t\to\infty} \mathbb{E}\left[\eta_{t,t+2h}\, \eta_{t+h,t+3h}\right] \\
&= \lim_{t\to\infty} \mathbb{E}\left[\left(\zeta_{t+h,t+2h} - \alpha\zeta_{t,t+h} - \beta\bar{\zeta}\right)\left(\zeta_{t+2h,t+3h} - \alpha\zeta_{t+h,t+2h} - \beta\bar{\zeta}\right)\right] \\
&= \lim_{t\to\infty} \mathbb{E}\left[\left(\zeta_{t+h,t+2h} - \bar{\zeta} - \alpha\left(\zeta_{t,t+h} - \bar{\zeta}\right)\right)\left(\zeta_{t+2h,t+3h} - \bar{\zeta} - \alpha\left(\zeta_{t+h,t+2h} - \bar{\zeta}\right)\right)\right]
\end{aligned}$$

Using the definition of V_j in equation 2.14 and the expressions in equations 2.15 to 2.17,

$$\begin{aligned}
U_1 &= \left(1 + \alpha^2\right) V_1 - \alpha\left(V_0 + V_2\right) \\
&= \left(1 + \alpha^2\right) V_1 - \alpha\left(V_0 + \alpha V_1\right) \\
&= V_1 - \alpha V_0 \\
&= \left(\frac{\gamma}{\kappa h}\right)^2 \frac{\beta^2}{2\kappa}\, \bar{\zeta} - \alpha \left(\frac{\gamma}{\kappa h}\right)^2 \left(h - \frac{1}{\kappa} + \frac{1}{\kappa} e^{-\kappa h}\right) \bar{\zeta} \\
&= \left(\frac{\gamma}{\kappa h}\right)^2 \left(\frac{1}{2\kappa} - h e^{-\kappa h} - \frac{1}{2\kappa} e^{-2\kappa h}\right) \bar{\zeta}
\end{aligned}$$

For $j \geq 2$, by the law of iterated expectations, I have

$$\begin{aligned} U_j &= \lim_{t\to\infty} \mathbb{E}\left[\eta_{t,t+2h}\ \eta_{t+jh,t+(j+2)h}\right] \\ &= \lim_{t\to\infty} \mathbb{E}\left[\mathbb{E}\left[\eta_{t,t+2h}\ \eta_{t+jh,t+(j+2)h} \mid \mathcal{F}_{t+2h}\right]\right] \\ &= \lim_{t\to\infty} \mathbb{E}\left[\eta_{t,t+2h}\ \mathbb{E}\left[\eta_{t+jh,t+(j+2)h} \mid \mathcal{F}_{t+2h}\right]\right] \\ &= \lim_{t\to\infty} \mathbb{E}\left[\eta_{t,t+2h} \cdot 0\right] \\ &= 0 \end{aligned}$$

where the conditional expectation is zero according to Proposition 1.1. □

Note that the autocovariances of $\eta_{t,t+2h}$ for all lags $j \geq 2$ are zero. This result has a natural interpretation: the two blocks associated with the two GMM errors do not overlap when $j \geq 2$, and consequently the GMM errors are uncorrelated.

I now consider the autocorrelations of $\eta_{t,t+2h}$. Let Q_j denote the asymptotic autocorrelation of $\eta_{t,t+2h}$ for lag j:

$$Q_j := \frac{U_j}{U_0} \tag{2.45}$$

It is easy to derive expressions for the autocorrelations of $\eta_{t,t+2h}$ based on the results in Proposition 2.5.

Corollary 2.2. *In the Heston model,*

$$Q_0 = 1 \tag{2.46}$$

$$Q_1 = \frac{\frac{1}{2} + (1-\beta)\log(1-\beta) - \frac{1}{2}(1-\beta)^2}{-\log(1-\beta) - 1 + (-\log(1-\beta) + 1)(1-\beta)^2} \tag{2.47}$$

$$Q_j = 0, \qquad j \geq 2 \tag{2.48}$$

Proof. Equation 2.46 is trivial.

Figure 2.2: Q_1 as a function of β in equation 2.47

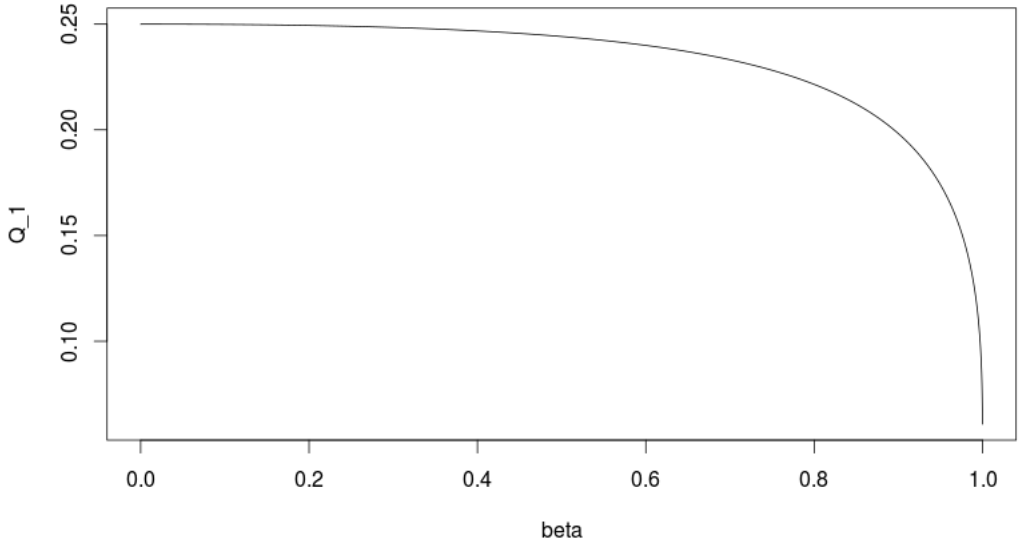

Equation 2.48 directly follows from the definition of Q_j in equation 2.45 and equation 2.44 in Proposition 2.5.

To establish equation 2.47, use the definition in equation 2.45 and equations 2.42 and 2.43 in Proposition 2.5:

$$\begin{aligned} Q_1 := \frac{U_1}{U_0} &= \frac{\frac{1}{2\kappa} - he^{-\kappa h} - \frac{1}{2\kappa}e^{-2\kappa h}}{h - \frac{1}{\kappa} + \left(h + \frac{1}{\kappa}\right)e^{-2\kappa h}} \\ &= \frac{\frac{1}{2} + (1-\beta)\log(1-\beta) - \frac{1}{2}(1-\beta)^2}{-\log(1-\beta) - 1 + (-\log(1-\beta) + 1)(1-\beta)^2} \end{aligned}$$

where in the last step I use the relationship $\beta = 1 - e^{-\kappa h}$. □

Note that the asymptotic autocorrelations of $\eta_{t,t+2h}$ for all lags depend only on the mean-reversion parameter β of the Heston model. They do not depend on $\bar{\zeta}$ or γ.

In particular, equation 2.47 expresses Q_1, the autocorrelation of $\eta_{t,t+2h}$ for lag 1 as a function of β. Figure 2.2 displays the graph of this function. It suggests

that Q_1 is approximately equal to 0.25 for a very wide range of values of β that encompasses both the median value of $\beta = 0.10$ and the upper quantile value of $\beta = 0.14$.

2.3 Errors in Variables

In Section 1.1.2 I addressed the errors in variables introduced by using the observable realized variation $\varphi_{t,t+h}$ in place of the unobservable quadratic variation $\zeta_{t,t+h}$. I showed that the moment condition equation 1.19 is unaffected under a weak assumption.

The same error-in-variable problem occurs here: the observable realized variation is an error-ridden measure of the unobservable quadratic variation:

$$\varphi_{t,t+h} = \zeta_{t,t+h} + \nu_{t,t+h} \tag{2.49}$$

However, it is no longer true that the second moments of quadratic variation $\zeta_{t,t+h}$ and the GMM error $\eta_{t,t+2h}$ are unaffected by measurement errors. As Anderson and Bollerslev (1998) suggests, squared realized variation yields an upward biased estimate of true squared quadratic variation for any fixed sampling interval, even though realized variation itself is unbiased for quadratic variation.

To investigate the effects of measurement errors on the second moments of $\zeta_{t,t+h}$ and $\eta_{t,t+2h}$, I start with the following strong assumption:

Assumption 2.1. *$\nu_{t,t+h}$ is independent of the ζ process, and is i.i.d. $N(0, \nu^2)$ with variance $\nu^2 > 0$.*

Let $\widetilde{V}_j$ denote the asymptotic autocovariance of $\varphi_{t,t+h}$ for lag $j \geq 0$:

$$\widetilde{V}_j := \lim_{t \to \infty} \mathbb{E}\left[\left(\varphi_{t,t+h} - \bar{\zeta}\right)\left(\varphi_{t+jh,t+(j+1)h} - \bar{\zeta}\right)\right] \tag{2.50}$$

Define

$$\xi_{t,t+2h} := \varphi_{t+h,t+2h} - \alpha\, \varphi_{t,t+h} - \beta\, \bar{\zeta} \tag{2.51}$$

and so

$$\begin{aligned} \xi_{t,t+2h} &= (\zeta_{t+h,t+2h} + \nu_{t+h,t+2h}) - \alpha\, (\zeta_{t,t+h} + \nu_{t,t+h}) - \beta\, \bar{\zeta} \\ &= \eta_{t,t+2h} + (\nu_{t+h,t+2h} - \alpha\, \nu_{t,t+h}) \end{aligned} \tag{2.52}$$

Let $\widetilde{U}_j$ denote the asymptotic autocovariance of $\xi_{t,t+2h}$ for lag $j \geq 0$:

$$\widetilde{U}_j := \lim_{t\to\infty} \mathbb{E}\left[\xi_{t,t+2h}\, \xi_{t+jh,t+(j+2)h}\right] \tag{2.53}$$

Proposition 2.6. *Under Assumption 2.1,*

$$\widetilde{V}_0 = V_0 + \nu^2 \tag{2.54}$$

$$\widetilde{V}_1 = V_1 \tag{2.55}$$

$$\widetilde{V}_j = V_j, \qquad j \geq 2 \tag{2.56}$$

$$\widetilde{U}_0 = U_0 + \left(1 + \alpha^2\right) \nu^2 \tag{2.57}$$

$$\widetilde{U}_1 = U_1 - \alpha\nu^2 \tag{2.58}$$

$$\widetilde{U}_j = U_j, \qquad j \geq 2 \tag{2.59}$$

Proof. Using Assumption 2.1 and the definitions in equations 2.49, 2.50, 2.52 and 2.53,

$$\begin{aligned} \widetilde{V}_0 &= \lim_{t\to\infty} \mathbb{E}\left[\left(\varphi_{t,t+h} - \bar{\zeta}\right)^2\right] \\ &= \lim_{t\to\infty} \mathbb{E}\left[\left(\zeta_{t,t+h} + \nu_{t,t+h} - \bar{\zeta}\right)^2\right] \\ &= \lim_{t\to\infty} \mathbb{E}\left[\left(\zeta_{t,t+h} - \bar{\zeta}\right)^2 + \nu_{t,t+h}^2 + 2\left(\zeta_{t,t+h} - \bar{\zeta}\right) \nu_{t,t+h}\right] \\ &= V_0 + \nu^2 + 0 \end{aligned}$$

and

$$\begin{aligned}
\widetilde{V}_1 &= \lim_{t\to\infty} \mathbb{E}\left[\left(\varphi_{t,t+h} - \bar{\zeta}\right)\left(\varphi_{t+h,t+2h} - \bar{\zeta}\right)\right] \\
&= \lim_{t\to\infty} \mathbb{E}\left[\left(\zeta_{t,t+h} + \nu_{t,t+h} - \bar{\zeta}\right)\left(\zeta_{t+h,t+2h} + \nu_{t+h,t+2h} - \bar{\zeta}\right)\right] \\
&= \lim_{t\to\infty} \mathbb{E}\left[\left(\zeta_{t,t+h} - \bar{\zeta}\right)\left(\zeta_{t+h,t+2h} - \bar{\zeta}\right) + \nu_{t,t+h}\,\nu_{t+h,t+2h}\right. \\
&\qquad \left. + \left(\zeta_{t,t+h} - \bar{\zeta}\right)\nu_{t+h,t+2h} + \left(\zeta_{t+h,t+2h} - \bar{\zeta}\right)\nu_{t,t+h}\right] \\
&= V_1 + 0 + 0 + 0
\end{aligned}$$

Similarly,

$$\widetilde{V}_j = V_j, \qquad j \geq 2$$

Moreover,

$$\begin{aligned}
\widetilde{U}_0 &= \lim_{t\to\infty} \mathbb{E}\left[\xi^2_{t,t+2h}\right] \\
&= \lim_{t\to\infty} \mathbb{E}\left[\left(\eta_{t,t+2h} + \nu_{t+h,t+2h} - \alpha\,\nu_{t,t+h}\right)^2\right] \\
&= \lim_{t\to\infty} \mathbb{E}\left[\eta^2_{t,t+2h} + \nu^2_{t+h,t+2h} + \alpha^2\nu^2_{t,t+h}\right. \\
&\qquad \left. +2\,\eta_{t,t+2h}\,\nu_{t+h,t+2h} - 2\,\eta_{t,t+2h}\,\nu_{t,t+h} - 2\,\eta_{t,t+2h}\,\nu_{t,t+h}\right] \\
&= U_0 + \nu^2 + \alpha^2\nu^2 + 0 - 0 - 0
\end{aligned}$$

and

$$\begin{aligned}
\widetilde{U}_1 &= \lim_{t\to\infty} \mathbb{E}\left[\xi_{t,t+2h}\,\xi_{t+h,t+3h}\right] \\
&= \lim_{t\to\infty} \mathbb{E}\left[\left(\eta_{t,t+2h} + \nu_{t+h,t+2h} - \alpha\,\nu_{t,t+h}\right)\left(\eta_{t+h,t+3h} + \nu_{t+2h,t+3h} - \alpha\,\nu_{t+h,t+2h}\right)\right] \\
&= \lim_{t\to\infty} \mathbb{E}\left[\eta_{t,t+2h}\,\eta_{t+h,t+3h} + \left(\nu_{t+h,t+2h} - \alpha\,\nu_{t,t+h}\right)\eta_{t+h,t+3h}\right. \\
&\qquad +\eta_{t,t+2h}\left(\nu_{t+2h,t+3h} - \alpha\,\nu_{t+h,t+2h}\right) \\
&\qquad \left. +\nu_{t+h,t+2h}\,\nu_{t+2h,t+3h} - \alpha\,\nu_{t,t+h}\,\nu_{t+2h,t+3h} - \alpha\,\nu^2_{t+h,t+2h} + \alpha^2\,\nu_{t,t+h}\,\nu_{t+h,t+2h}\right] \\
&= U_1 + 0 + 0 + 0 - 0 - \alpha\nu^2 + 0
\end{aligned}$$

Similarly,

$$\widetilde{U}_j = U_j, \qquad j \geq 2$$

□

This proposition implies that, among the results on autocovariances of quadratic variation in Proposition 2.3, equation 2.16 and equation 2.17 are unaffected by measurement errors, while equation 2.15 is vulnerable to measurement error. Among the results on autocovariance of the GMM error in Proposition 2.5, both equation 2.42 and equation 2.43 are vulnerable to measurement error; equation 2.44 is clearly robust to measurement error.

2.4 Estimating the Volatility of Volatility Parameter γ

The analysis of measurement errors in the last section has a direct implication regarding estimation of γ: equations 2.16 and 2.17 are appropriate choices for the moment conditions.

To achieve efficiency in estimation, I use the generalized method of moments (GMM) rather than the method of moments (MM). In the empirical study below, I use the following two moment conditions:

$$\mathbb{E}\left[\left(\varphi_{t,t+h} - \hat{\bar{\zeta}}\right)\left(\varphi_{t+h,t+2h} - \hat{\bar{\zeta}}\right) - \left(\frac{\gamma}{\hat{\kappa}h}\right)^2 \frac{\hat{\beta}^2}{2\hat{\kappa}}\,\hat{\bar{\zeta}}\right] = 0 \tag{2.60}$$

$$\mathbb{E}\left[\left(\varphi_{t,t+h} - \hat{\bar{\zeta}}\right)\left(\varphi_{t+2h,t+3h} - \hat{\bar{\zeta}}\right) - \left(\frac{\gamma}{\hat{\kappa}h}\right)^2 \frac{\left(1-\hat{\beta}\right)\hat{\beta}^2}{2\hat{\kappa}}\,\hat{\bar{\zeta}}\right] = 0 \tag{2.61}$$

Because the error terms associated with these two moment conditions are possibly heteroscedastic and autocorrelated, I use a heteroscedasticity and autocorrelation consistent (HAC) covariance matrix estimator with a Bartlett-kernel (see Newey and West (1987)).

Table 2.1: Sample standard deviation of $\varphi_{t,t+h} \times 10^4$, good weeks

	sample standard deviation of $\varphi_{t,t+h}$ $\times 10^4$
median	0.42
5% percentile	0.14
25% percentile	0.26
75% percentile	0.81
95% percentile	5.8

Under the GMM setting, the minimized value of the objective function multiplied by the sample size is asymptotically chi-square distributed, which allows for a specification test of the overidentifying restrictions. Moreover, inference concerning the individual parameter is readily available from the standard formula for the asymptotic covariance matrix. Specifically, I will test the hypothesis that $\gamma = 0$.

2.5 Empirical Analysis of the Second Moments of $\varphi_{t,t+h}$

This section examines the empirical properties of the second moments of realized variation $\varphi_{t,t+h}$.

2.5.1 Sample standard deviation of $\varphi_{t,t+h}$

I start my empirical analysis with the sample standard deviation of $\varphi_{t,t+h}$, the (scaled) realized variation over blocks. I compute the standard deviation for each week (more precisely, each five-day collection of blocks). I exclude the first block for each day so that the standard deviation lines up with the sample used to compute the estimates in Chapter 1.

Table 2.1 reports the summary statistics of the weekly sample standard deviation of $\varphi_{t,t+h}$ for good weeks. The median sample standard deviation is 0.42×10^{-4}.

Recall that the median $\bar{\zeta}$ in the sample is 0.59×10^{-4}, so the sample standard deviation of realized variation has a sizable magnitude compared to the level of the asymptotic mean of volatility. The distribution of the sample standard deviation is highly skewed to the right — a few good weeks experience very large standard deviation of realized variation. The 95% percentile of the distribution is as high as 5.8×10^{-4}, or 14 times as large as the median.

Figure 2.3 plots the time series of the sample standard deviation of $\varphi_{t,t+h}$ for all good weeks in the sample period. This plot resembles the times series plot of estimates of $\bar{\zeta}$ in Figure 1.8. This is not surprising, given the linear relationship between the standard deviation and $\bar{\zeta}$ in equation 2.10, which implies that because $\bar{\zeta}$ varies a lot over my sample period according to Figure 1.8, so does the standard deviation of $\varphi_{t,t+h}$. The series looks persistent and slow-moving most of the time. However, it can move abruptly; for example, the "Great Recession" from the second half of 2008 to the beginning of 2009 witnessed exceptionally high levels of volatility of volatility, which is clear in the plot.

2.5.2 Sample autocorrelations of $\varphi_{t,t+h}$

I now examine the sample autocorrelations of $\varphi_{t,t+h}$, the (scaled) realized variation over blocks. Let $\widehat{R}_j$ denote the sample autocorrelation of $\varphi_{t,t+h}$ for lag j. As before, I compute the sample autocorrelations for each week, and exclude the first block for each day in my calculation.

Table 2.2 reports the summary statistics of $\widehat{R}_j$, the sample autocorrelations of $\varphi_{t,t+h}$, for $j = 1, 2, 3, 4, 5, 6$. The sample autocorrelation decreases as the lag increases: the median $\widehat{R}_1$ is 0.57, and the median declines gradually to 0.38 for $\widehat{R}_6$ (recall that realized variation is over a 100-second block, so lag 6 corresponds to a time difference of 600 seconds, or 10 minutes). This makes sense, since the volatility process is persistent, and it is able to deviate from its original value

Figure 2.3: Sample standard deviation of $\varphi_{t,t+h} \times 10^4$, good weeks

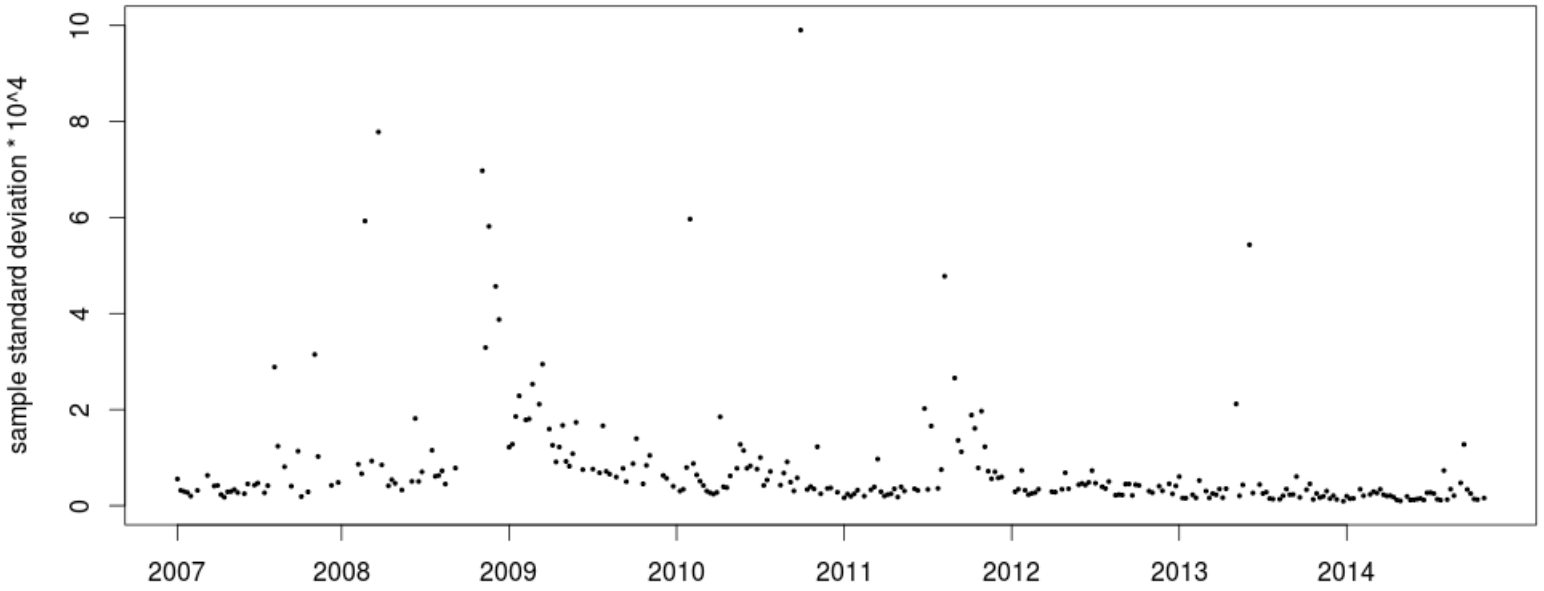

Table 2.2: Sample autocorrelations of $\varphi_{t,t+h}$, good weeks

	$\widehat{R}_1$	$\widehat{R}_2$	$\widehat{R}_3$	$\widehat{R}_4$	$\widehat{R}_5$	$\widehat{R}_6$
median	0.57	0.48	0.42	0.42	0.40	0.38
5% percentile	0.17	0.07	0.05	0.05	0.03	0.03
25% percentile	0.49	0.38	0.33	0.33	0.31	0.30
75% percentile	0.63	0.55	0.51	0.48	0.47	0.45
95% percentile	0.72	0.65	0.63	0.57	0.58	0.57
mean	0.54	0.45	0.42	0.39	0.37	0.36
standard deviation	0.16	0.16	0.15	0.15	0.15	0.14

as time passes. The mean is close to the median for each $\widehat{R}_j$, suggesting that its distribution is roughly symmetric about the median. The standard deviations of $\widehat{R}_j$'s are strikingly close to each other, with the maximum of 0.16 for $\widehat{R}_1$ and minimum of 0.14 for $\widehat{R}_6$.

I now compare $\widehat{R}_1$, the sample autocorrelation of realized variation $\varphi_{t,t+h}$ for lag 1, to the value of the asymptotic autocorrelation of quadratic variation $\zeta_{t,t+h}$ for lag 1 given by equation 2.24 with the parameter β replaced by its estimate $\hat{\beta}$ obtained in Chapter 1. Let R_1^β denote this value:

$$R_1^\beta = \frac{\hat{\beta}^2}{2\left(-\log\left(1-\hat{\beta}\right)-\hat{\beta}\right)} \tag{2.62}$$

Figure 2.4 plots the sample autocorrelation $\widehat{R}_1$ on the vertical axis and R_1^β on the horizontal axis, together with a 45 degree line. The plot shows that sample autocorrelation $\widehat{R}_1$ is almost always smaller than R_1^β. $\widehat{R}_1$ has a median of 0.57, much smaller than the median R_1^β of 0.93. This suggests that equation 2.24 fails to explain the sample autocorrelations for lag 1 observed in data.

This failure might be caused by two factors. The first factor is the measurement error. According to equations 2.54 and 2.55 in Proposition 2.6, the measurement

Figure 2.4: The sample autocorrelation $\widehat{R}_1$ versus R_1^{β}, good weeks

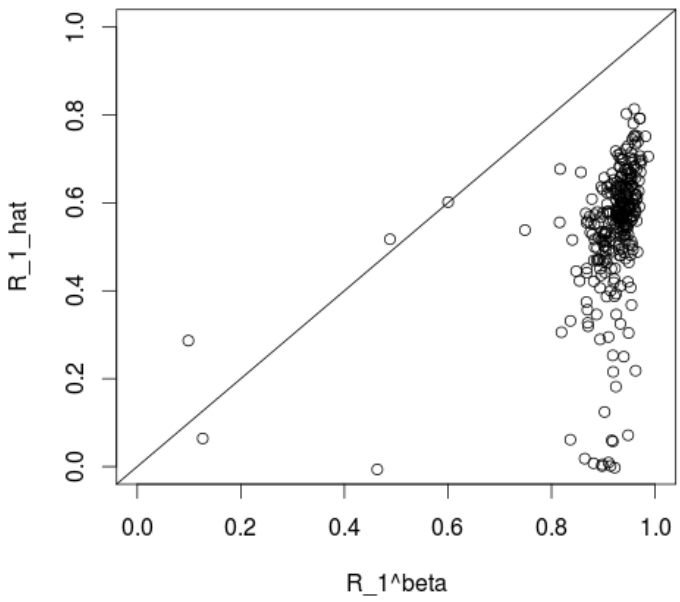

error in realized variation as a proxy for quadratic variation increases the variance but does not affect the autocovariance for lag 1, as long as the measurement error has zero mean and is independent across blocks. Consequently, measurement error lowers the sample autocorrelation. Under this explanation, the ratio of the medians, $0.57/0.93 = 61\%$, roughly measures the percentage in the sample variance of realized variation that can be contributed to the Heston dynamics of quadratic variation as opposed to measurement errors. The second factor is non-stationarity at the beginning of each day. Strictly speaking, equation 2.24 is an asymptotic formula that exploits the stationarity property of the quadratic variation process, and it might not be accurate if there is severe non-stationarity at the beginning of each day. However, this argument is mitigated by the fact that mean reversion is very fast, which suggests that the limiting approximation is a good approximation for most of the trading day.

I also examine $\widehat{R}_j$, the sample autocorrelations of $\varphi_{t,t+h}$ for higher lags $j \geq 2$.

In particular, I compute the ratio $\widehat{R}_j/\widehat{R}_1$, and compare this ratio to $\left(1-\hat{\beta}\right)^{j-1}$, the ratio of corresponding autocorrelations of quadratic variation given by equation 2.25 with the parameter β replaced by its estimate $\hat{\beta}$ obtained in Chapter 1. Figure 2.5 plots the ratios $\widehat{R}_j/\widehat{R}_1$ for $j = 2, 3, 4, 5$ on the vertical axis and $\left(1-\hat{\beta}\right)^{j-1}$ on the horizontal axis, together with a 45 degree line. In all subplots, the dots are reasonably close to the 45 degree line. This suggests that equation 2.25 succeeds in explaining the relative sizes of autocorrelations for lags $j \geq 1$.

This success can be explained by equations 2.55 and 2.56 in Proposition 2.6: the measurement error in realized variation as a proxy for quadratic variation does not affect the autocovariances for lags $j \geq 1$.

2.6 Empirical Analysis of the Second Moments of $\widehat{\xi}_{t,t+2h}$

This section examines the empirical properties of the second moments of the GMM error. Let $\widehat{\xi}_{t,t+2h}$ denote the empirical GMM error:

$$\widehat{\xi}_{t,t+2h} := \varphi_{t+h,t+2h} - \hat{\alpha}\,\varphi_{t,t+h} - \hat{\beta}\,\widehat{\bar{\zeta}} \tag{2.63}$$

where $\hat{\alpha}$, $\hat{\beta}$ and $\widehat{\bar{\zeta}}$ are the estimates of the parameters obtained in Chapter 1.

2.6.1 Sample standard deviation of $\widehat{\xi}_{t,t+2h}$

I start with the sample standard deviation of the GMM error $\widehat{\xi}_{t,t+2h}$. I compute the standard deviation for each week, or precisely, each five-day collection of blocks. Each trading day contains 232 GMM errors (recall that the first block for each day is used as an instrument and that a GMM error is associated with two adjacent blocks).

Table 2.3 reports the summary statistics of weekly sample standard deviation

Figure 2.5: $\widehat{R}_j/\widehat{R}_1$ versus $\left(1-\hat{\beta}\right)^{j-1}$ for $j = 2, 3, 4, 5$, good weeks

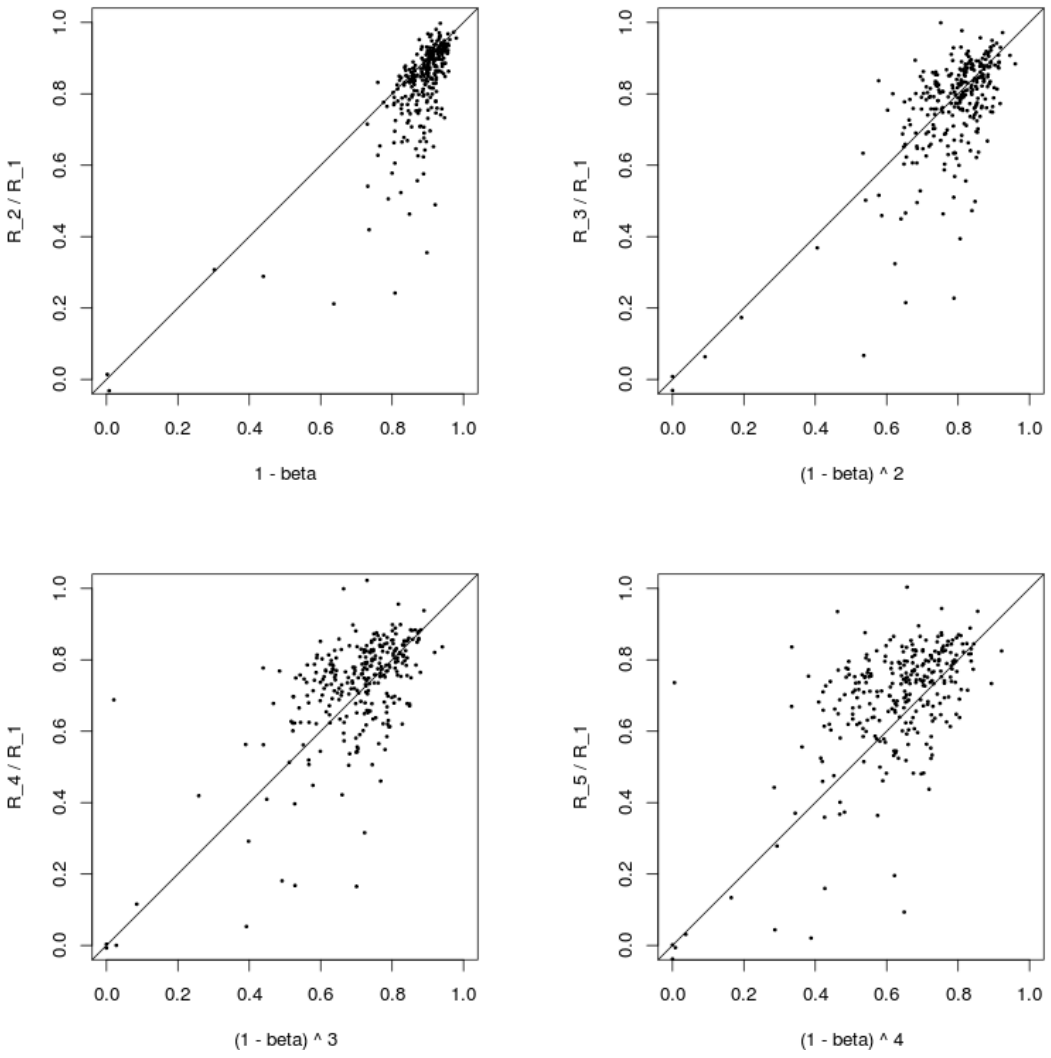

Table 2.3: Sample standard deviation of $\widehat{\xi}_{t,t+2h} \times 10^4$, good weeks

	sample standard deviation of $\widehat{\xi}_{t,t+2h} \times 10^4$
median	0.36
5% percentile	0.12
25% percentile	0.22
75% percentile	0.73
95% percentile	4.5

of the GMM error $\widehat{\xi}_{t,t+2h}$. The median sample standard deviation is 0.36×10^{-4}. Recall that the median $\bar{\zeta}$ in the sample is 0.59×10^{-4}, so the standard deviation has a sizable magnitude compared to the asymptotic mean of quadratic variation. The distribution of the sample standard deviation is highly skewed to the right — a few good weeks experience very large standard deviation of GMM errors.

Figure 2.6 plots the time series of the sample standard deviation of GMM errors $\widehat{\xi}_{t,t+2h}$ for good weeks in the bottom subplot, compared with Figure 2.3, the time series plot of the sample standard deviation of $\varphi_{t,t+h}$, in the top subplot. The two series resemble each other. Their correlation coefficient is 0.91. This is not surprising given the parallel between equation 2.10 in Proposition 2.1 and equation 2.35 in Proposition 2.4: the variance of quadratic variation and that of the GMM error are both proportional to the asymptotic variance of ζ_t, and they vary as the parameters $\bar{\zeta}$ and γ vary.

2.6.2 Sample autocorrelations of $\widehat{\xi}_{t,t+2h}$

I now examine the sample autocorrelations of $\widehat{\xi}_{t,t+2h}$, the empirical GMM error. Let $\widehat{Q}_j$ denote the sample autocorrelation of $\widehat{\xi}_{t,t+2h}$ for lag j. As before, I compute the sample autocorrelations for each week, and exclude the first block for each day in my calculation.

Figure 2.6: Sample standard deviation of $\varphi_{t,t+h}$ and $\widehat{\xi}_{t,t+2h}$, good weeks

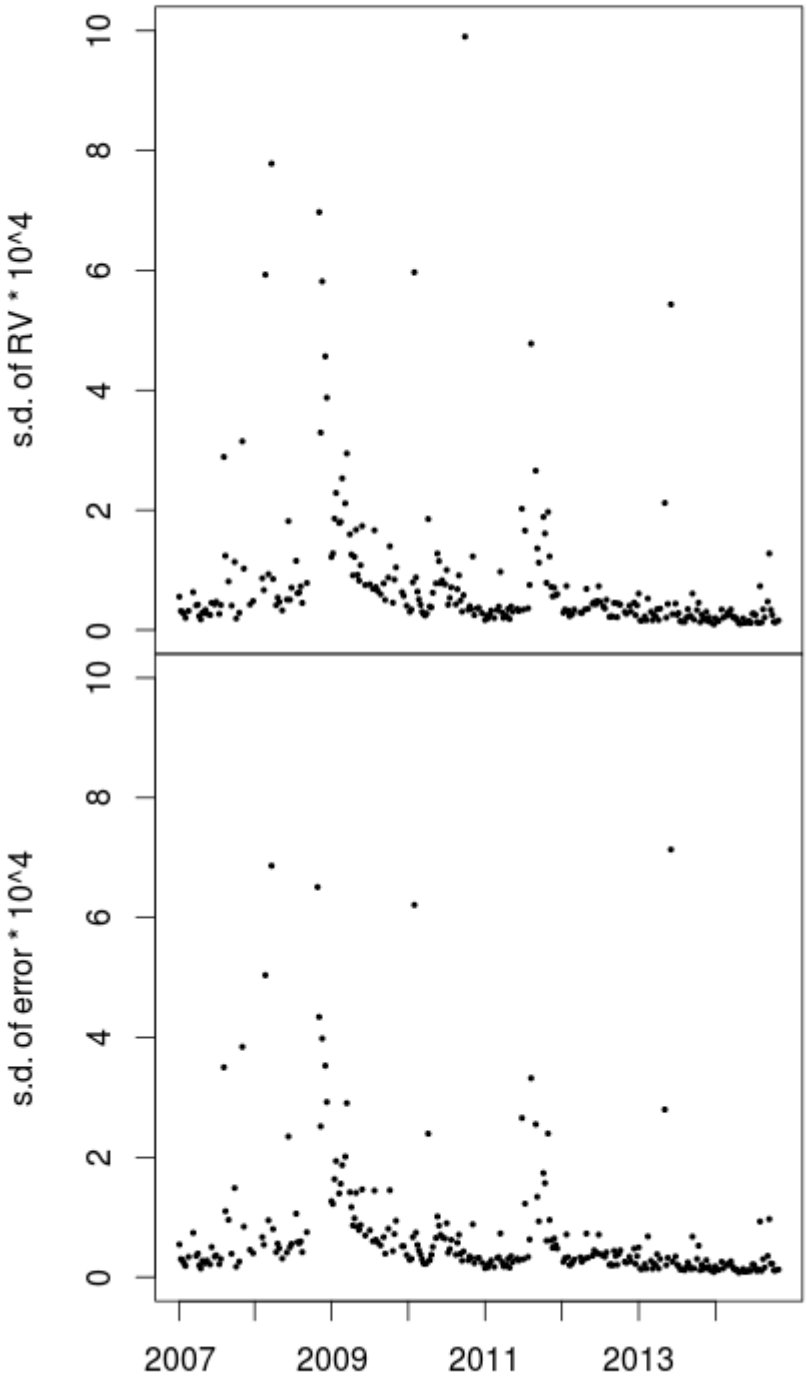

Figure 2.7: Sample autocorrelation function of $\widehat{\xi}_{t,t+2h}$, a good week, SPY

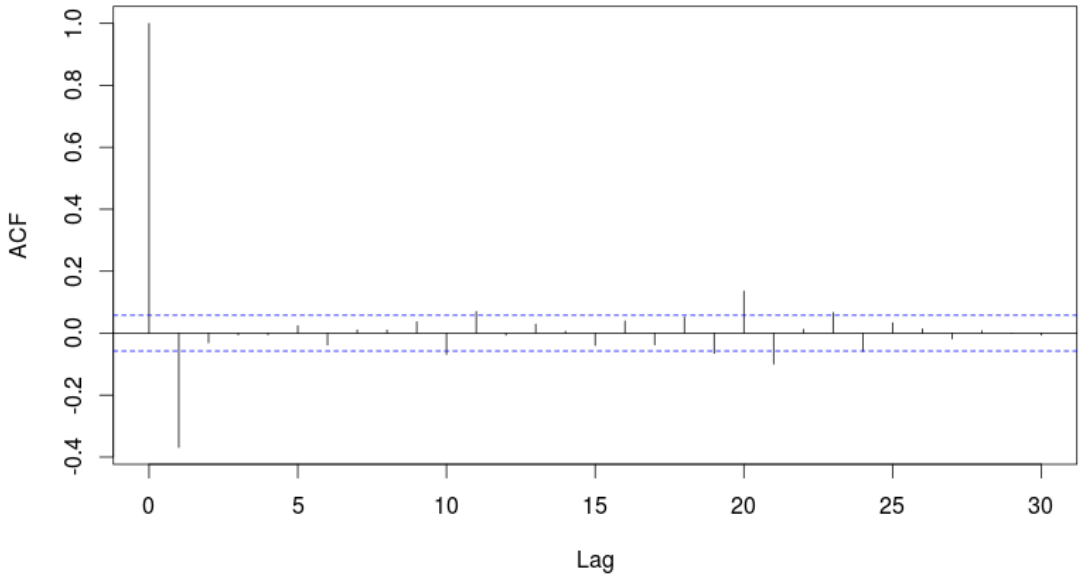

Figure 2.7 displays the autocorrelation function of the GMM error term for a typical good week, together with a band marked by dashed lines as indicating the threshold of significance at the 95% level. The sample autocorrelation for lag 1 is significantly negative, and those for higher lags are not significantly different from 0 (with a few minor exceptions).

Table 2.4 reports the summary statistics of $\widehat{Q}_j$, the sample autocorrelations of $\widehat{\xi}_{t,t+2h}$ for $j = 1, 2, 3$ (recall that realized variation is over a 100-second block, so lag 3 corresponds to a time difference of 300 seconds, or 5 minutes).

The first column of Table 2.4 shows that $\widehat{Q}_1$ is almost always negative. The median is -0.39 and the mean is -0.37. The 95% percentile is -0.19, which is still significantly negative. This is in sharp contrast to the implication of equation 2.47 that Q_1 is positive. This contrast might be caused by the measurement error. According to equations 2.58 in Proposition 2.6, the measurement error in realized

Table 2.4: Sample autocorrelations of $\widehat{\xi}_{t,t+2h}$, good weeks

	$\widehat{Q}_1$	$\widehat{Q}_2$	$\widehat{Q}_3$
median	-0.39	-0.04	-0.00
5% percentile	-0.48	-0.16	-0.08
25% percentile	-0.42	-0.07	-0.04
75% percentile	-0.35	-0.01	0.02
95% percentile	-0.19	0.04	0.08
mean	-0.37	-0.05	-0.00
standard deviation	0.12	0.07	0.06

variation as a proxy for quadratic variation negatively affects the autocorrelation of the GMM error for lag 1. If the measurement error is large, the autocorrelation can turn negative (the variance is also affected by the measurement error but it cannot change sign).

The second and third columns of Table 2.4 show that $\widehat{Q}_2$ and $\widehat{Q}_3$ are very close to 0. This agrees with equation 2.48 in Proposition 2.5. This agreement is likely because the measurement error does not affect the autocovariances of the GMM error for lags $j \geq 2$, according to equation 2.59 in Proposition 2.6.

2.7 Estimation Results of γ

This section reports the estimation results of the volatility of volatility parameter γ of the Heston model. I estimate γ using GMM based on the two moment conditions given by equations 2.60 and 2.61 for every good week as defined in Chapter 1.

Table 2.5: Estimates of $\gamma^2 \times 10^3$, good weeks

	$\gamma^2 \times 10^3$
median	0.83
5% percentile	0.21
25% percentile	0.42
75% percentile	1.45
95% percentile	7.46
median standard error	0.21
median z-score	4.01

2.7.1 Estimates of γ^2

Table 2.5 reports the summary statistics of the estimates of γ^2. The median is 0.83×10^{-3}. This median is much larger than the median estimate of $\bar{\zeta}$, which is 0.59×10^{-4} according to Table 1.2. Thus, γ^2 dominates $\bar{\zeta}$ by an order of magnitude in determining the asymptotic variance of ζ_t, which equals $\gamma^2\bar{\zeta}/2\kappa$ (see equation 2.4).

Figure 2.8 plots the time series of the estimates of γ^2 (the estimates are multiplied by 10^3). This series is persistent and slow-moving, most of the time, although this is less noticeable than the volatility clustering shown in Figure 1.8. However, volatility of volatility can move abruptly; for example, the "Great Recession" from the second half of 2008 to the beginning of 2009 witnessed exceptionally high levels of volatility of volatility, which is clear in the plot.

Figure 2.9 displays the histogram of the estimates of γ^2 (the estimates are multiplied by 10^3). The two highest bars lie in the range of $[0, 2] \times 10^{-3}$, which encompass the median and the lower and upper quantiles reported in Table 2.5. The distribution is highly skewed to the right, with a few outliers that are larger than 10×10^{-3}, as represented by the bar I label "infinity" at the very right of the histogram. However, these outliers are not a problem but rather represent a good

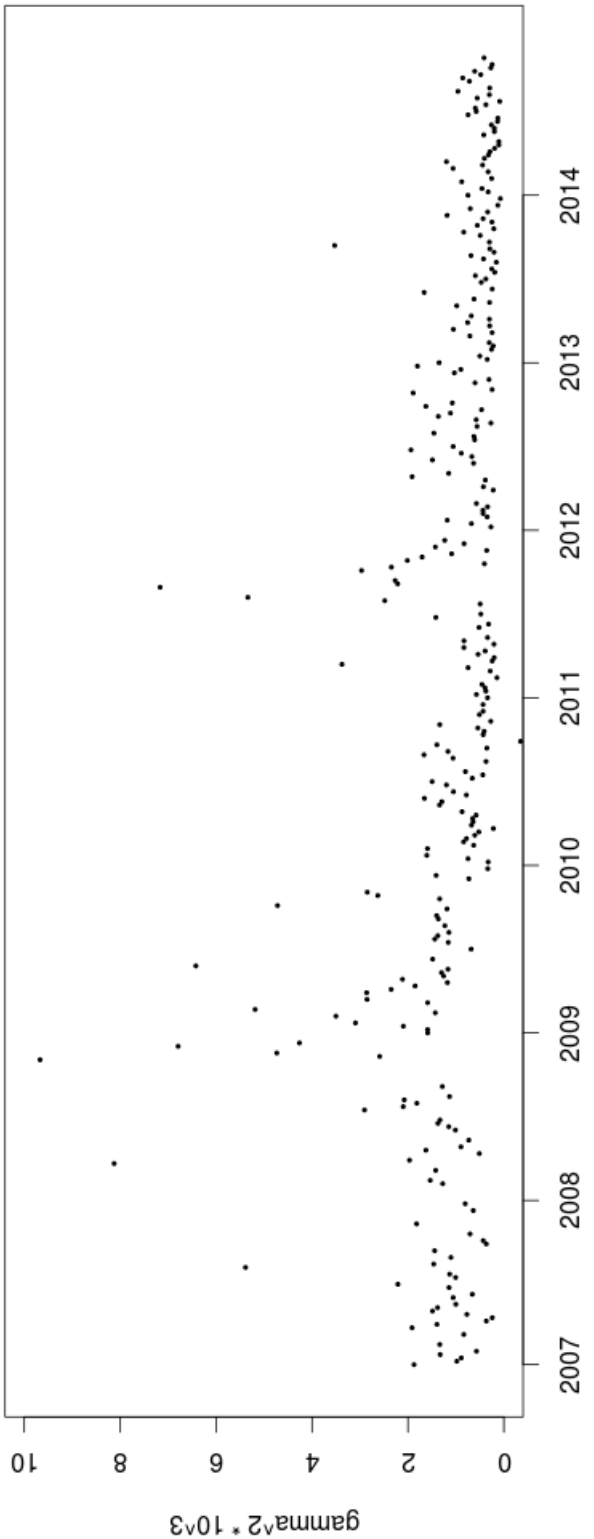

Figure 2.8: Estimates of $\gamma^2 \times 10^3$, good weeks

Figure 2.9: Histogram of estimates of $\gamma^2 \times 10^3$, good weeks

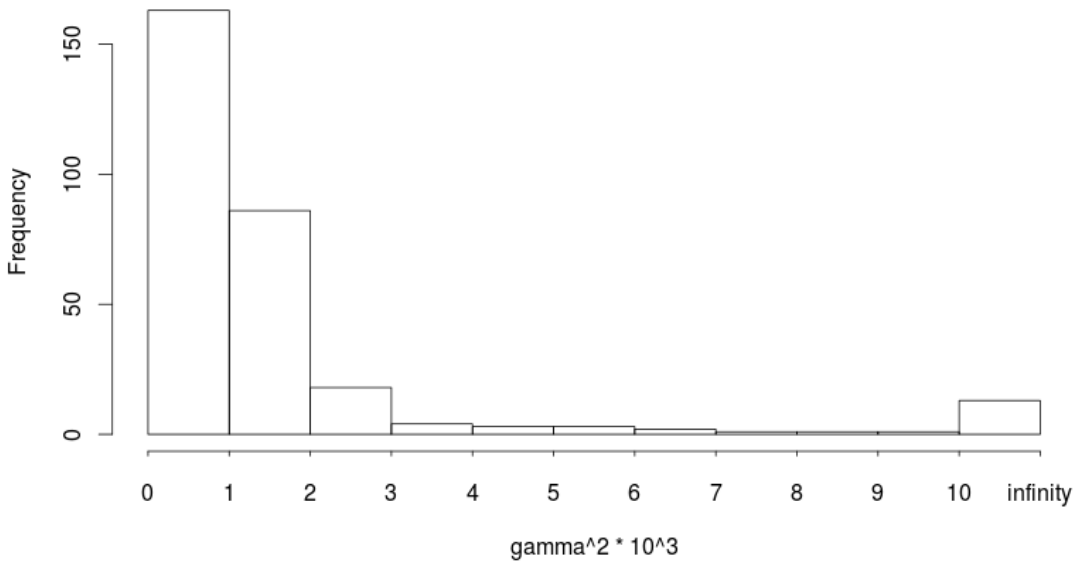

feature of the estimation: volatility of volatility can sometimes be exceptionally high, for example, during the financial crisis of 2008 - 2009.

2.7.2 Evidence of stochastic volatility

I am now ready to answer a key question raised in the introduction of Chapter 1: is the variation in realized variation over blocks, for example, in Figure 1.2, due to sampling error around a deterministic trend (as for a deterministic volatility model) or even a constant value (as for a geometric Brownian motion) or does this variation actually represent stochastic volatility? I answer this question by testing the hypothesis that $\gamma = 0$ — the null is accepted under deterministic volatility and rejected under stochastic volatility. The crucial point is that my GMM estimates are robust to measurement error by design thanks to a judicious choice of moment conditions, so the estimates of γ faithfully reflects the magnitude

of stochastic volatility despite the presence of measurement error.

92% of the good weeks feature stochastic volatility. The null is rejected at a 5% significance level, or equivalently, the estimates of γ^2 are positive and significant. This is strong evidence of stochastic volatility. Volatility starts the day high, and quickly declines towards its asymptotic mean $\bar{\zeta}$ at a fast rate κ. However, stochastic shocks to volatility constantly occur. This force is balanced by the force of strong mean reversion toward the asymptotic mean. The two forces jointly determine the stationary distribution of stock-price volatility.

For the other 8% of the good weeks the null hypothesis $\gamma = 0$ is not rejected at the 5% significance level. This is the case of deterministic volatility. Volatility starts the day high, but it declines deterministically at rate κ. The Heston stochastic differential equation becomes a deterministic ordinary differential equation: $d\zeta_t = \kappa(\bar{\zeta} - \zeta_t)dt$. The solution is $\zeta_t = e^{-\kappa t}\zeta_0 + (1 - e^{-\kappa t})\bar{\zeta}$. Because I find that mean-reversion is fast, this deterministic volatility model is approximately a geometric Brownian motion for most of the trading day.

I now examine the Feller condition in all good weeks. Recall that the Feller condition states that $\gamma^2 < 2\kappa\bar{\zeta}$, and it guarantees that ζ_t is almost surely positive for all t. Figure 2.10 plots $2\hat{\kappa}\widehat{\bar{\zeta}} \times 10^3$ on the horizontal axis against $\hat{\gamma}^2 \times 10^3$ on the vertical axis, together with a 45 degree line. 95% of the dots lie below the 45 degree line, indicating that the Feller condition is satisfied in the weeks they represent. 5% of the dots lie above the 45 degree line, indicating that the Feller condition is violated in those weeks. This is an evidence of model mis-specification, including price jumps or volatility jumps. Some of these 5% of good weeks belong to the 8% deterministic cases, suggesting that the GMM estimation of γ occasionally breaks down.

I further assess the performance of the Heston model using the GMM specification test. Figure 2.11 displays the histogram of the p-values of GMM J-tests for good weeks in which γ^2 is significantly positive and satisfies the Feller condition,

Figure 2.10: The Feller condition, good weeks

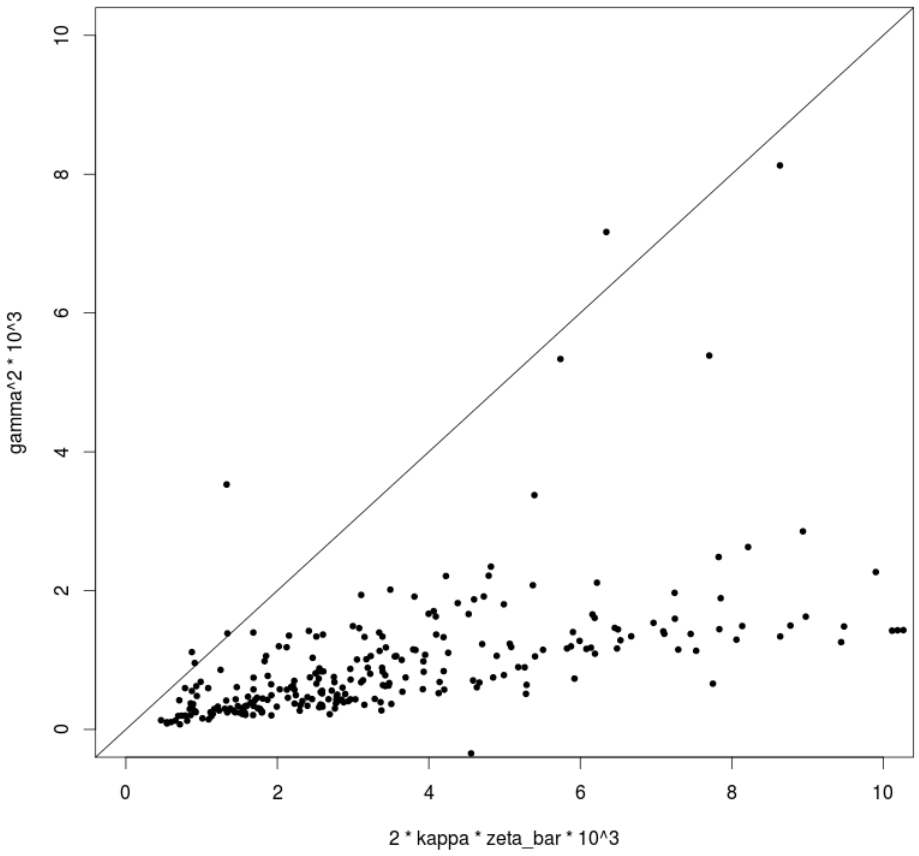

Figure 2.11: Histogram of p-values of GMM J-test, good weeks

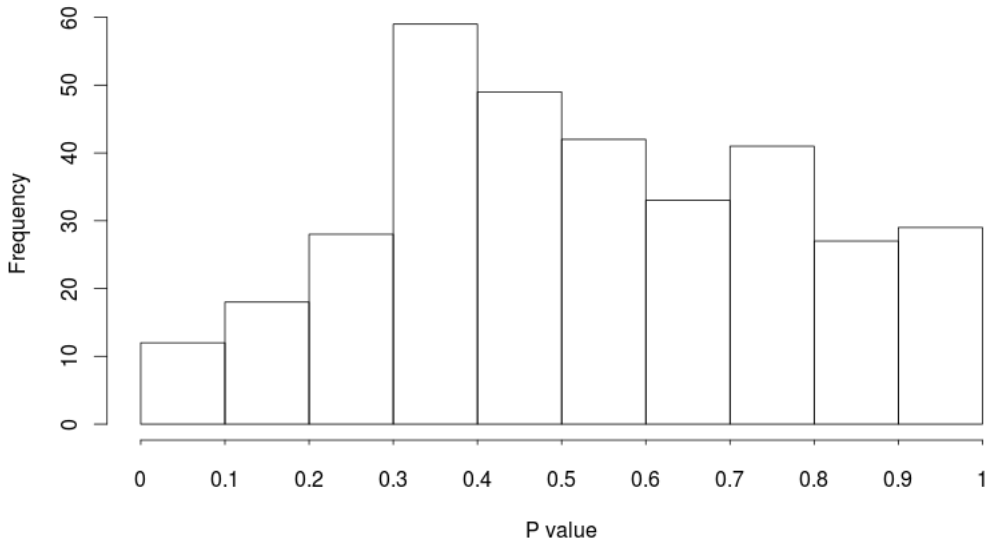

which account for 91% of the good weeks. The p-values are not small most of the time, indicating no evidence that the model is mis-specified. Only in 11 out of 268 weeks does the GMM specification test reject the model at 10% significance level.

To summarize, the Heston model works very well empirically in 65% (257 out of 393) of weeks in the sample, in the sense that all three parameters are significant, the model passes the GMM specifications tests, and the Feller condition is satisfied.

CHAPTER 3

Outliers

In Chapters 1 and 2 I reformulated the Heston stochastic volatility model to develop a model of the high-frequency evolution of the scaled increments $\zeta_{t,t+h}$ of quadratic variation. I used the generalized method of moments to estimate three of the parameters of the Heston model, the speed of mean reversion κ (or equivalently, β), the asymptotic mean $\bar{\zeta}$, and the volatility of volatility γ, and found that the estimation is successful most of the time. I established the validity of the Heston model also by examining as many structural implications of the model as I could find.

However, the continuous-path Heston model is not the whole story. An attractive alternative is to allow for jumps, either in the price process or the volatility process, but to claim that they are rare. Small jumps may be common but indistinguishable from a Heston model empirically. But I can allow for rare large jumps. To identify blocks where large jumps are likely present, I look for blocks where large realized variation occurs. What these "bad blocks" are picking up are very large shocks that are not well approximated by the Heston model. The arrival rate of the large shocks is very low (on the order of a few per day) in contrast to ordinary shocks (which have arrival rates on the order of a few per second). Bad blocks represent deviations that are not handled well by the stationary error terms of our model. They show up only when we examine the "path behavior" of the realized variation process. The larger point is that distinguishing between jumps and continuous movements is hard, but I may be able to approximate the general

Table 3.1: Number of bad blocks

$\varphi_{t,t+h}$ over weekly median	Good weeks	Bad weeks	Total
$(10, 100)$	301	422	723
$(100, 1000)$	32	157	189
$(1000, +\infty)$	3	41	44
Total bad blocks	336	620	956
Total per week	1.13	6.39	2.43
Total percentage	0.10%	0.55%	0.21%

case with my continuous-path model most of the time except for a collection of relatively infrequent bad blocks.

3.1 The Effect of Bad Blocks

In this section, I identify bad blocks, shrink them, and re-estimate the model, and analyze the effects of bad blocks on estimation results.

I start by identifying bad blocks. A bad block is a 100-second block in which the realized variation $\varphi_{t,t+h}$ exceeds 10 times the median of realized variation in all blocks in that week. This definition of the bad block has an important advantage that it is independent of any model.

Based on this definition, I identify all bad blocks in the entire sample period from 2007 to 2014. Table 3.1 reports the breakdown of all bad blocks. There are 956 bad blocks in total, or 2.43 per week (there are 393 weeks in the sample), accounting for 0.21% of all blocks (there are $234 \times 5 \times 393 = 459,810$ blocks in the sample). Among them 336 bad blocks occur in the 296 good weeks, or 1.13 bad blocks per good week, accounting for 0.10% of all blocks in good weeks. The remaining 620 bad blocks occur in the 97 bad weeks, or 6.39 bad blocks per bad week, accounting for 0.55% of all blocks in bad weeks. These numbers are

Table 3.2: Distribution of the number of bad blocks for each week

Number of bad blocks	Good weeks	Bad weeks	Total
0	158	28	186
1	63	18	85
2	36	14	50
3	13	9	22
4	7	2	9
5	4	2	6
6	4	3	7
7	2	1	3
8	3	3	6
9	2	1	3
10	1	0	1
11	1	2	3
12	0	1	1
13	1	1	2
14	0	2	2
20	0	1	1
21	0	1	1
23	0	1	1
25	0	1	1
44	0	1	1
75	0	1	1
184	0	1	1
Total	296	97	393

consistent with the idea that bad blocks represent large and rare jumps (either in the price process or in the volatility process).

Table 3.2 reports the distribution of the number of bad blocks for each week. The first column reports the distribution for good weeks. More than half of good weeks have no bad blocks. The good weeks with 0, 1 or 2 bad blocks account for 87% of all good weeks. The good weeks with the largest number of bad blocks has 13 bad blocks. This distribution looks like a Poisson distribution, as expected. An estimate of the parameter of the Poisson distribution is 1.13, the average number of bad blocks per week shown in Table 3.1. This estimate has the dimension of a

Figure 3.1: Histogram of the number of blocks for each week

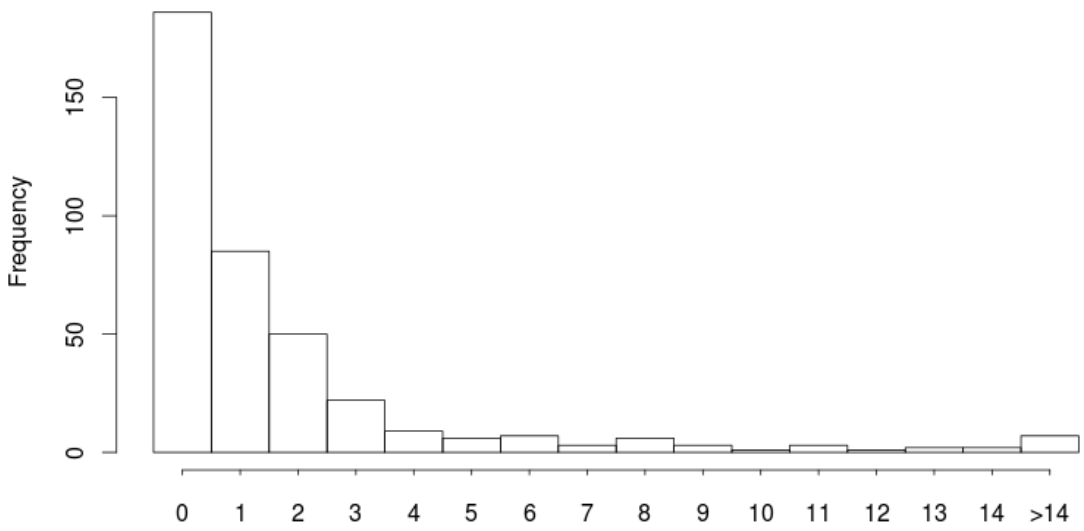

rate per week, and corresponds to a parameter value of 0.23 with the dimension of a rate per day.

The second column of Table 3.2 reports the distribution for bad weeks. 29% of bad weeks have no bad blocks. This percentage is significantly lower than for good weeks, but it is still a considerable portion. In these weeks, the failure of my GMM estimation in Chapter 1 cannot be explained by bad blocks. The bad weeks with 0, 1 or 2 bad blocks account for 62% of all bad weeks. This distribution looks like a Poisson distribution, as expected, except for its fat right tail. The bad weeks with the largest number of bad blocks has 184 bad blocks. This week includes February 27, 2007, when the S&P 500 Index dropped 3.5% in volatile trading following a 9% sell-off in China's stock market overnight.

The third column of Table 3.2 reports the distribution for all weeks. Figure 3.1 displays the histogram of this distribution. The distribution looks like a Poisson

Figure 3.2: Histogram of the block index of bad blocks

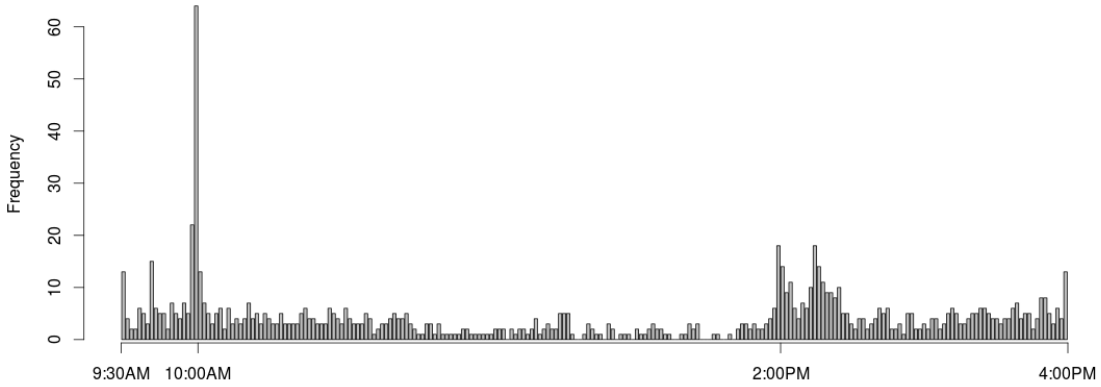

distribution, except for its fat right tail. The weeks containing more than 14 bad blocks are represented by the bar at the very right end labeled ">14".

Do bad blocks tend to occur more frequently in some part of a trading day than other parts? Figure 3.2 displays the histogram of the block index of bad blocks. Bad blocks are more common in four parts of a trading day, the beginning, 10:00AM, 2:00PM and the end. 10:00AM corresponds to various macroeconomic announcements[1], and 2:00PM is the time when FOMC releases its policy statement.

I now "shrink" the bad blocks. Specifically, I divide $\varphi_{t,t+h}$ by 10 for blocks in the first row of Table 3.1, by 100 for blocks in the second row and by 1000 for blocks in the third row. This procedure of shrinking bad blocks also has the advantage that it is independent of any model. There are of course other reasonable and model-independent ways of shrinking bad blocks, but I perform this procedure for simplicity.

I am now ready to re-estimate the parameters for a day or a week, using the

[1]They include Purchasing Managers Index (PMI), Consumer Conference (Conference Board), and Consumer Sentiment (University of Michigan, preliminary), among others. See Siegel, "Stocks in the Long Run", Fourth Edition, Table 14.1, p. 243.

Table 3.3: Reproduced Table 1.1: joint estimation of $\bar{\zeta}$ and β, before shrinkage

	Daily (1969)	Weekly (393)
Good β, Good $\bar{\zeta}$	53% (1041/1969)	88% (344/393)
Good β, Bad $\bar{\zeta}$	0% (7/1969)	1% (2/393)
Bad β, Good $\bar{\zeta}$	37% (737/1969)	9% (36/393)
Bad β, Bad $\bar{\zeta}$	9% (184/1969)	3% (11/393)
Good J-stat	88% (1732/1969)	87% (340/393)
Bad J-stat	12% (237/1969)	13% (53/393)
Good (β, $\bar{\zeta}$ and J-stat)	45% (894/1969)	75% (296/393)

Table 3.4: Performance of joint estimation of $\bar{\zeta}$ and β, after shrinkage

	Daily (1969)	Weekly (393)
Good β, Good $\bar{\zeta}$	54% (1061/1969)	92% (363/393)
Good β, Bad $\bar{\zeta}$	0% (0/1969)	0% (0/393)
Bad β, Good $\bar{\zeta}$	36% (716/1969)	7% (28/393)
Bad β, Bad $\bar{\zeta}$	10% (192/1969)	1% (2/393)
Good J-stat	92% (1806/1969)	89% (351/393)
Bad J-stat	8% (163/1969)	11% (42/393)
Good (β, $\bar{\zeta}$ and J-stat)	49% (961/1969)	83% (325/393)

shrunk data for bad blocks.

Table 3.4 displays measures of statistical performance of daily and weekly joint estimation of $\bar{\zeta}$ and β after shrinking bad blocks. This table is parallel to Table 1.1 in Chapter 1, reproduced here for convenience as Table 3.3.

The first column reports the statistical performance of daily estimation. The parameter significance is not very different from before shrinkage. The percentage of days passing the GMM J-test increases to 92% after shrinkage from 88% before. The percentage of good days is unchanged at 49%.

The second column reports the statistical performance of weekly estimation.

The parameter significance improves, with the percentage of both parameters being significant increasing to 92% after shrinkage from 88% before. Meanwhile, the percentage of days passing the GMM J-test increases to 89% after shrinkage from 87% before. Overall, the percentage of good weeks increases to 83% after shrinkage from 75% before.

In summary, shrinking bad blocks modestly improves daily joint estimation of $\bar{\zeta}$ and β, and significantly improves weekly joint estimation. Pooling is still appropriate.

3.1.1 The effect of bad blocks in good weeks

I now examine parameter estimates after shrinking bad blocks, in each of the 138 good weeks with at least one bad block.

Figure 3.3 plots parameter estimates in all good weeks with bad blocks, before shrinking on the horizontal axis versus after shrinking on the vertical axis, together with a 45 degree line. Clockwise from the upper left corner, I present plots for the three estimated parameters $\bar{\zeta}$, β, γ^2 followed by a plot of the p-value of the J-test. Each of these graphs plots estimates for all 138 good weeks with at least one bad block. Figure 3.4 is organized in the same way, but with axes truncated to better display the majority of the results, except for the graph for the p-value, which is simply reproduced. Because of the truncation, the plots in Figure 3.4 have fewer observations: 135, 133, 132 and 138.

The upper-left subplot of Figure 3.3 shows that $\bar{\zeta}$ is almost unaffected by bad blocks, even for some good weeks with large estimates of $\bar{\zeta}$. The upper-left subplot of Figure 3.4 has 135 dots, and it confirms that all relatively small estimates of $\bar{\zeta}$ are unaffected by bad blocks. One might be inclined to think this is because bad blocks are rare, however, this argument is not valid because it also predicts other parameter estimates are almost unaffected, which is not the case as I explain

Figure 3.3: Good weeks with bad blocks, before shrinking and after

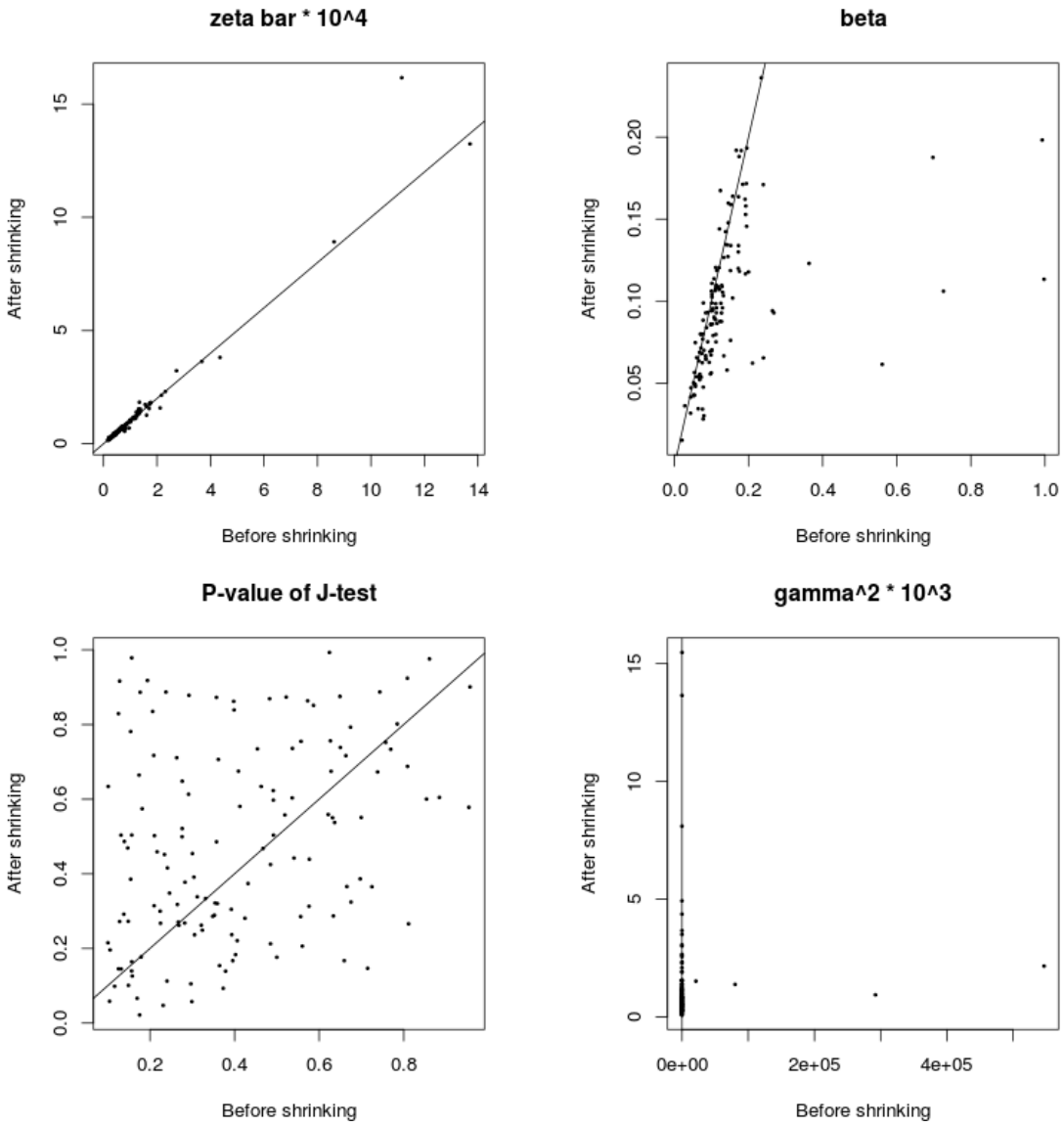

Figure 3.4: Good weeks with bad blocks, before shrinking and after, truncated

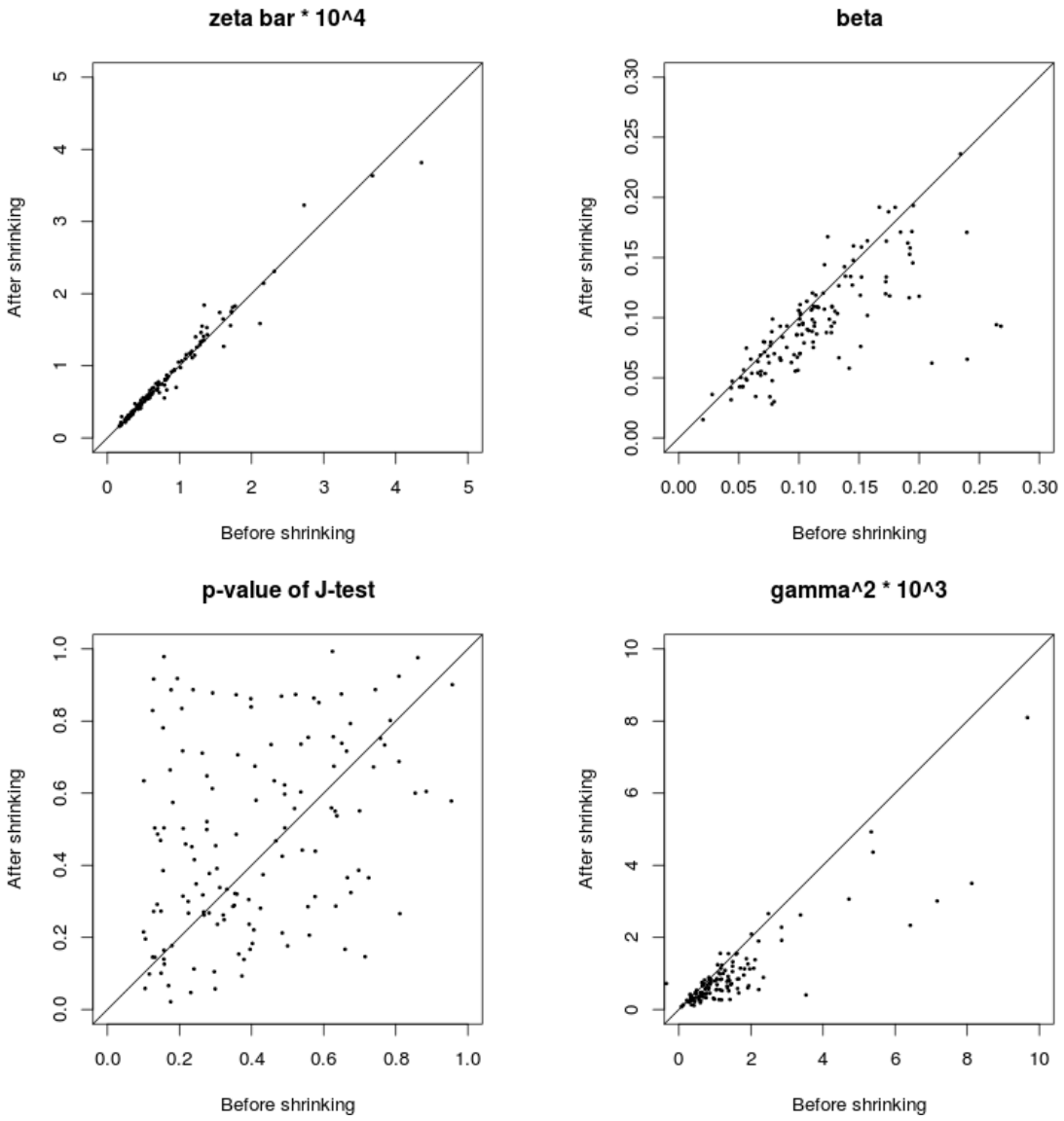

the paragraphs that follow. The reason is likely that a bad block affects two GMM errors with almost the same magnitude (because α is close to 1) but with opposite signs, and hence the time-average sample versions of equation 1.28 are almost equal with or without bad blocks.

The upper-right subplot of Figure 3.3 shows that β is unaffected most of the time, but shrinking eliminates large estimates that are suspicious. The upper-left subplot of Figure 3.4 has 133 dots, and it confirms that relatively small estimates of β are almost unaffected by bad blocks, except for 3 cases. The percentage of the estimates before and after shrinking being roughly equal is $130/138 = 94\%$. The argument in the last paragraph can explain why estimates of β are unaffected most of the time. The fact that shrinking eliminates all large estimates indicates that sometimes estimates of β are probably driven by a single pair of blocks where the first block is bad while the second is on the border of being bad or not (an immediate decline of realized variation from a large positive shock to a level about $\bar{\zeta}$ corresponds to β close to 1).

The lower-right subplot of Figure 3.3 shows that γ is unaffected or modestly smaller most of the time, but like β shrinking eliminates all large estimates that are suspicious (the line that looks like a vertical axis is indeed a 45 degree line). The upper-left subplot of Figure 3.4 has 132 dots, and it confirms that relatively small estimates of γ are unaffected or modestly smaller after shrinking, with a few more exceptions than for β. A change in the value of γ might be due to a change in the value of β, and the estimation procedure of γ developed in Chapter 2 itself might or might not be affected.

The lower-left subplots of Figure 3.3 and Figure 3.4 show that the P-value of the GMM J-test of Chapter 1 estimation is affected in an unclear way.

3.1.2 The effect of bad blocks in bad weeks

I now examine parameter estimates after shrinking bad blocks, in each of the 69 bad weeks with at least one bad block.

Figure 3.5 plots parameter estimates in all bad weeks with bad blocks, before shrinking on the horizontal axis versus after on the vertical axis, together with a 45 degree line. This figure is not truncated, so it contain estimates in all 69 bad weeks with at least one bad block. Figure 3.6 does the same, but is truncated to better display the majority of the results.

The upper-left subplot of Figure 3.5 shows that shrinking eliminates all extremely large and all negative estimates that are suspicious (the line that looks like a vertical axis in is indeed a 45 degree line). The upper-left subplot of Figure 3.6 contains 63 dots, and it shows that almost all estimates of $\bar{\zeta}$ are unaffected.

The upper-right subplots show that estimates of β are unaffected most of the time, but shrinking eliminates most of the large estimates that are suspicious. This pattern is similar to those in good weeks with bad blocks but is less prominent.

The lower-right subplots show that estimates of γ is unaffected or modestly smaller most of the time, but like β shrinking eliminates all extremely large estimates that are suspicious. This pattern is similar to those in good weeks with bad blocks but is less prominent.

The lower-left subplots show that the p-value of the GMM J-test of Chapter 1 estimation is affected in an unclear way, except that shrinking eliminates almost all p-values smaller than 0.1, but this might be artificial since 0.1 is the threshold of the p-value for "good J-test" and "bad J-test".

Figure 3.5: Bad weeks with bad blocks, before shrinking and after

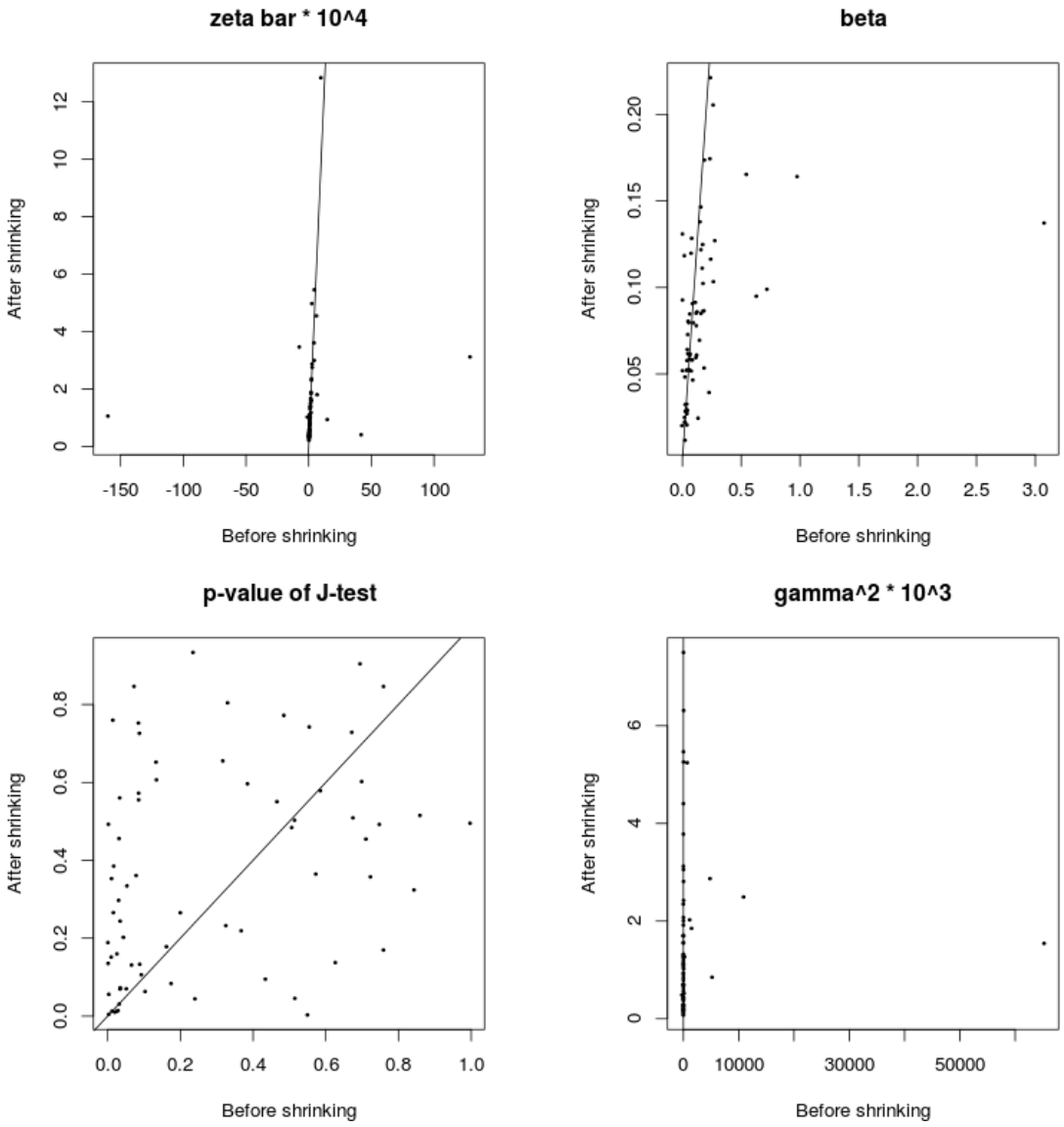

Figure 3.6: Bad weeks with bad blocks, before shrinking and after, truncated

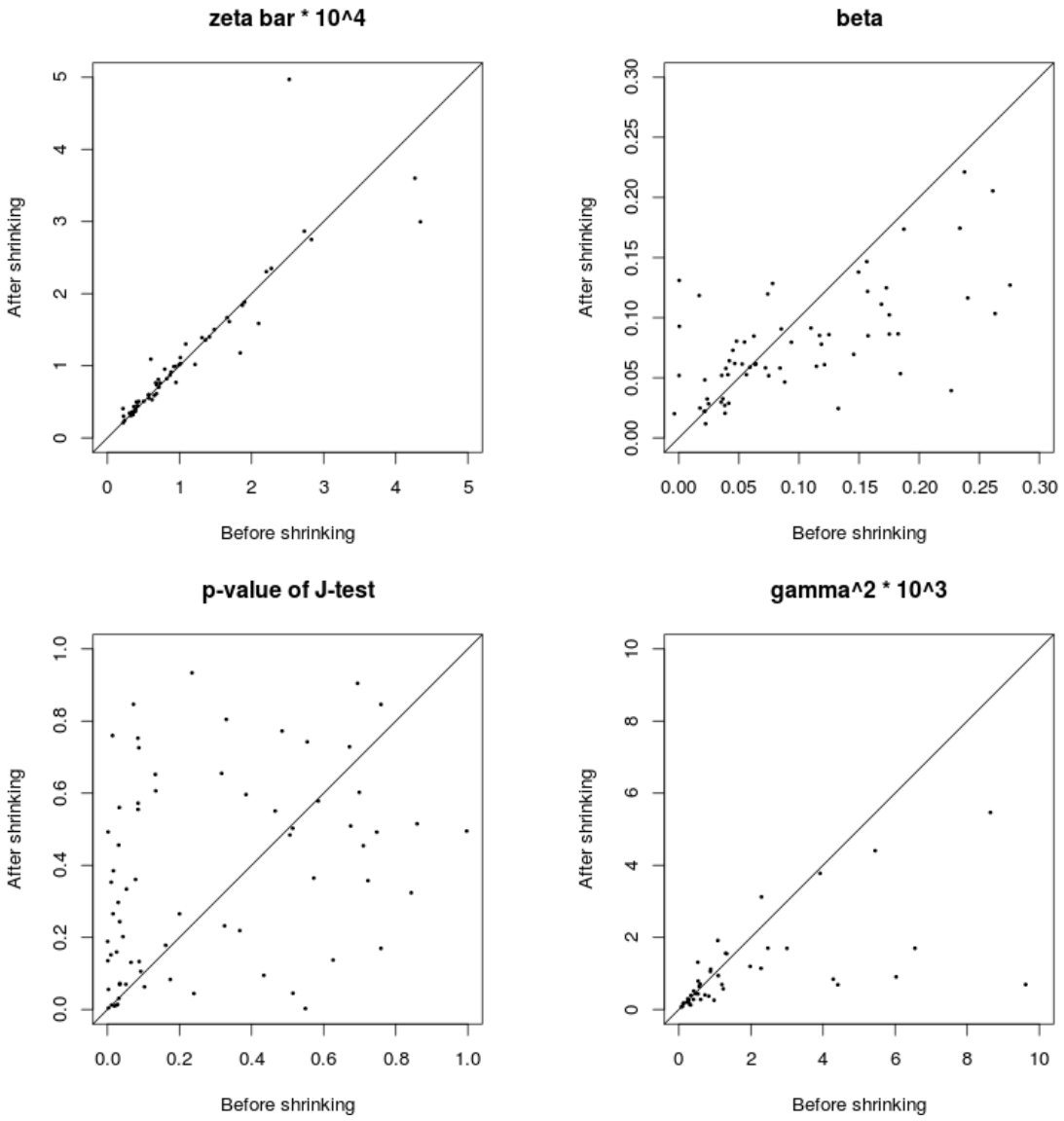

Table 3.5: Estimation results, two bad weeks

	Week 123	Week 323
$\bar{\zeta} \times 10^4$	81	0.81
standard error of $\bar{\zeta} \times 10^4$	7.3×10^4	0.49
β	5.3×10^{-5}	0.012
standard error of β	4.8×10^{-2}	0.017
p-value of J-test	0.62	0.13
median $\varphi_{t,t+h} \times 10^4$	1.33	0.57
mean $\varphi_{t,t+h} \times 10^4$	1.53	0.72

3.1.3 Two Bad Weeks

There are still 393 - 325 = 68 bad weeks after shrinking, according to Table 3.4. These bad weeks are not likely caused by a few bad blocks but rather by some other forms of model misspecification. I will only examine the two weeks that fall into the "bad $\bar{\zeta}$, bad β" category after shrinking.

One such bad week is a five-day collection of 02/27/2007 - 03/05/2007, which is not a calendar week from Monday to Friday; I will refer to this week as "week 123" henceforth. Figure 3.7 plots the realized variation over blocks for this week. This is a typical week: volatility starts high on each trading day and quick declines towards its long-run mean value, and moves slightly higher at the end of the day. No block in this week is identified as a bad block. The first column of Table 3.5 reports the estimation results for this week. The estimate of $\bar{\zeta}$ is too large. Clearly, the jointly estimation breaks down in this week. The reason is unclear.

The other bad week is a five-day collection of 06/17/2013 - 06/21/2013, which happens to be a calendar week from Monday to Friday; I will refer to this week as "week 323". Figure 3.8 plots the realized variation over blocks for this week. Volatility suddenly moved high at 2:00PM on 06/19/2013. This was the time the FOMC released a statement that it might "taper" its quantitative easing

Figure 3.7: Realized variation by block, 02/27/2007 - 03/05/2007 (week 123)

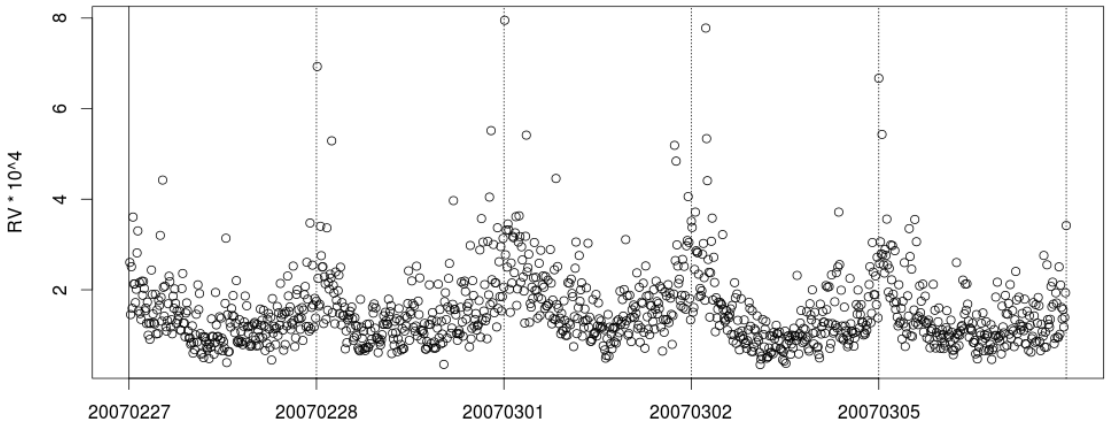

Figure 3.8: Realized variation by block, 06/17/2013 - 06/21/2013 (week 323)

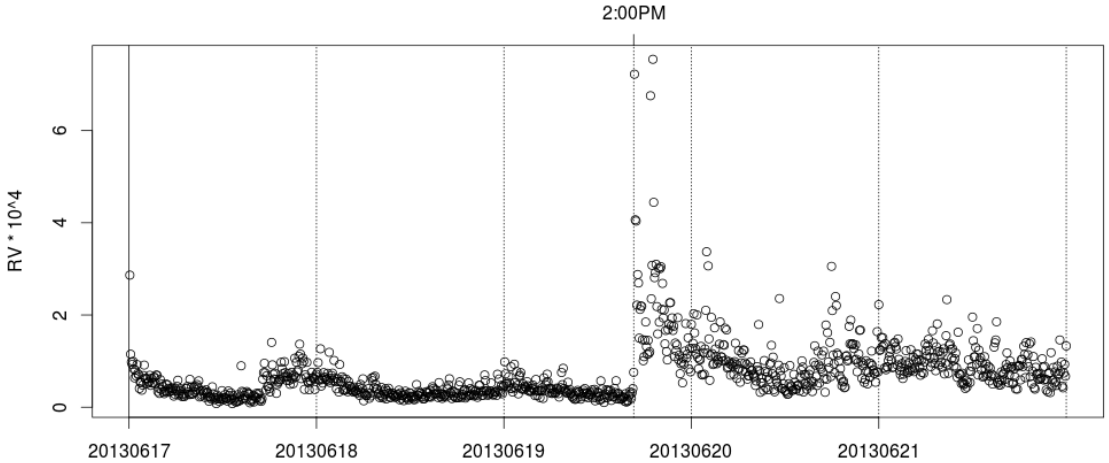

program sooner than the market assumed. The market experienced significantly higher volatility for the rest the week than before the FOMC announcement. The second column of Table 3.5 reports the estimation results for this week. The estimate of $\bar{\zeta}$ looks plausible in the sense that it is close to weekly median and mean, but its standard error is very high. This is because there was a structural break: volatility switched from a low volatility regime to a high volatility regime. Pooling might harm rather than help because the parameter values clearly change over this week.

3.2 Conclusion and Future Research

In conclusion, the continuous-path model of Chapters 1 and 2 works very well "most of the time", and most of the failures are localized to a few bad blocks — the equilibrium behavior is interrupted at relatively infrequent intervals with the arrival of big junks of information that disrupt the market. That immediately suggests a disjunction between price behavior at high frequency and price behavior on longer time scales (days, weeks, months).

References

Aît-Sahalia, Yacine, and Jean Jacod, 2014, *High-Frequency Financial Econometrics*, Princeton University Press.

Anderson, Torbin, Tim Bollerslev, Francis X. Diebold, and Paul Labys, 2000, Great Realizations, *Risk* 13, 105–108.

Anderson, Torbin, and Tim Bollerslev, 1998, Answering the Skeptics: Yes, Standard Volatility Models Do Provide Accurate Forecasts, *International Economic Review* 3, 885-905.

Ellickson, Bryan, Benjamin Hood, Tin Shing Liu, Duke Whang, and Peilan Zhou, 2012, Stocks in the Short Run.

Cox, John, Jonathan Ingersoll, and Stephen Ross, 1993, A Theory of the Term Structure of Interest Rates, *Econometrica* 53, 385–407.

Feller, William, 1951, Two Singular Diffusion Problems, *Annals of Mathematics* 54(2), 173–182.

Hansen, Lars Peter, 1982, Large Sample Properties of Generalized Method of Moments Estimators, *Econometrica* 50, 1029-1054.

Heston, Steven, 1993, A Closed-Form Solution for Options with Stochastic Volatility with Aplications to Bond and Currency Options, *Review of Financial Studies* 6, 327–343.

Hayashi, Fumio, 2000, *Econometrics*, Princeton University Press.

Hood, Benjamin, 2011, Essays on Intraday Stock Price Volatility, Ph.D. dissertation, UCLA.

Liu, Tin Shing, 2011, Stock Price Volatility within a Trading Day, Ph.D. dissertation, UCLA.

Newey, Whitney, and Kenneth West, 1987, A Simple, Positive Semi-definite, Heteroskedasticity and Autocorrelation Consistent Covariance Matrix, *Econometrica* 55, 703-708.

Protter, Philip, 2004, *Stochastic Integration and Differential Equations*, Springer-Verlag.

Shreve, Steven, 2004, *Stochastic Calculus for Finance: II*, Springer-Verlag.

Whaley, Robert, 1993, Derivatives on Market Volatility: Hedging Tools Long Overdue, *Journal of Derivatives* 1, 71–84.

Whaley, Robert, 2009, Understanding VIX, *Journal of Portfolio Management* 35 (Spring), 98–105.

Whang, Duke, 2012, Volatility at High Frequency, Ph.D. dissertation, UCLA.

Zhou, Peilan, 2007, Essays on Financial Asset Return Volatility, Ph.D. dissertation, UCLA.